Cook Inlet Circulation Modeling - Freshwater Forcing Experiment and Lagrangian Analysis

Contents

Contents

Final Report to the National Oceanic Atmospheric Administration National Centers for Coastal Ocean Science Kasitsna Bay Lab

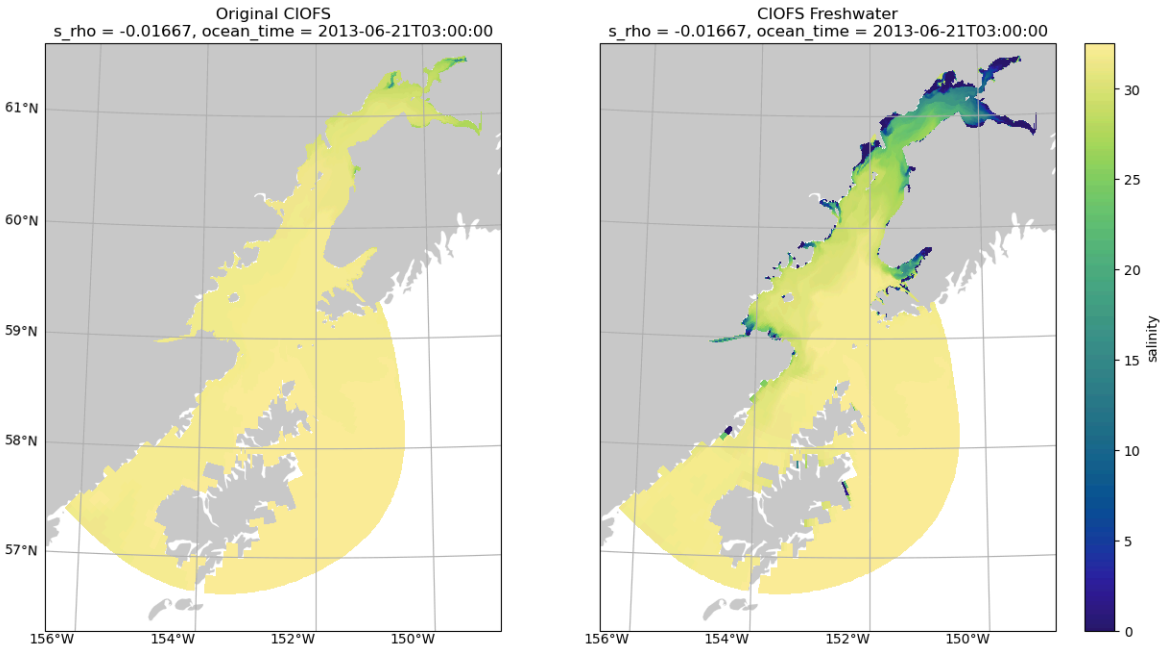

This project has been supported by the National Oceanic Atmospheric Administration National Centers for Coastal Ocean Science Kasitsna Bay Lab.

October 11, 2024

Citation: Thyng, K. M., C. Liu, 2024. Cook Inlet Circulation Modeling - Freshwater Forcing Experiment and Lagrangian Analysis, Final Report to the National Oceanic Atmospheric Administration National Centers for Coastal Ocean Science Kasitsna Bay Lab, Axiom Data Science, Anchorage, AK.

Online report: https://ciofs-fresh.axds.co/

PDFs of parts of report:

- Main content
- Model-data comparison: moorings
- Model-data comparison: CTD transects
- Model-data comparison: CTD profiles
- Model-data comparison: HF Radar
- Model-data comparison: ADCP
- Model-data comparison: drifters

1. Summary and Recommendations

1.1. Summary

A new hindcast version of the Cook Inlet Operational Forecast System (CIOFS) model (the CIOFS Freshwater model[1]) has been run with improved freshwater forcing for two time period: 2003–2006 and 2012–2014, selected to overlap with the maximum amount of historical data. This project follows from the previous hindcast CIOFS model project[2], in which a similar CIOFS model (the CIOFS Hindcast model[3]) was run with only gauged rivers for freshwater forcing. That project found that the model was severely lacking freshwater in the system. These two models are compared in detail in the present report.

1.2. Key Outcomes

Because much more freshwater is input to the newer model, salinity is captured much more accurately in the CIOFS Freshwater model, as compared with CIOFS Hindcast. The impact is also seen in the drifter simulations that are at 7.5m and shallower, which are close enough to the surface to be impacted by the presence of freshwater. For these drifter simulations, the CIOFS Freshwater particle tracks are more likely to follow the *in situ* drifter than the CIOFS Hindcast are, and that is borne out in the area-based skill scores found. Subtidal sea surface height for CIOFS Freshwater is also improved, demonstrating how this measure is impacted by the freshwater input. Temperature is also improved in the CIOFS Freshwater model, but only by a small margin.

1.3. Recommendations

Given the success and large improvements seen in the CIOFS Freshwater version of the CIOFS model, the time range of the simulation should be expanded as long as possible, to something similar as the CIOFS Hindcast 1999–2022. When running a new long simulation, it would also be a good time to make other improvements in the model setup, such as improved stretching in the vertical grid, improved tracer advection, and improved turbulence closure scheme. Additionally, another model such as the Global Ocean Physics Reanalysis model (GLORYS12V1) should be evaluated a possible alternative for forcing the horizontal open boundaries.

---

[1] CIOFS Freshwater visualization: https://portal.aoos.org/#module-metadata/43596105-4a50-4528-985f-bb65e1c08e2c

[2] CIOFS Hindcast report: https://ciofs.axds.co/

[3] CIOFS Hindcast visualization: https://portal.aoos.org/#metadata/7840770a-c04f-4b37-aba4-12094c8e1a5a/

2. Model Descriptions

2.1. CIOFS Models

There are three models being actively run in and/or used in Cook Inlet which are all referred to as CIOFS models since they use the same grid and domain:

- CIOFS operational: Run as a nowcast/forecast since Aug 31, 2021 and forecast 48 hours. Portal link
- CIOFS hindcast: from 1999 through 2022. Portal link
- CIOFS freshwater forcing: 2003–2006 and 2012–2014. Portal link

where CIOFS originally stood for Cook Inlet Operational Forecast System.

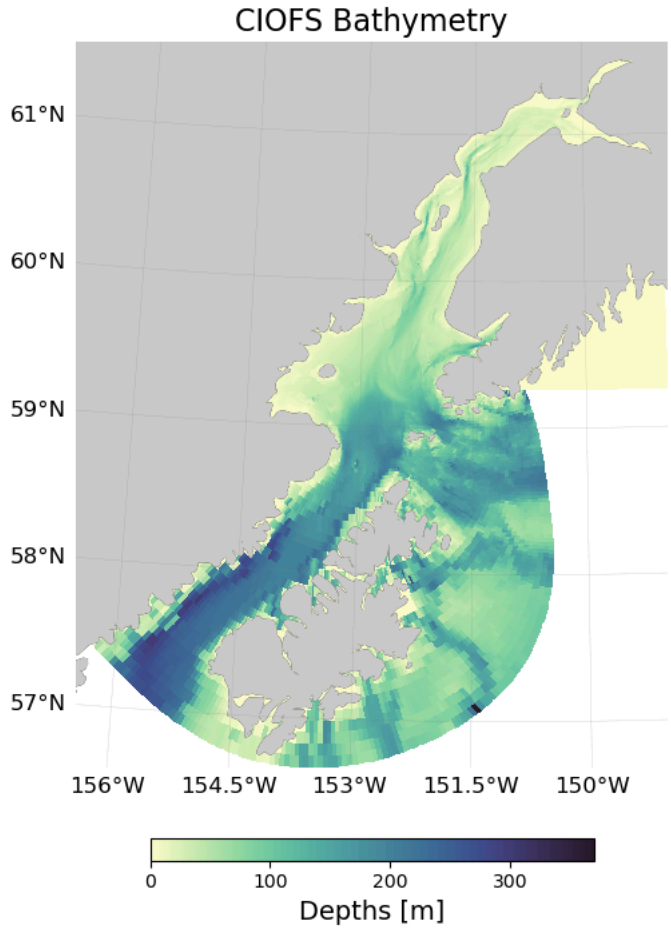

Fig. 2.1 Bathymetry for all CIOFS models.

All CIOFS models are run using Regional Ocean Modeling System (ROMS) [Shchepetkin and McWilliams [SM05], McWilliams [McW09]] using the same horizontal grid and number of vertical levels and stretching/transform functions (see bathymetry in Fig. 2.1). The horizontal grid ranges from 10 meters to 3.5 kilometers resolution and the vertical grid has 30 sigma levels with Vstretching=1 and Vtransform=1.

Since the current project uses output from the CIOFS hindcast and freshwater models (see example animation in Fig. 2.2), we will present the forcing for those models here.

0:00

_images/ciofs_freshwater.mp4

Fig. 2.2 Example animation showing the surface salinity for CIOFS Hindcast (left) and CIOFS Freshwater (right).

2.1.1. Both CIOFS Hindcast and CIOFS Freshwater

Time-varying surface forcing for both models comes from ECMWF Reanalysis v5 (ERA5) for wind, temperature, and humidity [HBB+20]. Boundary forcing is from HYCOM Global Ocean Forecasting System (GOFS) 3.1 Reanalysis and is for temperature, salinity, and sub-tidal water levels [NavalRLaboratory21]. The open boundary forcing for tides is from the NOS CO-OPS version of CIOFS [NOAA [NOA19]; Zhang [Zha19]] which is derived from the ADCIRC tidal database [ADCd.].

Each modeling period required a 1 year spin up time period that was discarded.

The difference between the two models was in how the freshwater forcing was implemented. That is described in the following sections for each model.

2.1.1.1. CIOFS Hindcast

The CIOFS Hindcast model used river inputs with real-time discharge observations from 12 major rivers supplied by the USGS for freshwater forcing [USGS16].

Additional details about the CIOFS Hindcast model forcing are included in the original CIOFS Hindcast report [TLFD23].

2.1.1.2. CIOFS Freshwater-Forced

2.1.1.2.1. Hydrology Model

The CIOFS Freshwater model used output from a watershed model as the freshwater forcing, similar to what is described in [DHH+20]. The hydrology model of the Gulf of Alaska watershed provided by David Hill, Oregon State University [[BHAL16], [HBC+15]] was used to create the ROMS river (point sources) input files. The data made available to Axiom contains daily discharge values at coastal grid points along the Gulf of Alaska from the hydrology model's native grid.

Python scripts created by Kate Hedstrom were used to generate the ROMS point source input files for the CIOFS freshwater hindcast. The scripts transform the discharge values from the hydrology model into a ROMS grid-specific format, including identifying discharge points in the ROMS grid, mapping and re-indexing discharge values from the input points to ROMS discharge points, and other necessary calculations to prepare the data for the ROMS model. Modifications to the scripts were made so that the generated input files work with the CIOFS grid. An additional measure to increase the model stability was to redistribute extremely high discharge at a single point across several nearby points. To account for large discharge from point sources, the maximum speed in ROMS was increased from 20 to 80 m/s by modifying mod_scalars.F in ROMS source code, following the ROMS manual [Hedstrom18].

The resulting difference in the total amount of volumetric rate of freshwater input for each model is shown in Fig. 2.3.

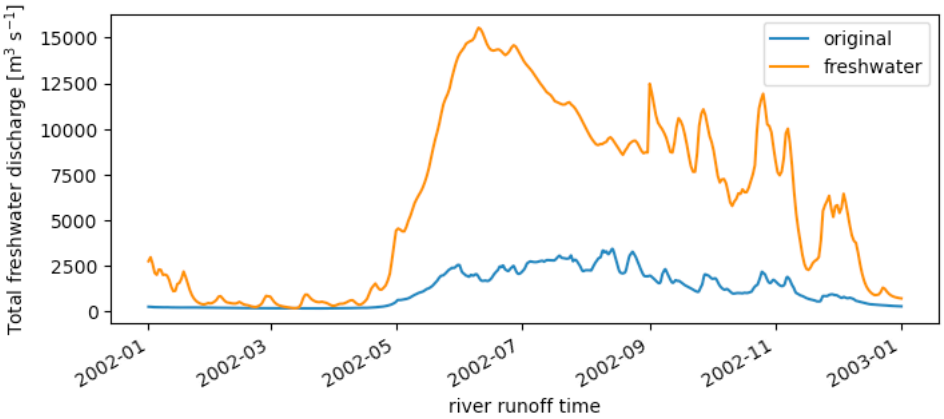

Fig. 2.3 Overall freshwater input for CIOFS Hindcast (blue) and CIOFS Freshwater (orange) models for the first year of spin-up time, 2002.

2.1.1.2.2. Computation

The CIOFS freshwater simulations were performed using the Intel Fortran Compiler and Intel MPI, which are provided in the oneAPI base toolkit and HPC toolkit, version 2023, for parallelization on a local cluster consisting of 23 nodes. A total of 9 nodes each contained 40 Intel Xeon Gold 6148 (Skylake) CPU cores, allowing for a total of 360 cores to perform the 2003-2006 simulation. The remaining 14 nodes each contained 48 Intel Xeon Gold 6262 (Cascade Lake) CPU cores, allowing for a total of 672 cores to perform the 2012-2014 simulation. Both model simulations were performed concurrently. Nodes were connected via QDR InfiniBand fabric, which enabled the two groups of hindcast simulations over 7 years in total to complete within one and a half months. This performance demonstrates efficient scaling, enabling the high-resolution simulations required for this project to be feasibly executed within a reasonable timeframe. The Intel compiler and MPI implementation tailored for the Xeon architecture was critical in maximizing utilization of the available compute capability.

3. Monthly Mean Salinity

Plots of monthly mean surface salinity are shown in this section.

Differences between the USGS river-forced CIOFS model (left) and the watershed model-forced CIOFS model (right) are stark in both winter and summer. The differences are less widespread in the winter (Fig. 3.1) as compared with the summer (Fig. 3.2).

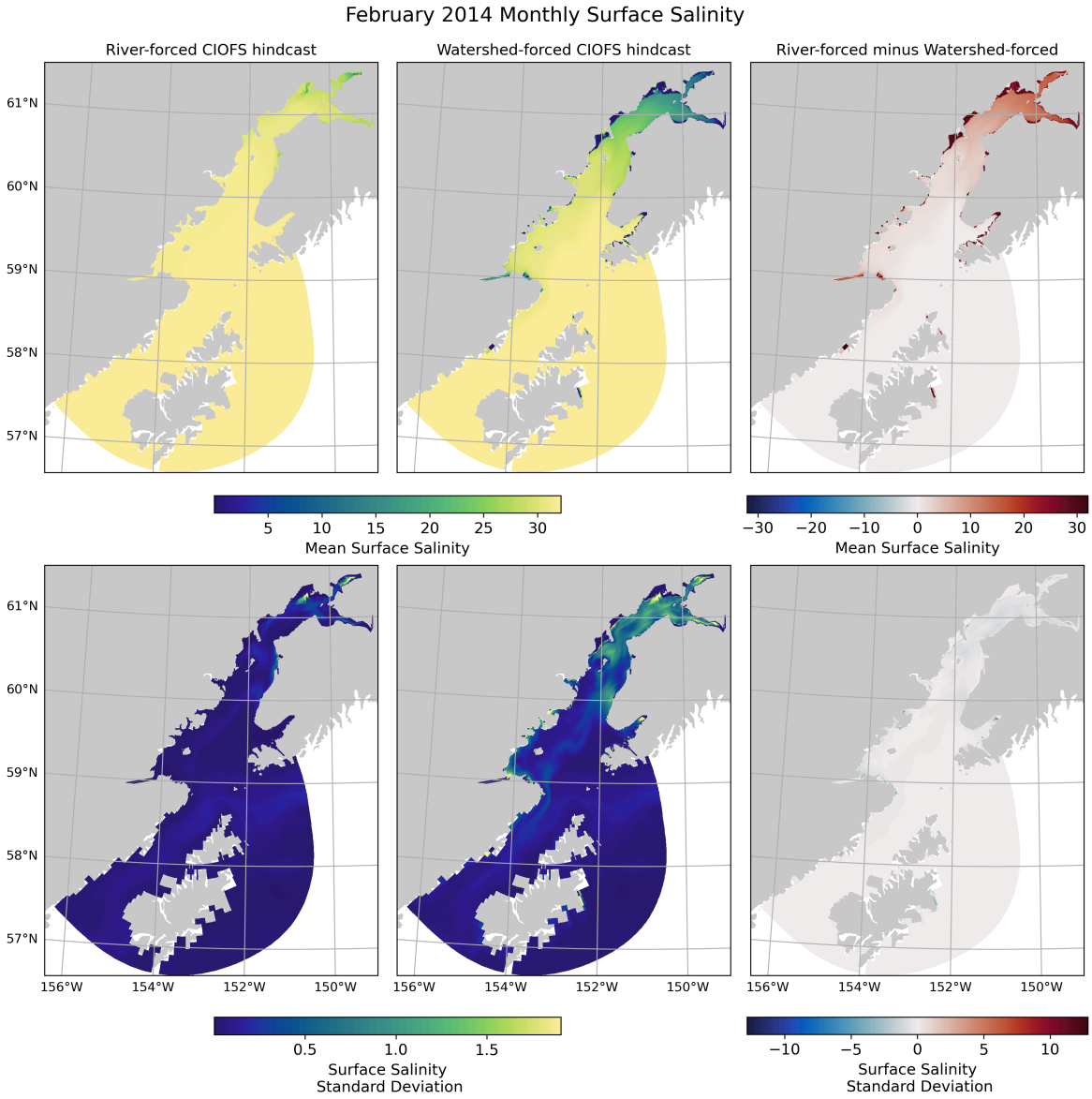

Fig. 3.1 Mean surface salinity between the USGS river-forced CIOFS model (left) and watershed model-forced CIOFS model (right) in February 2014.

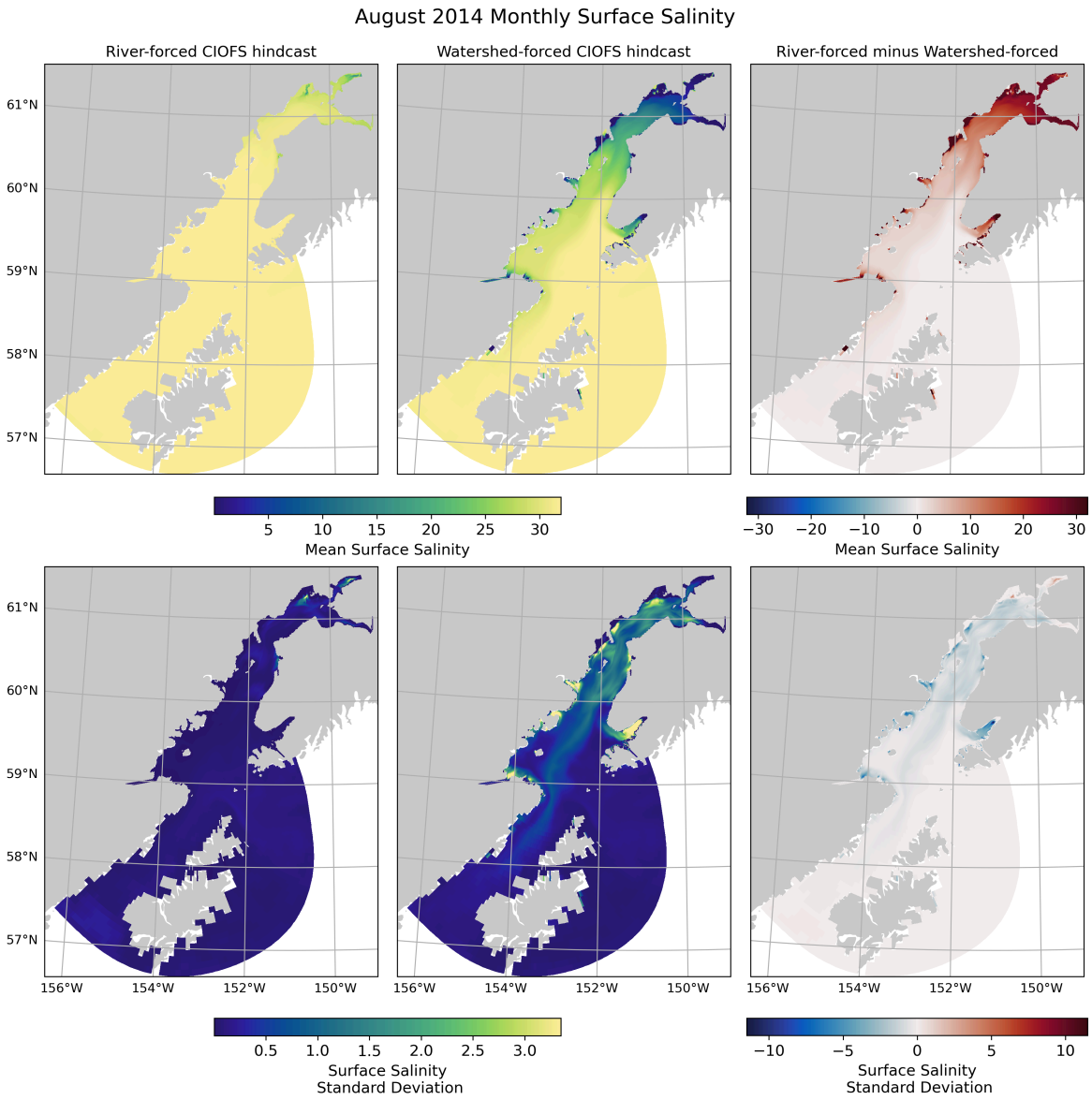

Fig. 3.2 Mean surface salinity between the USGS river-forced CIOFS model (left) and watershed model-forced CIOFS model (right) in August 2014.

4. Dataset Pages

4.1. Cook Inlet 2005 Current Survey

- Moored ADCP (NOAA): ADCP survey Cook Inlet 2005
- Moored NOAA ADCP surveys in Cook Inlet

ADCP data has been converted to eastward, northward velocities as well as along- and across-channel velocities, in the latter case using the NOAA-provided rotation angle for the rotation. The along- and across-channel velocities are additionally filtered to show the subtidal signal, which is what is plotted in the dataset page.

- Dataset description, link to page in CIOFS Hindcast report [TLFD23].
- Catalog page, link to page in GitHub repository documentation.

4.2. Cook Inlet 2002/2003/2004/2008/2012 Current Survey

- Moored ADCP (NOAA): ADCP survey Cook Inlet, multiple years
- Moored NOAA ADCP surveys in Cook Inlet

ADCP data has been converted to eastward, northward velocities as well as along- and across-channel velocities, in the latter case using the NOAA-provided rotation angle for the rotation. The along- and across-channel velocities are additionally filtered to show the subtidal signal, which is what is plotted in the dataset page.

- Dataset description, link to page in CIOFS Hindcast report [TLFD23].
- Catalog page, link to page in GitHub repository documentation.

4.3. Barabara to Bluff 2002-2003

- CTD transects: Barabara to Bluff
- Repeat CTD transect from Barabara to Bluff Point in Cook Inlet from 2002 to 2003.
- Dataset description, link to page in CIOFS Hindcast report [TLFD23].
- Catalog page, link to page in GitHub repository documentation.

4.4. CTD Transects 2004-2006 - CMI KBNERR

- CTD Transects, Moored CTD (CMI KBNERR): Six repeat, one single transect, one moored CTD
- Seasonality of Boundary Conditions for Cook Inlet, Alaska

During 2004 to 2006 we collected hydrographic measurements along transect lines crossing: 1) Kennedy Entrance and Stevenson Entrance from Port Chatham to Shuyak Island; 2) Shelikof Strait from Shuyak Island to Cape Douglas; 3) Cook Inlet from Red River to Anchor Point; 4) Kachemak Bay from Barbara Point to Bluff Point, and 5) the Forelands from East Foreland to West Foreland. During the third year we added two additional lines; 6) Cape Douglas to Cape Adams, and 7) Magnet Rock to Mount Augustine. The sampling in 2006 focused on the differences in properties during the spring and neap tide periods.

CTD profiles 2004-2005 - CMI UAF seems to be transect 5 of this project.

Part of the project: Seasonality of Boundary Conditions for Cook Inlet, Alaska Steve Okkonen Principal Investigator Co-principal Investigators: Scott Pegau Susan Saupe Final Report OCS Study MMS 2009-041 August 2009 Report: https://researchworkspace.com/files/39885971/2009_041.pdf

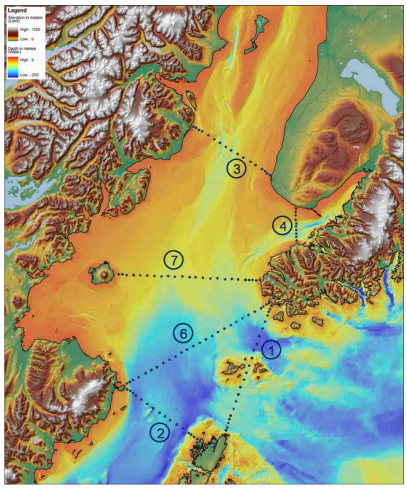

- Dataset description, link to page in CIOFS Hindcast report [TLFD23].
- Catalog page, link to page in GitHub repository documentation.

4.5. CTD profiles 2004-2005 - CMI UAF

- CTD Transect (CMI UAF): from East Foreland Lighthouse
- Seasonality of Boundary Conditions for Cook Inlet, Alaska: Transect (3) at East Foreland Lighthouse.

9 CTD profiles at stations across 10 cruises in (approximately) the same locations. Approximately monthly for summer months, 2004 and 2005.

Part of the project: Seasonality of Boundary Conditions for Cook Inlet, Alaska Steve Okkonen Principal Investigator Co-principal Investigators: Scott Pegau Susan Saupe Final Report OCS Study MMS 2009-041 August 2009 Report: https://researchworkspace.com/files/39885971/2009_041.pdf

- Dataset description, link to page in CIOFS Hindcast report [TLFD23].
- Catalog page, link to page in GitHub repository documentation.

4.6. CTD profiles 2012-2021 - GWA

- CTD Transects (GWA): Six repeat transects in Cook Inlet
- The Kachemak Bay Research Reserve (KBRR) and NOAA Kasitsna Bay Laboratory jointly work to complete oceanographic monitoring in Kachemak Bay and lower Cook Inlet, in order to provide the physical data needed for comprehensive restoration monitoring in the Exxon Valdez oil spill (EVOS) affected area. This project utilized small boat oceanographic and plankton surveys at existing KBRR water quality monitoring stations to assess spatial, seasonal and inter-annual variability in water mass movement. In addition, this work leveraged information from previous oceanographic surveys in the region, provided environmental information that aided a concurrent Gulf Watch benthic monitoring project, and benefited from a new NOAA ocean circulation model for Cook Inlet.

Surveys are conducted annually along five primary transects; two in Kachemak Bay and three in lower Cook Inlet, Alaska. Oceanographic data were collected via vertical CTD casts from surface to bottom, zooplankton and phytoplankton tows were made in the upper water column, and seabird and marine mammal observations were performed opportunistically. We also collect meteorological data and water quality measurements in Homer Harbor and Anchor Point year-round at stations as part of our National Estuarine Research Reserve (NERR) System-wide Monitoring program in Seldovia and Homer harbors, and in ice-free months at a mooring near the head of Kachemak Bay.

Project files and further description can be found here: https://gulf-of-alaska.portal.aoos.org/#metadata/4e28304c-22a1-4976-8881-7289776e4173/project

- Dataset description, link to page in CIOFS Hindcast report [TLFD23].
- Catalog page, link to page in GitHub repository documentation.

4.7. CTD profiles 2003-2006 - OTF KBNERR

- CTD Transect (OTF KBNERR): Repeated from Anchor Point
- CTD Transect Across Anchor Point, for GEM Project 030670.

This project used a vessel of opportunity to collect physical oceanographic and fisheries data at six stations along a transect across lower Cook Inlet from Anchor Point (AP) to the Red River delta each day during July. Logistical support for the field sampling was provided in part by the Alaska Department of Fish and Game which has chartered a drift gillnet vessel annually to fish along this transect providing inseason projections of the size of sockeye salmon runs entering Cook Inlet. This project funded collection of physical oceanographic data on board the chartered vessel to help identify intrusions of the Alaska Coastal Current (ACC) into Cook Inlet and test six hypotheses regarding effects of changing oceanographic conditions on migratory behavior and catchability of sockeye salmon entering Cook Inlet. In 2003-2007, a conductivity-temperature-depth profiler was deployed at each station. In 2003-2005, current velocities were estimated along the transect using a towed acoustic Doppler current profiler, and salmon relative abundance and vertical distribution was estimated using towed fisheries acoustic equipment.

Willette, T.M., W.S. Pegau, and R.D. DeCino. 2010. Monitoring dynamics of the Alaska coastal current and development of applications for management of Cook Inlet salmon - a pilot study. Exxon Valdez Oil Spill Gulf Ecosystem Monitoring and Research Project Final Report (GEM Project 030670), Alaska Department of Fish and Game, Commercial Fisheries Division, Soldotna, Alaska.

Report: https://evostc.state.ak.us/media/2176/2004-040670-final.pdf Project description: https://evostc.state.ak.us/restoration-projects/project-search/monitoring-dynamics-of-the-alaska-coastal-current-and-development-of-applications-for-management-of-cook-inlet-salmon-040670/

- Dataset description, link to page in CIOFS Hindcast report [TLFD23].
- Catalog page, link to page in GitHub repository documentation.

4.8. CTD time series UAF

- CTD Transects (UAF): Repeated in central Cook Inlet
- Observations of hydrography and currents in central Cook Inlet, Alaska during diurnal and semidiurnal tidal cycles

Surface-to-bottom measurements of temperature, salinity, and transmissivity, as well as measurements of surface currents (vessel drift speeds) were acquired along an east-west section in central Cook Inlet, Alaska during a 26-hour period on 9-10 August 2003. These measurements are used to describe the evolution of frontal features (tide rips) and physical properties along this section during semidiurnal and diurnal tidal cycles. The observation that the amplitude of surface currents is a function of water depth is used to show that strong frontal features occur in association with steep bathymetry. The positions and strengths of these fronts vary with the semidiurnal tide. The presence of freshwater gradients alters the phase and duration of tidal currents across the section. Where mean density-driven flow is northward (along the eastern shore and near Kalgin Island), the onset of northward tidal flow (flood tide) occurs earlier and has longer duration than the onset and duration of northward tidal flow where mean density-driven flow is southward (in the shipping channel). Conversely, where mean density-driven flow is southward (in the shipping channel), the onset of southward tidal flow (ebb tide) occurs earlier and has longer duration than the onset and duration of southward tidal flow along the eastern shore and near Kalgin Island.

Observations of hydrography and currents in central Cook Inlet, Alaska during diurnal and semidiurnal tidal cycles Stephen R. Okkonen Institute of Marine Science University of Alaska Fairbanks Report: https://www.circac.org/wp-content/uploads/Okkonen_2005_hydrography-and-currents-in-Cook-Inlet.pdf

- Dataset description, link to page in CIOFS Hindcast report [TLFD23].
- Catalog page, link to page in GitHub repository documentation.

4.9. CTD profiles 2005 - NOAA

- CTD Profiles (NOAA): across Cook Inlet
- CTD Profiles from NOAA.
- Dataset description, link to page in CIOFS Hindcast report [TLFD23].
- Catalog page, link to page in GitHub repository documentation.

4.10. Kachemak Kuletz 2005-2007

- CTD Profiles (Kachemak Kuletz 2005-2007)
- CTD Profiles in Cook Inlet
- Dataset description, link to page in CIOFS Hindcast report [TLFD23].
- Catalog page, link to page in GitHub repository documentation.

4.11. KB small mesh 2006

- CTD Profiles (KB small mesh 2006)

- CTD Profiles in Cook Inlet
- Dataset description, link to page in CIOFS Hindcast report [TLFD23].
- Catalog page, link to page in GitHub repository documentation.

4.12. Drifters: Ecosystems & Fisheries-Oceanography Coordinated Investigations (EcoFOCI)

- Drifters (EcoFOCI)
- EcoFOCI Project.

As described on the main project website for EcoFOCI:

> We study the ecosystems of the North Pacific Ocean, Bering Sea and U.S. Arctic to improve understanding of ecosystem dynamics and we apply that understanding to the management of living marine resources. EcoFOCI scientists integrate field, laboratory and modeling studies to determine how varying biological and physical factors influence large marine ecosystems within Alaskan waters.

> EcoFOCI is a joint research program between the Alaska Fisheries Science Center (NOAA/ NMFS/ AFSC) and the Pacific Marine Environmental Laboratory (NOAA/ OAR/ PMEL).

Drifter data are being pulled from this webpage: https://www.ecofoci.noaa.gov/drifters/efoci_drifterData.shtml which also has a plot available for each drifter dataset.

Several years of EcoFOCI drifter data are also available in a private Research Workspace project: https://researchworkspace.com/project/41531085/files.

- Catalog page, link to page in GitHub repository documentation.

4.13. Drifters (UAF), multiple projects

- Drifters (UAF)
- Drifters run by Mark Johnson and others out of UAF with various years and drogue depths.
- 2003: 7.5m (Cook Inlet)
- 2004: 5m (Cook Inlet)
- 2005: 5m, 80m (Cook Inlet)
- 2006: 5m (Cook Inlet)
- 2012: 1m (Cook Inlet), 15m (Cook Inlet)
- 2013: 1m (Cook Inlet), 15m (Cook Inlet)
- 2014: 1m (Cook Inlet)
- 2019: 1m (Kachemak Bay, Lynn Canal)
- 2020: 1m (Kachemak Bay, Lynn Canal)

Descriptive summary of later drifter deployment: https://www.alaska.edu/epscor/about/newsletters/May-2022-feature-current-events.php, data portal: https://ak-epscor.portal.axds.co/

- Catalog page, link to page in GitHub repository documentation.

4.14. HF Radar - UAF

- HF Radar (UAF)
- HF Radar from UAF.

Files are:

- Upper Cook Inlet (System A): 2002-2003 and 2009
- Lower Cook Inlet (System B): 2006-2007

Data variables available include tidally filtered and weekly averaged along with tidal constituents calculated from hourly data.

Several new datasets were derived in 2024 with the CIOFS freshwater project which narrow the full time datasets (lower-ci_system-B_2006-2007.nc and upper-ci_system-A_2002-2003.nc) in time to just 2003 and 2006, respectively, before running processing in Research Workspace and are otherwise identical. See processing notebook https://researchworkspace.com/file/44879475/add_variables_to_notebooks_limited_time_range.ipynb:

- lower-ci_system-B_2006_subtidal_daily_mean.nc
- lower-ci_system-B_2006_tidecons_base.nc
- lower-ci_system-B_2006_subtidal_weekly_mean.nc
- upper-ci_system-A_2003_subtidal_daily_mean
- upper-ci_system-A_2003_tidecons_base
- upper-ci_system-A_2003_subtidal_weekly_mean.nc

Some of the data is written up in reports:

- https://espis.boem.gov/final%20reports/5009.pdf
- https://www.govinfo.gov/app/details/GOVPUB-I-47b721482d69e308aec1cca9b3e51955

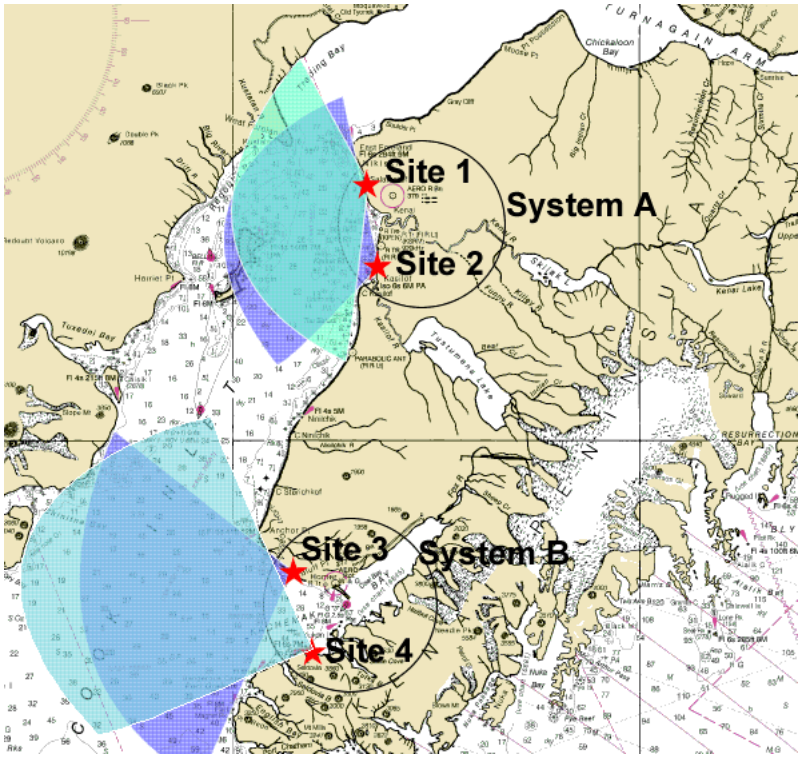

- Dataset description, link to page in CIOFS Hindcast report [TLFD23].
- Catalog page, link to page in GitHub repository documentation.

4.15. Moorings from Alaska Ocean Observing System (AOOS)/ Coastal Data Information Program (CDIP)

- Moorings (CDIP): Lower and Central Cook Inlet, Kodiak Island
- Moorings from AOOS/CDIP
- Dataset description, link to page in CIOFS Hindcast report [TLFD23].

- Catalog page, link to page in GitHub repository documentation.

4.16. Mooring from CIRCAC

- Mooring (CIRCAC): Central Cook Inlet Mooring
- Central Cook Inlet Mooring from: Seasonality of Boundary Conditions for Cook Inlet, Alaska

CIRCAC is the Cook Inlet Regional Citizens Advisory Council. It was funded by MMS (pre-BOEM), OCS Study MMS 2009-041 funneled through the Coastal Marine Institute (University of Alaska Fairbanks).

This mooring was damaged so it was removed.

Part of the project: Seasonality of Boundary Conditions for Cook Inlet, Alaska Steve Okkonen Principal Investigator Co-principal Investigators: Scott Pegau Susan Saupe Final Report OCS Study MMS 2009-041 August 2009 Report: https://researchworkspace.com/files/39885971/2009_041.pdf

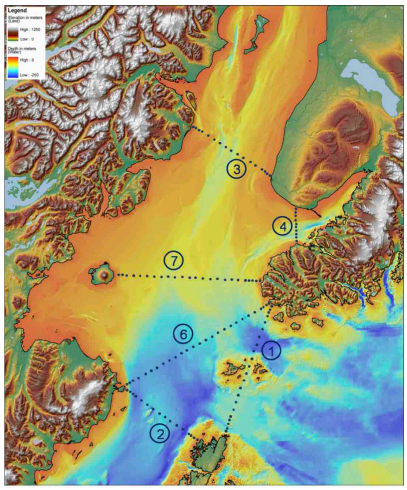

- Dataset description, link to page in CIOFS Hindcast report [TLFD23].
- Catalog page, link to page in GitHub repository documentation.

4.17. Moorings from Kachemak Bay National Estuarine Research Reserve (KBNERR)

- Moorings (KBNERR): Lower Cook Inlet Mooring
- Lower Cook Inlet Mooring from: Seasonality of Boundary Conditions for Cook Inlet, Alaska

CIRCAC is the Cook Inlet Regional Citizens Advisory Council. It was funded by MMS (pre-BOEM), OCS Study MMS 2009-041 funneled through the Coastal Marine Institute (University of Alaska Fairbanks).

Part of the project: Seasonality of Boundary Conditions for Cook Inlet, Alaska Steve Okkonen Principal Investigator Co-principal Investigators: Scott Pegau Susan Saupe Final Report OCS Study MMS 2009-041 August 2009 Report: https://researchworkspace.com/files/39885971/2009_041.pdf

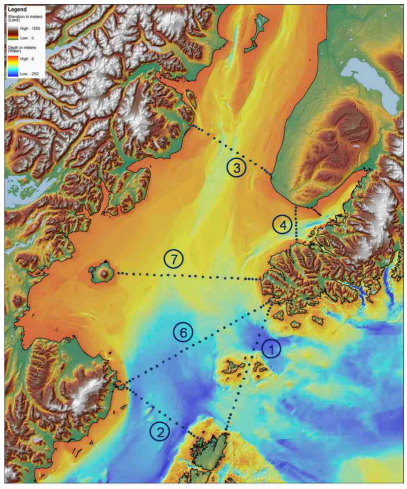

- Dataset description, link to page in CIOFS Hindcast report [TLFD23].
- Catalog page, link to page in GitHub repository documentation.

4.18. Moorings from Kachemak Bay National Estuarine Research Reserve (KBNERR)

- Moorings (KBNERR): Kachemak Bay: Bear Cove, Seldovia
- Moorings from Kachemak Bay National Estuarine Research Reserve (KBNERR)

Station mappings from AOOS/ERDDAP to KBNERR station list:

- nerrs_kacsdwq :: kacsdwq
- nerrs_kacsswq :: kacsswq
- cdmo_nerrs_bearcove :: This is a different station than kacbcwq, which was active 2002-2003 while this is in 2015. They are also in different locations.

More information: https://accs.uaa.alaska.edu/kbnerr/

- Dataset description, link to page in CIOFS Hindcast report [TLFD23].
- Catalog page, link to page in GitHub repository documentation.

4.19. Historical moorings from Kachemak Bay National Estuarine Research Reserve (KBNERR)

- Moorings (KBNERR): Historical, Kachemak Bay
- Historical moorings from Kachemak Bay National Estuarine Research Reserve (KBNERR)

More information: https://accs.uaa.alaska.edu/kbnerr/

- Dataset description, link to page in CIOFS Hindcast report [TLFD23].
- Catalog page, link to page in GitHub repository documentation.

4.20. Moorings from Kachemak Bay National Estuarine Research Reserve (KBNERR)

- Moorings (KBNERR): Kachemak Bay, Homer stations
- Moorings from Kachemak Bay National Estuarine Research Reserve (KBNERR)

Station mappings from AOOS/ERDDAP to KBNERR station list:

- nerrs_kachdwq :: kachdwq

- homer-dolphin-surface-water-q :: kachswq
- nerrs_kach3wq :: kach3wq

More information: https://accs.uaa.alaska.edu/kbnerr/

- Dataset description, link to page in CIOFS Hindcast report [TLFD23].
- Catalog page, link to page in GitHub repository documentation.

4.21. Moorings from NOAA

- Moorings (NOAA): across Cook Inlet
- Moorings from NOAA

Geese Island, Sitkalidak Island, Bear Cove, Anchorage, Kodiak Island, Alitak, Seldovia, Old Harbor, Boulder Point, Albatross Banks, Shelikof Strait

- Dataset description, link to page in CIOFS Hindcast report [TLFD23].
- Catalog page, link to page in GitHub repository documentation.

4.22. Moorings from University of Alaska Fairbanks (UAF)

- Moorings (UAF): Kodiak Island, Peterson Bay
- Moorings from UAF
- Dataset description, link to page in CIOFS Hindcast report [TLFD23].
- Catalog page, link to page in GitHub repository documentation.

5. Model Assessment Summary

A summary of the model comparisons with the data variables is given in this section. The “Overview” pages have Taylor diagrams and plots that show the skill score as a summary metric from each model-data comparison shown in the subpages (see Methodology).

The previous report [TLFD23] demonstrated that the CIOFS Hindcast model does not having enough freshwater input into the system to have realistic salinity variability, nor accurate salinity. The CIOFS Hindcast model performs better for other variables. The major seasonal sea water temperature signal is well-captured, though temperature anomaly is not. CIOFS Hindcast captures the tidal sea surface height well, and mostly does well at subtidal sea surface height as well. It also captures horizontal speed reasonably well.

Next we will summarize how the CIOFS Hindcast and CIOFS Freshwater models perform when compared with the data across these variables. See Methodology for how to read in the individual model-data comparison figures.

5.1. Salinity

The CIOFS Freshwater model is forced with freshwater accounting for the whole watershed, and the amount of freshwater input into the model is much higher than is input into the CIOFS Hindcast model (see details in Model Descriptions). Given this, we can expect there to be much fresher water in the salinity field compared to the CIOFS Hindcast.

The salinity field is captured much better by CIOFS Freshwater than CIOFS Hindcast when looking at CTD transects (see Fig. 8.3). For example, whereas a CIOFS Hindcast CTD transect (Fig. 5.1) is nearly uniformly salty, the equivalent CIOFS Freshwater transect (Fig. 5.2) has good horizontal variability and some vertical variability.

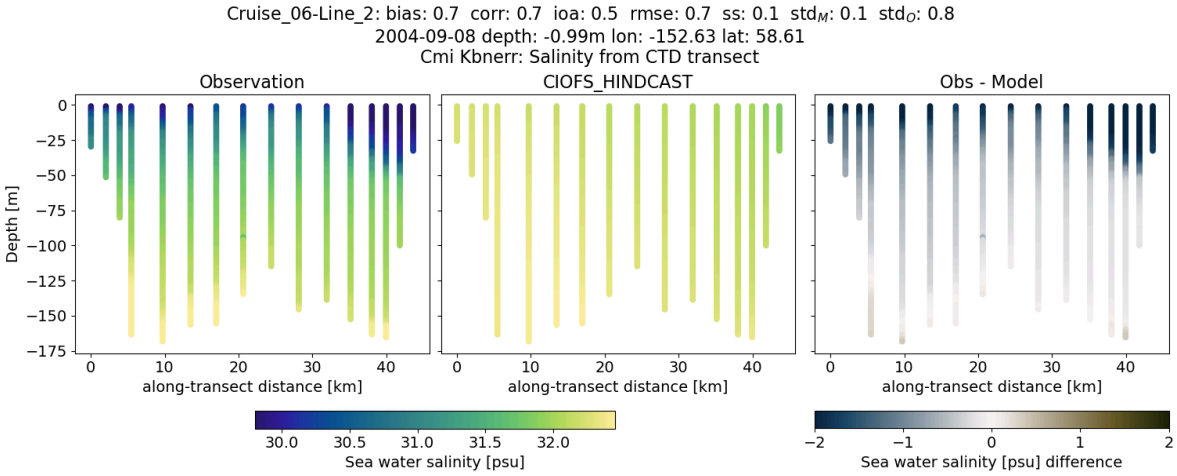

Fig. 5.1 Example of CIOFS Hindcast CTD transect comparison with salinity data (from the CMI KBNERR project of repeated transects across Cook Inlet).

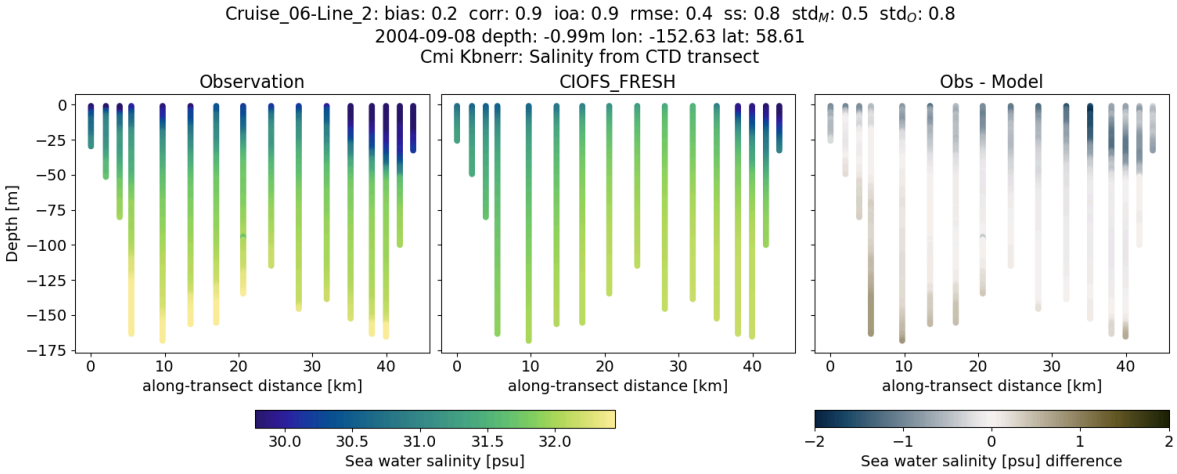

Fig. 5.2 Example of CIOFS Freshwater CTD transect comparison with salinity data (from the CMI KBNERR project of repeated transects across Cook Inlet).

Similarly, a CIOFS Hindcast along-bay CTD transect (Fig. 5.3) is nearly uniformly salty, while the equivalent CIOFS Freshwater transect (Fig. 5.4) has good horizontal variability and vertical variability, though the water is still too salty.

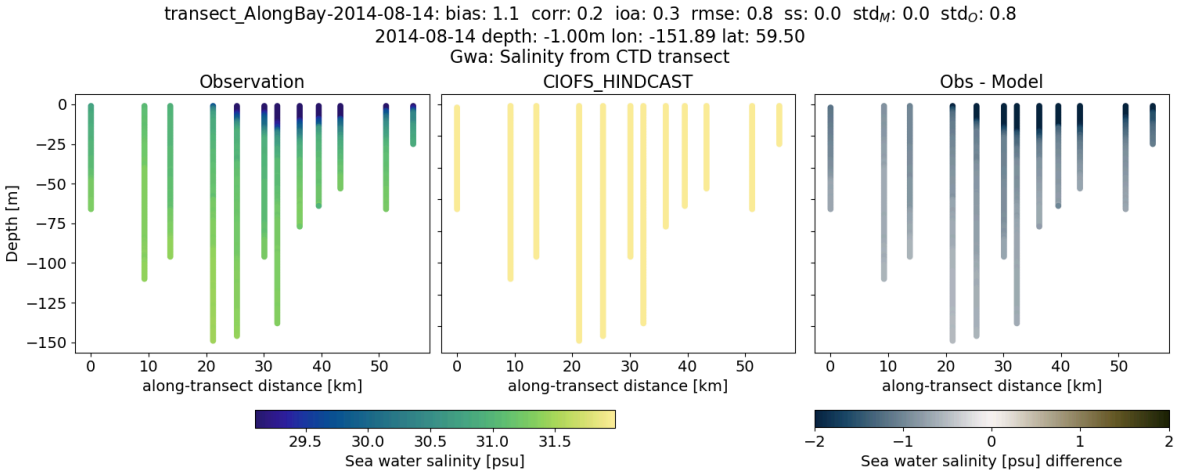

Fig. 5.3 Example of CIOFS Hindcast CTD transect comparison with salinity data (from the GWA project of repeated transects across Cook Inlet).

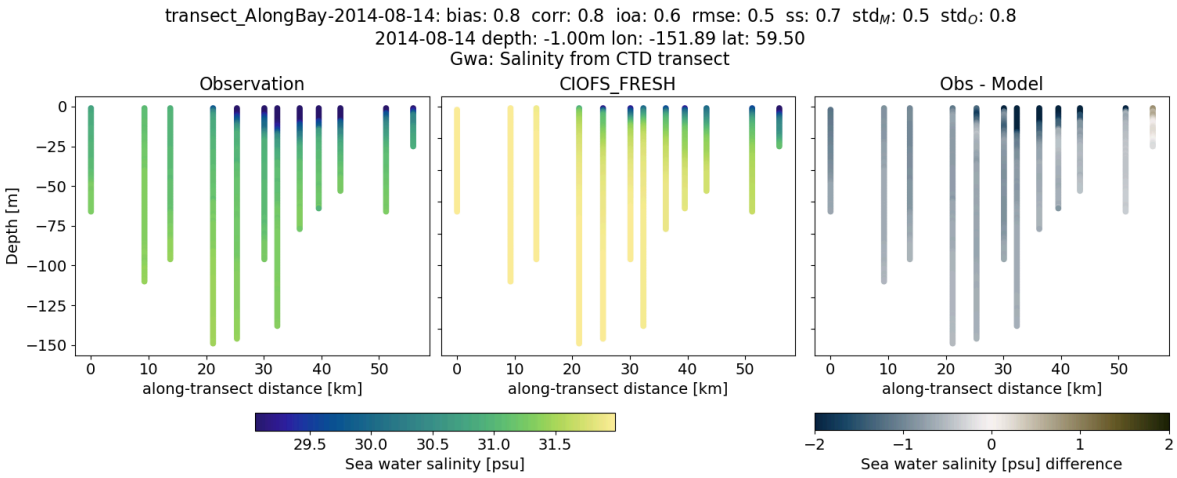

Fig. 5.4 Example of CIOFS Freshwater CTD transect comparison with salinity data (from the GWA project of repeated transects across Cook Inlet).

Looking at CTD profiles, CIOFS Freshwater has both better correlation and improved variance over CIOFS Hindcast (see Fig. 9.3). Salinity profiles in Kachemak Bay are better in CIOFS Freshwater. In the example profiles below, CIOFS Hindcast has a well-mixed profile that is salty whereas CIOFS Freshwater has a more realistic, fresh surface layer.

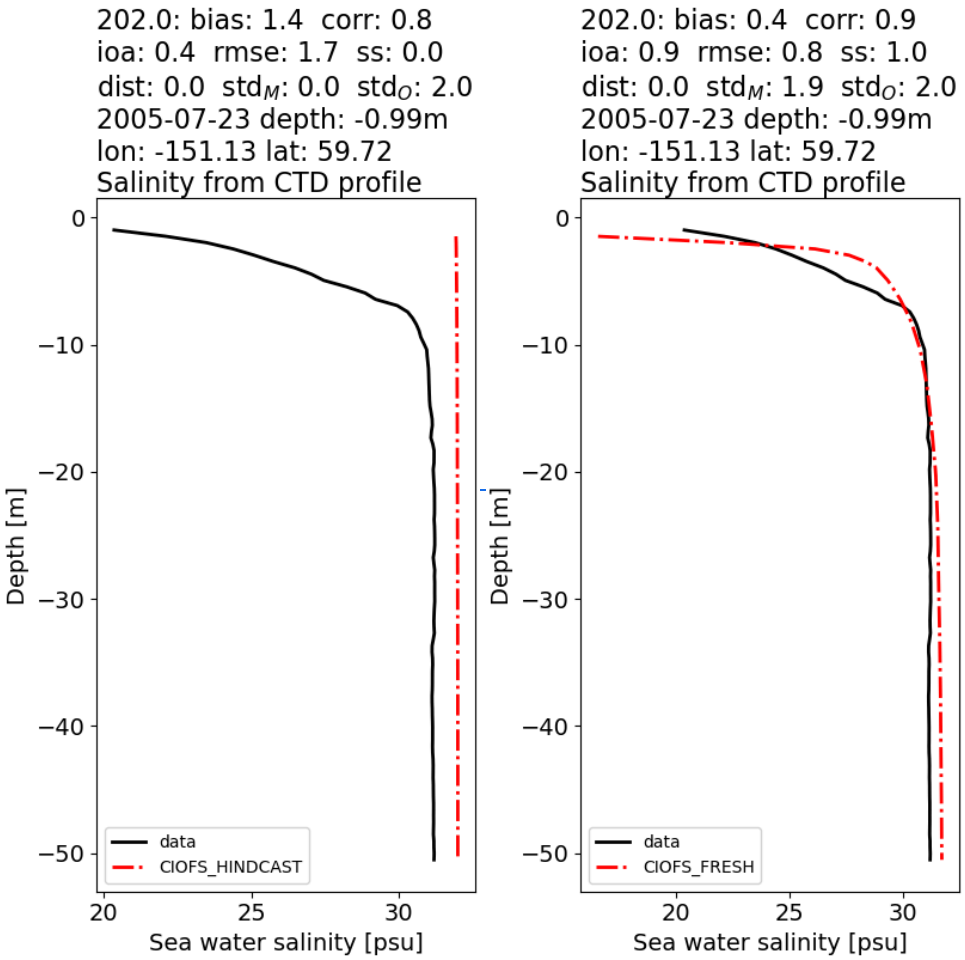

Salinity time series are not well-represented by either model (see Fig. 7.5). While we find some improved skill score for CIOFS Freshwater, primarily we find substantially more variability as compared with CIOFS Hindcast. For example, this is noticeable at a deep mooring where the subtidal salinity time series from CIOFS Hindcast across a year is relatively constant (Fig. 5.5) but the additional freshwater leads to increased variability in the CIOFS Freshwater model (Fig. 5.6), though not much improved skill score (0.3 vs 0.1).

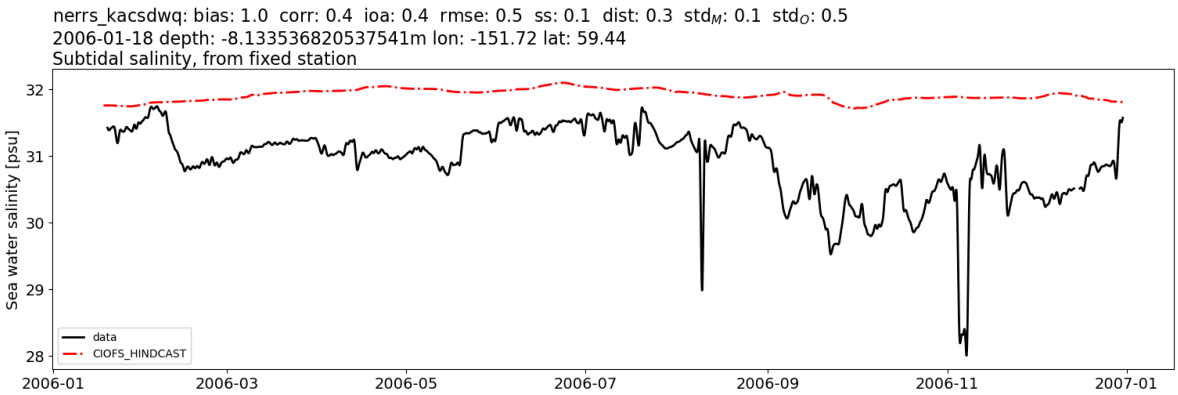

Fig. 5.5 Example of CIOFS Hindcast deep water subtidal time series comparison with salinity data (Station `nerrs-kacsdwq`).

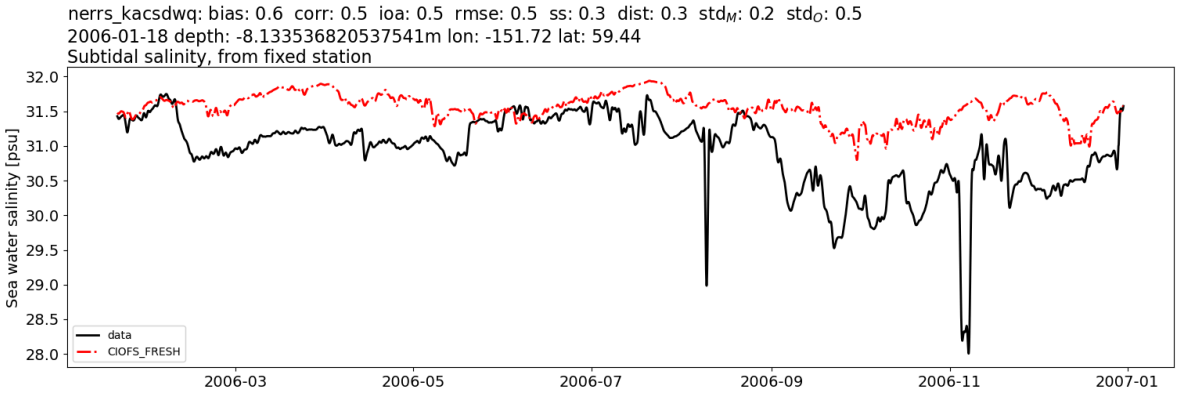

Fig. 5.6 Example of CIOFS Freshwater deep water subtidal time series comparison with salinity data (Station `nerrs-kacsdwq`).

5.2. Currents

The currents are mostly captured similarly for the two models for HF Radar and ADCP data, though generally the subtidal time series from CIOFS Fresh have improved variance.

However, comparisons between *in situ* drifters and numerical particle simulations show differences between the models depending on the area and depth of the domain in which the drifter was traveling. The EcoFOCI drifters mostly traveled outside of Cook Inlet in the Gulf of Alaska where differences in freshwater due to the improved freshwater forcing in CIOFS Freshwater are minimal. Accordingly, the particle simulations and skill scores there are similar between the two models. These and deeper UAF drifter results can particularly be seen in the overview plots at 15m and 40m depth (see salinity profile above for variability with depth for example).

The UAF drifters are in Cook Inlet where freshwater is potentially an important feature, and they were run at multiple depths. The rest of the UAF drifters besides those run at 15m depth were run at 7.5, 5, and 1m depth, and with shallower depth there is increasing difference between the CIOFS Hindcast and CIOFS Freshwater particle simulations as the freshwater takes on a more important role. For example, the CIOFS Hindcast 1m particles (Fig. 5.7) are limited in transport compared to the CIOFS Freshwater particles (Fig. 5.8), which travel much farther through the Inlet with the freshwater present in the system. The CIOFS Freshwater particles are much more accurate than the CIOFS Hindcast particles.

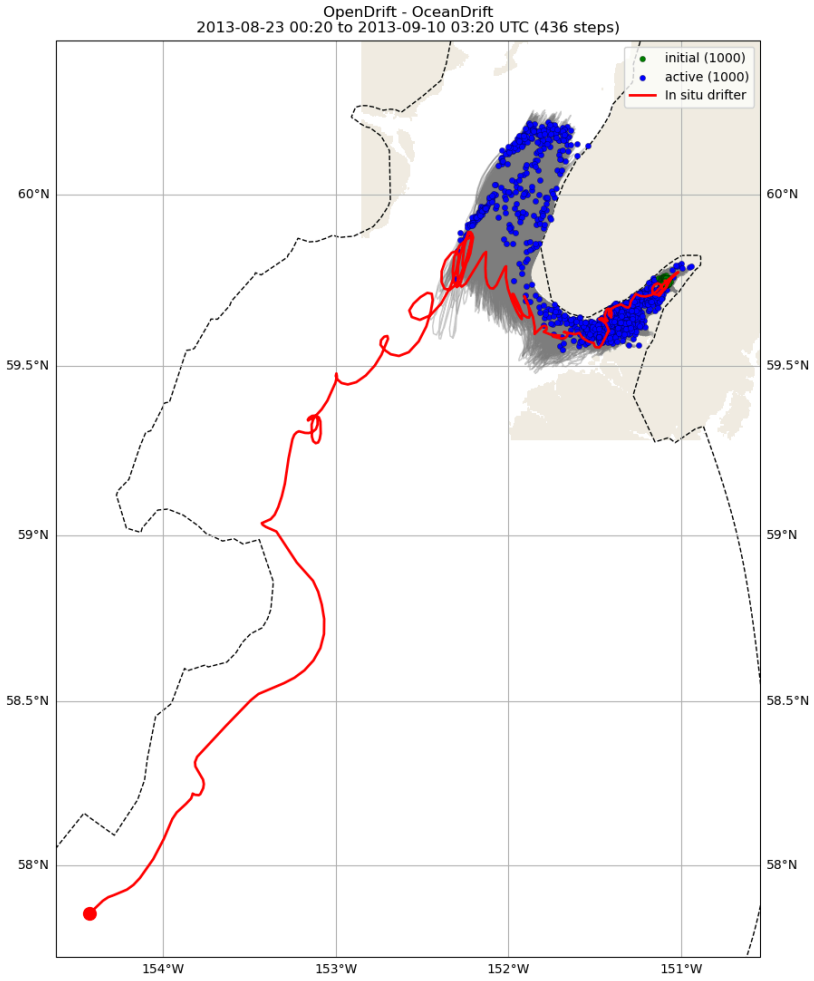

Fig. 5.7 Example of CIOFS Hindcast 1m drifter and particle simulations (drifter `CIDrifter0008Y2013_MicrostarSurfaceAt1M_deployment4`).

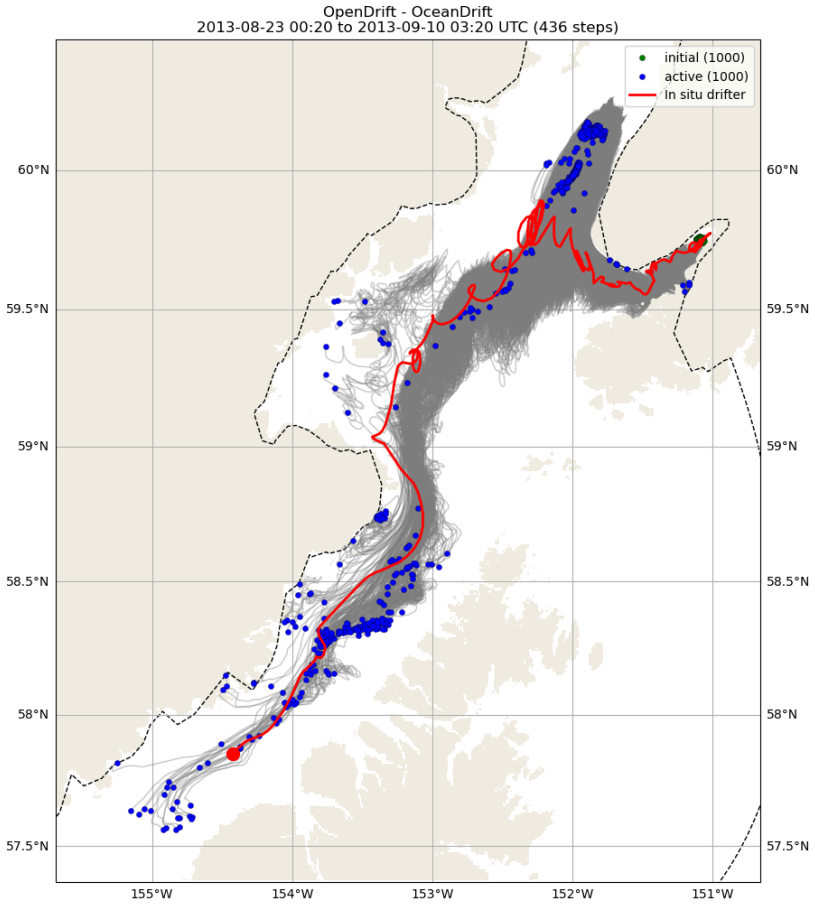

Fig. 5.8 Example of CIOFS Freshwater 1m drifter and particle simulations (drifter `CIDrifter0008Y2013_MicrostarSurfaceAt1M_deployment4`).

5.3. Temperature

The seasonal temperature range is relatively easy to capture by a numerical model, and both the CIOFS Hindcast and Freshwater models often capture the full tidal or subtidal temperature time series shown in the moorings data. However, they do have differences. While the CIOFS Hindcast model has the full seasonal temperature range at the head of the Inlet (NOAA 9455920, Fig. 5.9) and the south end of Kodiak Island (NOAA 9457804), it is a bit too cool relative to the data in the summer west of Kodiak Island (WMO 46077) and in the spring and summer east of Kodiak Island (NOAA 9457292). In Kachemak Bay, the CIOFS Hindcast model is more likely to be somewhat cold relative to the data throughout the year at the surface (Fig. 5.10) and at depth (Fig. 5.11), except in the summer.

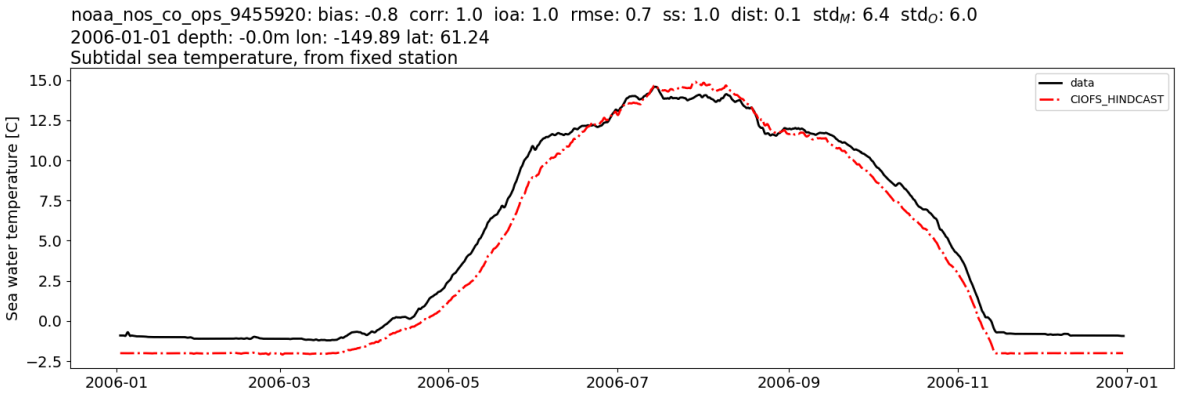

Fig. 5.9 Example of CIOFS Hindcast surface water subtidal time series comparison at the head of the Inlet with temperature data (Station `noaa_nos_co_ops_9455920`).

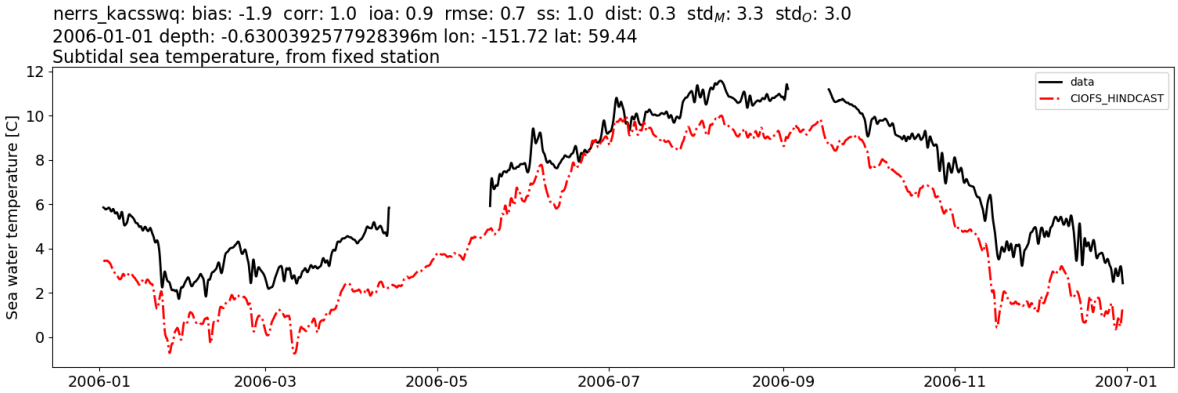

Fig. 5.10 Example of CIOFS Hindcast surface water subtidal time series comparison in Kachemak Bay with temperature data (Station `nerrs_kacsswq`).

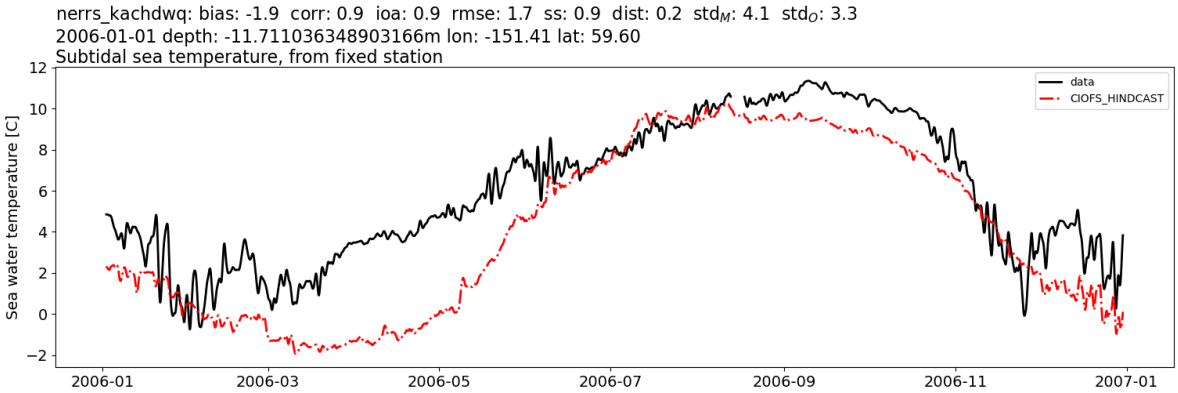

Fig. 5.11 Example of CIOFS Hindcast deep water subtidal time series comparison in Kachemak Bay with temperature data (Station `nerrs_kachdwq`).

CIOFS Freshwater shows consistently low temperatures in the subtidal temperature signal across the year in the same locations shown for CIOFS Hindcast: NOAA 9455920 (Fig. 5.12), Kachemak Bay surface (Fig. 5.13), and Kachemak Bay deep (Fig. 5.14).

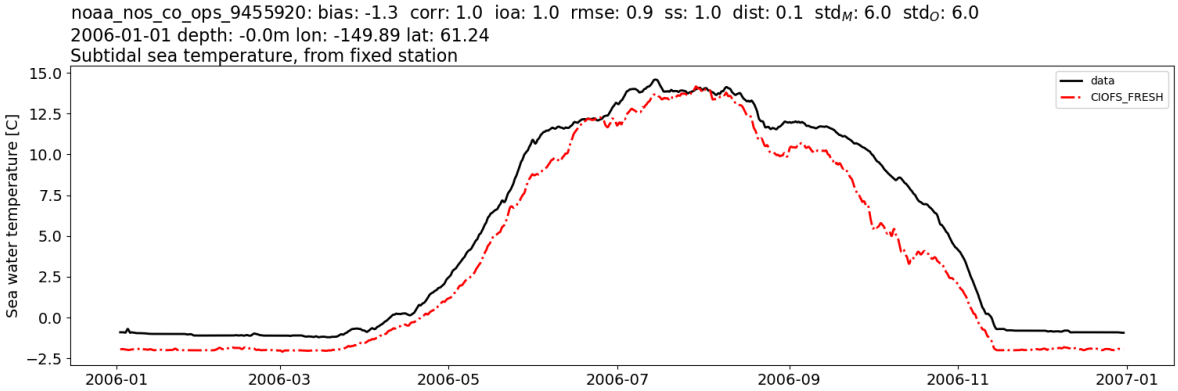

Fig. 5.12 Example of CIOFS Freshwater surface water subtidal time series comparison at the head of the Inlet with temperature data (Station `noaa_nos_co_ops_9455920`).

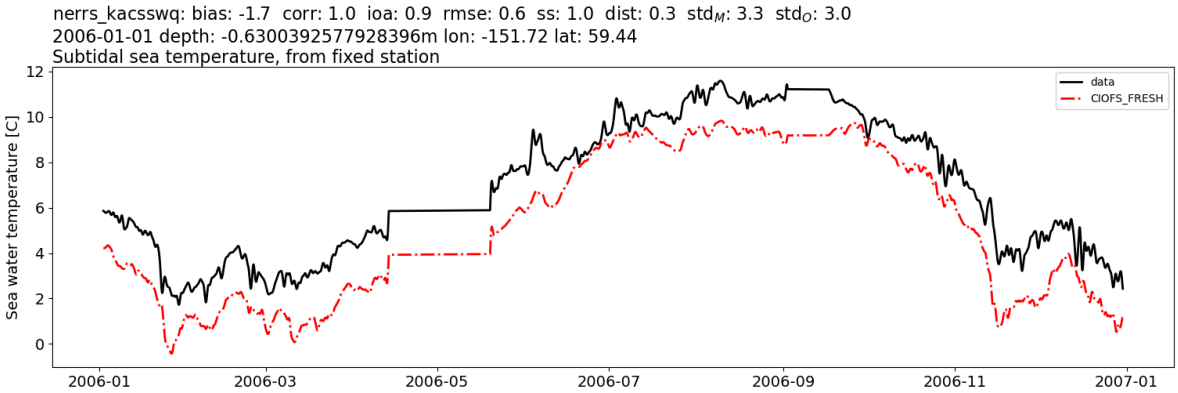

Fig. 5.13 Example of CIOFS Freshwater surface water subtidal time series comparison in Kachemak Bay with temperature data (Station `nerrs_kacsswq`).

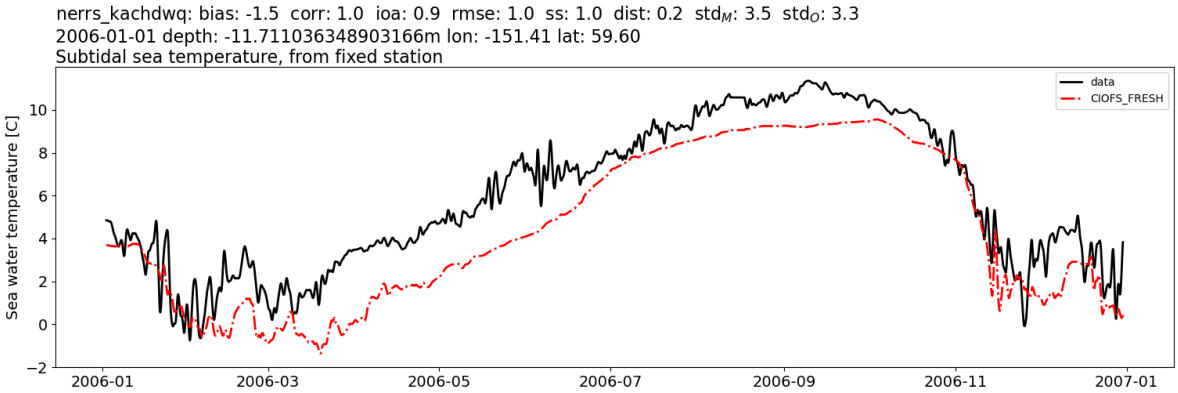

Fig. 5.14 Example of CIOFS Freshwater deep water subtidal time series comparison in Kachemak Bay with temperature data (Station `nerrs_kachdwq`).

CIOFS Freshwater saw some small improvement in the difficult measure of temperature anomaly. For example, showing the same year as the other examples, whereas CIOFS Hindcast demonstrates only moderate skill in this measure with a skill score of 0.6, CIOFS Freshwater has 0.9 and visually follows the trend of the data through the year.

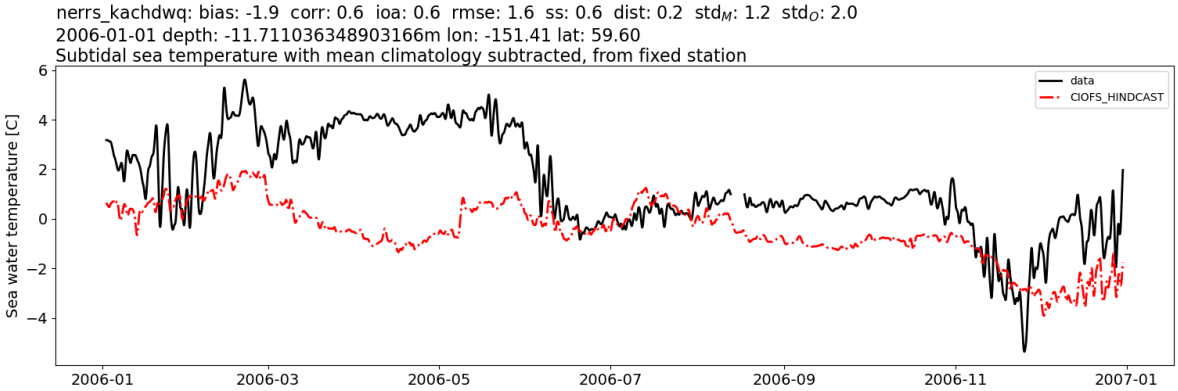

Fig. 5.15 Example of CIOFS Freshwater deep water subtidal temperature anomaly time series comparison in Kachemak Bay with temperature data (Station `nerrs_kachdwq`).

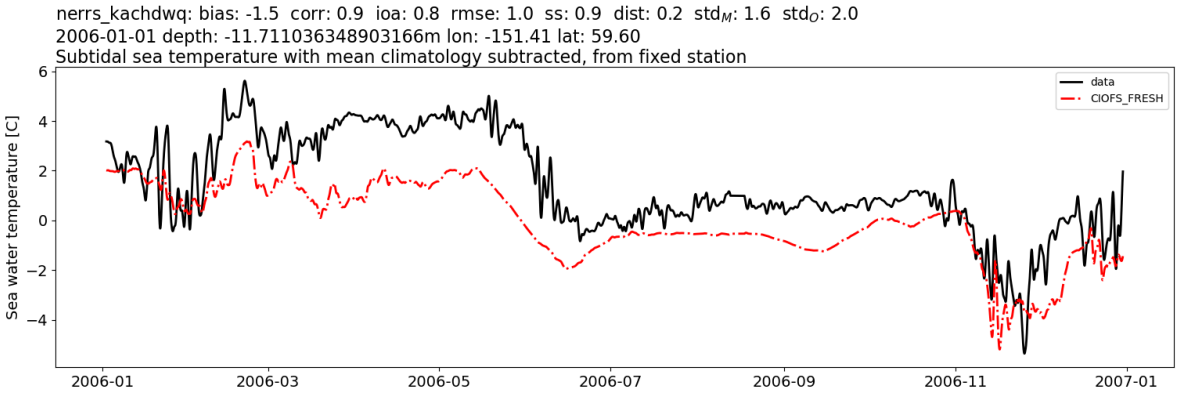

Fig. 5.16 Example of CIOFS Freshwater deep water subtidal temperature anomaly time series comparison in Kachemak Bay with temperature data (Station `nerrs_kachdwq`).

CTD transects for temperature are similar between CIOFS Hindcast and CIOFS Freshwater, but CIOFS Freshwater does perform better, as seen in Figs. 8.3 and 8.4.

5.4. Sea Surface Height

Both models capture the tidal sea surface height well. CIOFS Freshwater represents the subtidal sea surface height more accurately than CIOFS Hindcast (Fig. 7.3), and the highest skill scores are at station 9455920 near Anchorage. However, note an important difference in how the CIOFS Freshwater model is able to capture peaks in a way that the CIOFS Hindcast model is not. CIOFS Hindcast for an example year at this station (Fig. 5.17) shows subtidal variability, but it misses most unique peaks and troughs. CIOFS Freshwater (Fig. 5.18) captures many of these, implying that these peaks and troughs are due to freshwater input.

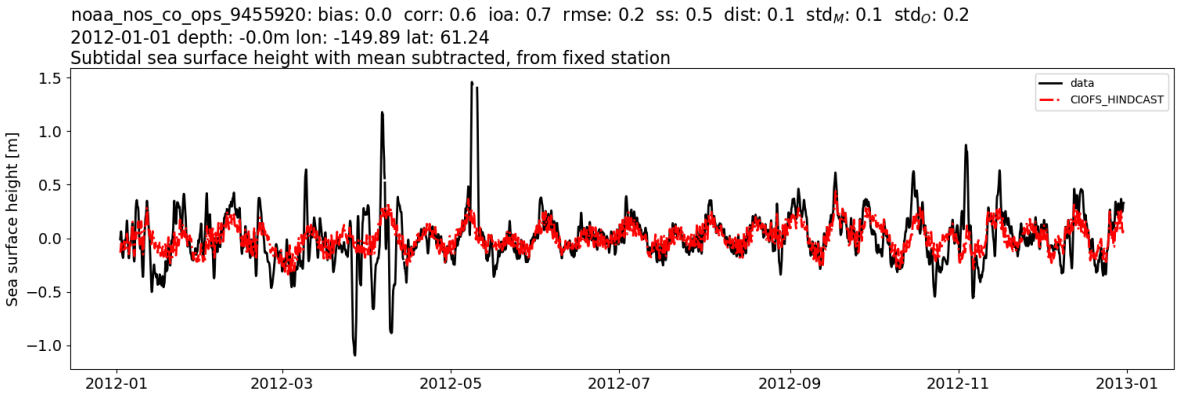

Fig. 5.17 Example of CIOFS Hindcast subtidal time series comparison with sea surface height data (Station `noaa_nos_co_ops_9455920`).

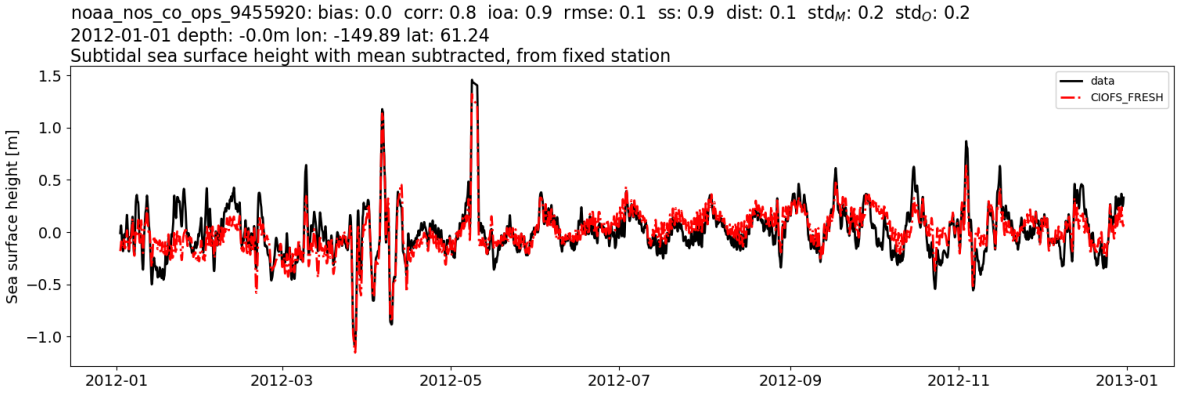

Fig. 5.18 Example of CIOFS Freshwater subtidal time series comparison with sea surface height data (Station `noaa_nos_co_ops_9455920`).

6. Methodology

6.1. Software

The datasets are compared with model output from the CIOFS and NWGOA models using the `ocean-model-skill-assessor` (`OMSA`) framework, as well as dependencies therein and software written for this report. Detailed documentation is available for OMSA.

6.2. Taylor Diagram

Taylor diagrams are used to summarize in one diagram several pieces of information about how accurately a model captures the behavior in a set of observations [Tay01]. They directly represent the correlation coefficient and the standard deviation of the model and observations, and due to geometric relationships, also the root mean squared error. Taylor diagrams are used to demonstrate the overall performance of the models in this study by concatenating all comparisons of a type (e.g., all CTD transects) and calculating the metrics to use in the diagram using the single concatenated model and data representations. The Taylor Diagram uses code from Copin [Cop12].

6.2.1. By Region

We split Cook Inlet into regions to give some spatial information in the region-based Taylor diagrams. The resulting regions are shown in Fig. 6.1.

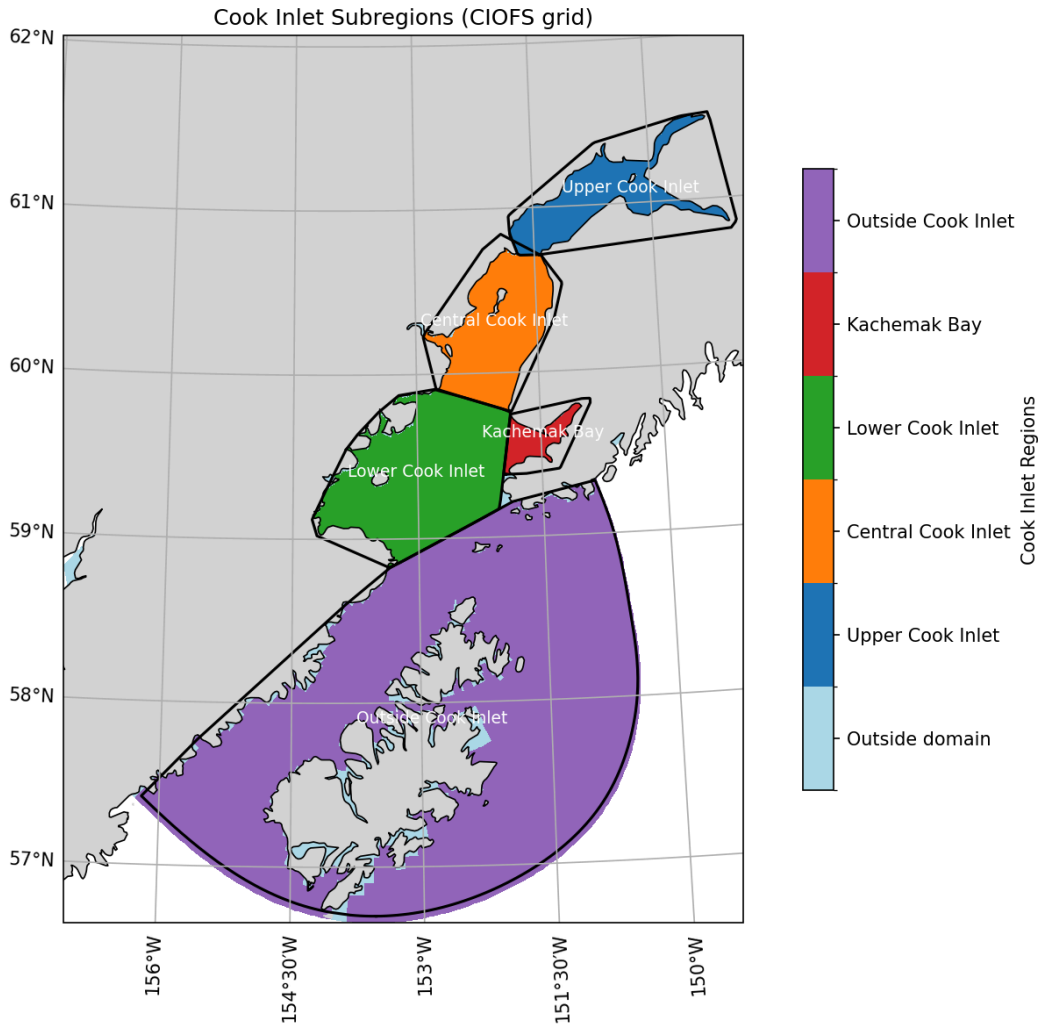

Fig. 6.1 Cook Inlet, split into named regions for analysis.

6.2.2. By Season

We split the year into seasons for grouping by time, defined as follows:

- Winter: December through March
- Spring: April and May
- Summer: June through August
- Fall: September through November

6.3. Comparison Metrics

Multiple statistical measures of the model-data comparison are given, though skill score is used as the main overview measure. To compare model and data output, the model output was interpolated in time and space to match the data.

6.3.1. All Metrics

The available statistical metrics are:

- Bias
- Correlation coefficient
- Index of agreement

- Root mean square error (RMSE)
- Skill score (SS)

6.3.2. Bias

The bias (the mean of the difference) is defined as:

$$\text{Bias} = \frac{1}{N}\sum_{i=1}^{N}(M_i - O_i),$$

where M_i is the model value at index i, O_i is the corresponding observation, and N is the total number of paired samples. A positive bias indicates the model overestimating the observations and a negative bias represents the model underestimating the observations.

6.3.3. Correlation Coefficient

The correlation coefficient [Pea95] is defined as:

$$r = \frac{\sum_{i=1}^{N}\left(M_i-\overline{M}\right)\left(O_i-\overline{O}\right)}{\sqrt{\sum_{i=1}^{N}\left(M_i-\overline{M}\right)^2}\sqrt{\sum_{i=1}^{N}\left(O_i-\overline{O}\right)^2}}$$

where M_i is the model value at index i, O_i is the corresponding observation, $\overline{M}$ is the mean of the model values, $\overline{O}$ is the mean of the observations, and N is the total number of paired samples. The correlation coefficient measures how much the model follows the temporal patterns of the observations and ranges from -1 (exactly negative linear relationship) to 1 (exactly positive linear relationship). Note that a model can have a correlation coefficient of 1 but still have a large bias.

6.3.4. Index of Agreement

The index of agreement Willmott [Wil81] is defined as:

$$d = 1 - \frac{\sum_{i=1}^{N}(M_i-O_i)^2}{\sum_{i=1}^{N}\left(\left|M_i-\overline{O}\right|+\left|O_i-\overline{O}\right|\right)^2}$$

where M_i is the model value at index i, O_i is the corresponding observation, $\overline{O}$ is the mean of the observations, and N is the total number of paired samples. The index of agreement measures both the pattern and magnitude of the model as compared with the observations, and ranges from 0 (no agreement) to 1 (perfect agreement). Because it measures both magnitude and patterns, it is a useful combined metrics, but it is harder to interpret than a single metric like correlation and it is sensitive to outliers.

6.3.5. Root Mean Squared Error (RMSE)

The root mean squared error (RMSE) is defined as:

$$\text{RMSE} = \sqrt{\frac{1}{N}\sum_{i=1}^{N}(M_i - O_i)^2},$$

where M_i is the model value at index i, O_i is the observation, and N is the total number of paired samples. The RMSE represents the model error relative to the observations, and is sensitive to outliers.

6.3.6. Skill score

Taylor suggests a skill score SS in Taylor [Tay01] that combines the information in the Taylor diagram to represent model skill with a single value:

$$S = \frac{4(1+r)^4}{\left(\frac{\sigma_m}{\sigma_o}+\frac{1}{\sigma_m/\sigma_o}\right)^2(1+r_0)^4}$$

where σ_m is the standard deviation of the model, σ_o is the standard deviation of the observations, r is the correlation coefficient between the model and observations, and r_0 is the maximum attainable correlation coefficient (often taken as 1). The maximum attainable correlation coefficient accounts for the fact that variability inherent in the system means that no two models will ever be exactly the same without the exact same forcing. The skill score is 1 when the model variance is the same as the observational variance and there is perfect correlation, and can be down to -1 for negative correlation values.

6.4. Details of comparisons

6.4.1. Units

Variable	Unit
Sea water temperature	Deg Celsius
Sea water salinity	PSU
Sea surface height	m
Along/across-channel velocity	m/s
Speed	m/s

6.4.2. Comparisons shown

One or more of the following time series modifications is used where noted to alter the data and model time series before comparison. Detailed explanations of each are given below, and which have been used are noted for each model-data comparison.

6.4.2.1. Tidal filtering

The tides are an important feature of Cook Inlet, and if we do not remove them from the time series we want to compare, they will dominate the model-data comparisons. Because the tides have a highly correlated signal, comparing time series with them intact from moment to moment gives a skewed comparison; if the model-data comparison at one time is close, it probably will also be at the next time. A better way to compare the model and data in a regime like this is by first filtering out the tides; we use the `pl33` filter to do so. We filter out the tides for most model-data comparisons presented here, though if a sea surface height time series is relatively short, we left it with tides to show the full comparison.

6.4.2.2. Long time series

Long time series of temperature or salinity tend to have significant annual cycles. In a similar way to the tides, this can skew the meaning of our statistical metrics because, for example, the large, expected temperature cycle dominates any smaller features. Because of this, we present long time series of temperature and salinity as the anomaly with respect to the monthly mean calculated from the data time series across the available years. We will often also show the comparisons without removing the monthly mean to help give an intuitive feel for how the model is behaving with respect to the data.

6.4.2.3. Mean subtracted

Numerical ocean models tend to not have a specific vertical datum that they are calculated with respect to. For this reason, when the sea surface height is compared between model and data, the mean of each is separately subtracted from the time series before comparison.

6.4.2.4. Harmonic tidal analysis

Harmonic tidal analysis was run to calculated tidal constants with the HF Radar data. We ran a Python version of the classic Matlab package T_Tide [PBL02].

6.5. How to read a model-data figure

Consider the example model-data comparison in Fig. 6.2 for a year of mooring data. The title contains a lot of information:

- station identifier
- statistical metric values
  - bias
  - correlation coefficient (“corr”)
  - index of agreement (“ioa”)
  - root mean squared error (“rmse”)
  - skill score (“ss”)
  - distance of model grid-node from actual data location, if relevant (“dist”)
  - standard deviation of the model and observations (std_M, std_O)
- date or start date of observations
- depth or first depth
- longitude and latitude location (“lon” and “lat”)
- descriptive title

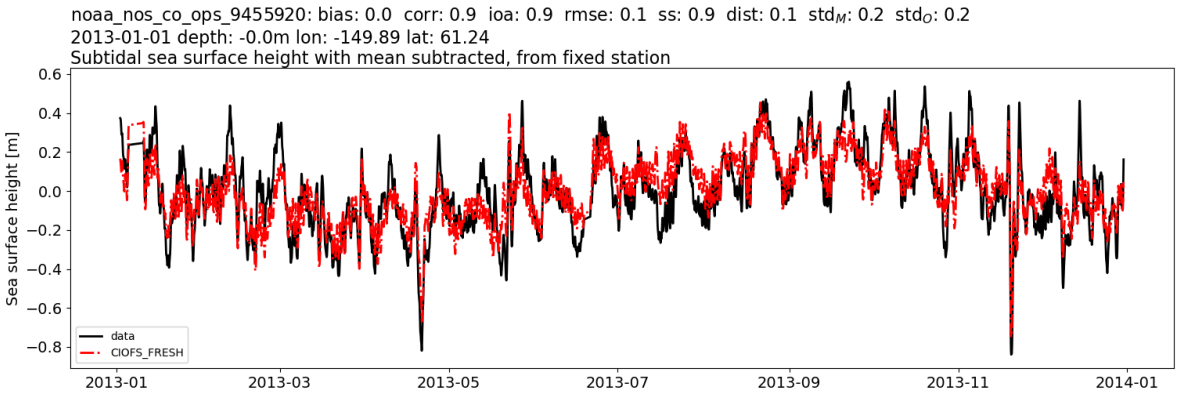

Fig. 6.2 Example of CIOFS Freshwater subtidal time series comparison with sea surface height data (Station `noaa_nos_co_ops_9455920`).

7. Overview Mooring Data

In the map below, some stations are at the same or nearly same location, in which case the marker representing their location is shifted slightly to allow for both to be seen. Datasets that span more than 1 year are represented by the number of years they span: one marker per year. By necessity these markers are moved in space from the actual station location and arranged into a grid so they can all be seen. Therefore, their locations in the skill score plots do not represent their actual locations.

The skill scores below represent the skill of each model by variable and processing listed. The models perform similarly for sea surface height: they capture the tidal signal well and the subtidal signal less well, though some improvement is noticeable for CIOFS fresh as compared with CIOFS hindcast for the subtidal sea surface height. The models perform similarly for temperature; they capture the tidal and subtidal seasonal cycles and do moderately well on the subtiddal temperature with the monthly anomaly subtracted. For salinity, CIOFS fresh shows moderate improvement over CIOFS hindcast.

91MB zipfile of plots and stats files

7.1. Map of Stations

Fig. 7.1 All mooring stations, by project. Click on a legend entry to toggle the transparency. (HTML plot, won't show up correctly in PDF.)

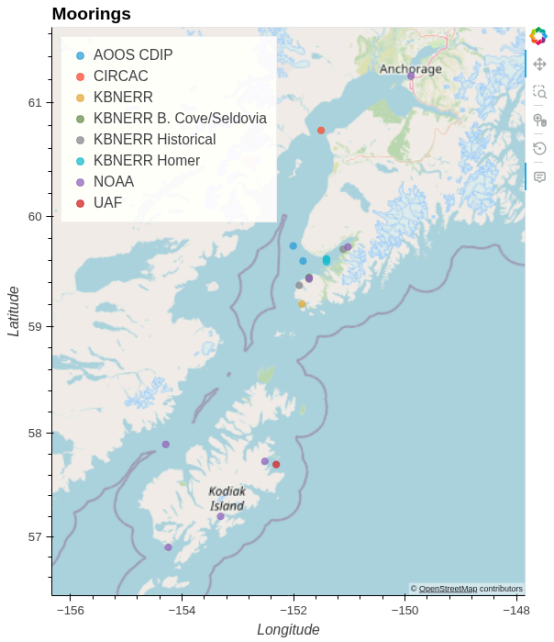

Fig. 7.2 All mooring stations, by project. (PNG screenshot, available for PDF and for saving image.)

7.2. Taylor Diagrams

Taylor diagrams summarize the skill of the two models in capturing the moorings datasets. The data has been grouped by region (Figs. 7.3, 7.4, and 7.5). Sea surface height (Fig. 7.3) is captured well by the models outside of Cook Inlet and in Upper Cook Inlet, but less well in Kachemak Bay. Both models have too low variance and correlation in capturing the subtidal sea surface height, but is better for CIOFS Fresh than Hindcast. Temperature (Fig. 7.4) is medium to well-captured in both models for the full and subtidal signals. For the subtidal anomaly, the models perform similarly to each other but none of the regions show good performance. Salinity time series (Fig. 7.5) are poorly captured across the board for both models. Skill scores are shown in the next plots for each dataset.

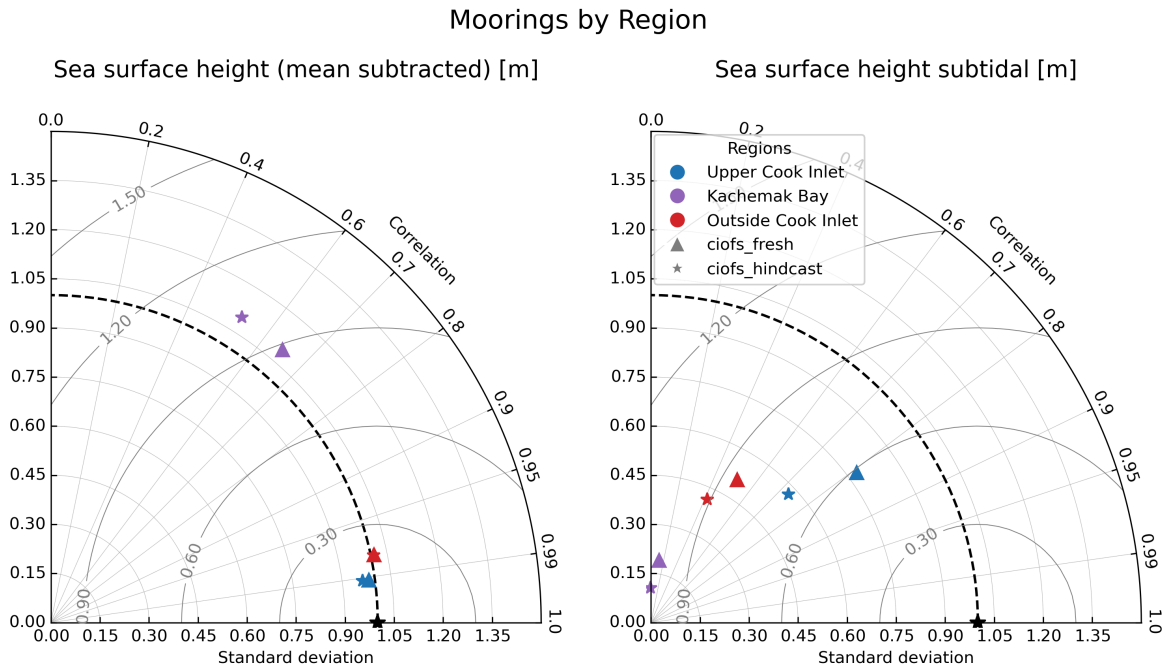

Fig. 7.3 Taylor Diagram summarizing skill of CIOFS Hindcast (stars) and CIOFS Fresh (triangles) for sea surface height: full signal minus the mean (left) and subtidal, grouped by region of Cook Inlet, for moorings.

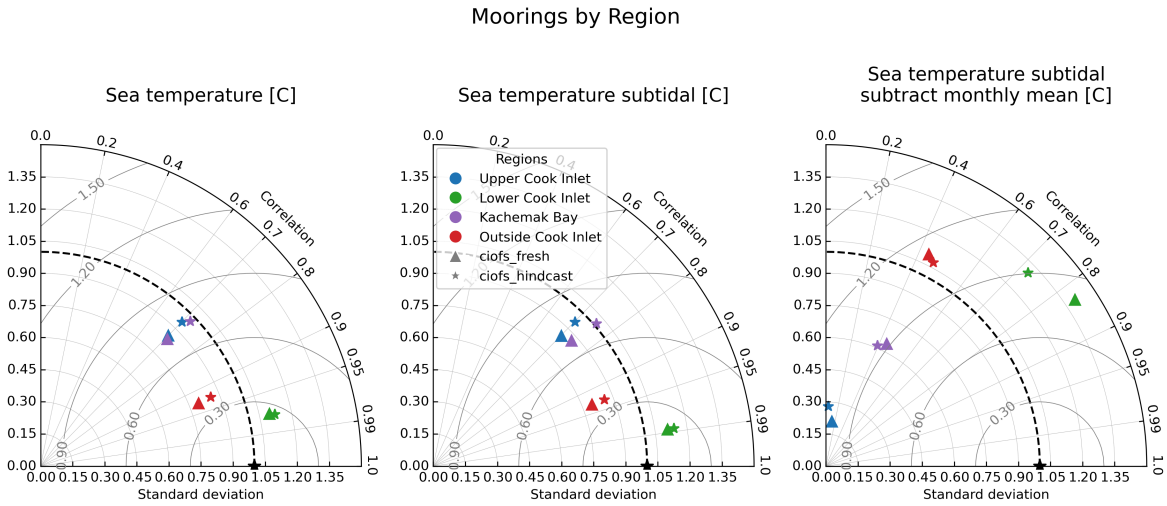

Fig. 7.4 Taylor Diagram summarizing skill of CIOFS Hindcast (stars) and CIOFS Fresh (triangles) for temperature: full signal (left), subtidal (center), and subtidal (right) minus the monthly mean, grouped by region of Cook Inlet, for moorings.

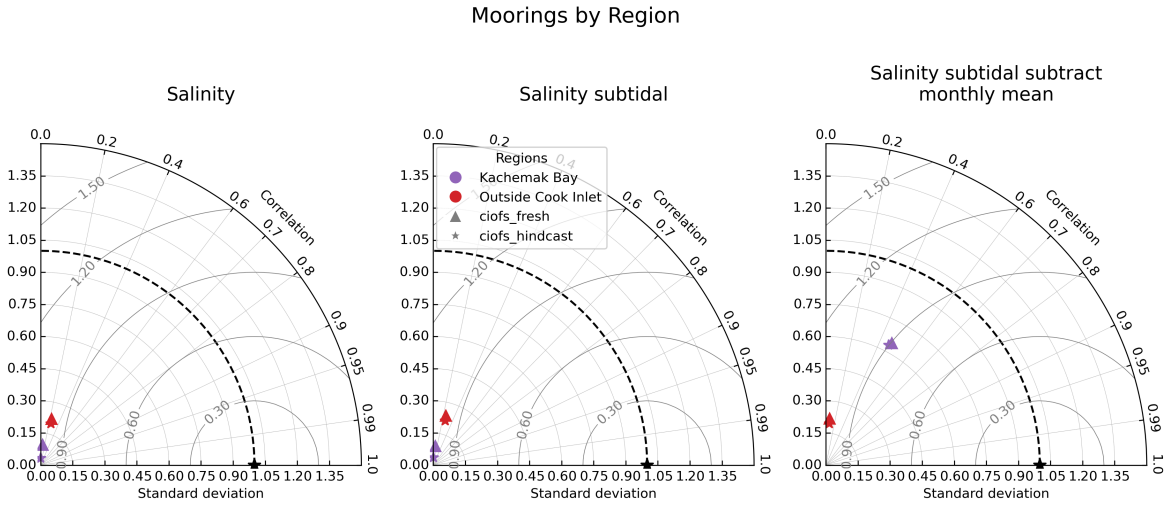

Fig. 7.5 Taylor Diagram summarizing skill of CIOFS Hindcast (stars) and CIOFS Fresh (triangles) for salinity: full signal (left), subtidal (center), and subtidal (right) minus the monthly mean, grouped by region of Cook Inlet, for moorings.

7.3. Sea Surface Height

7.3.1. Full signal, mean subtracted

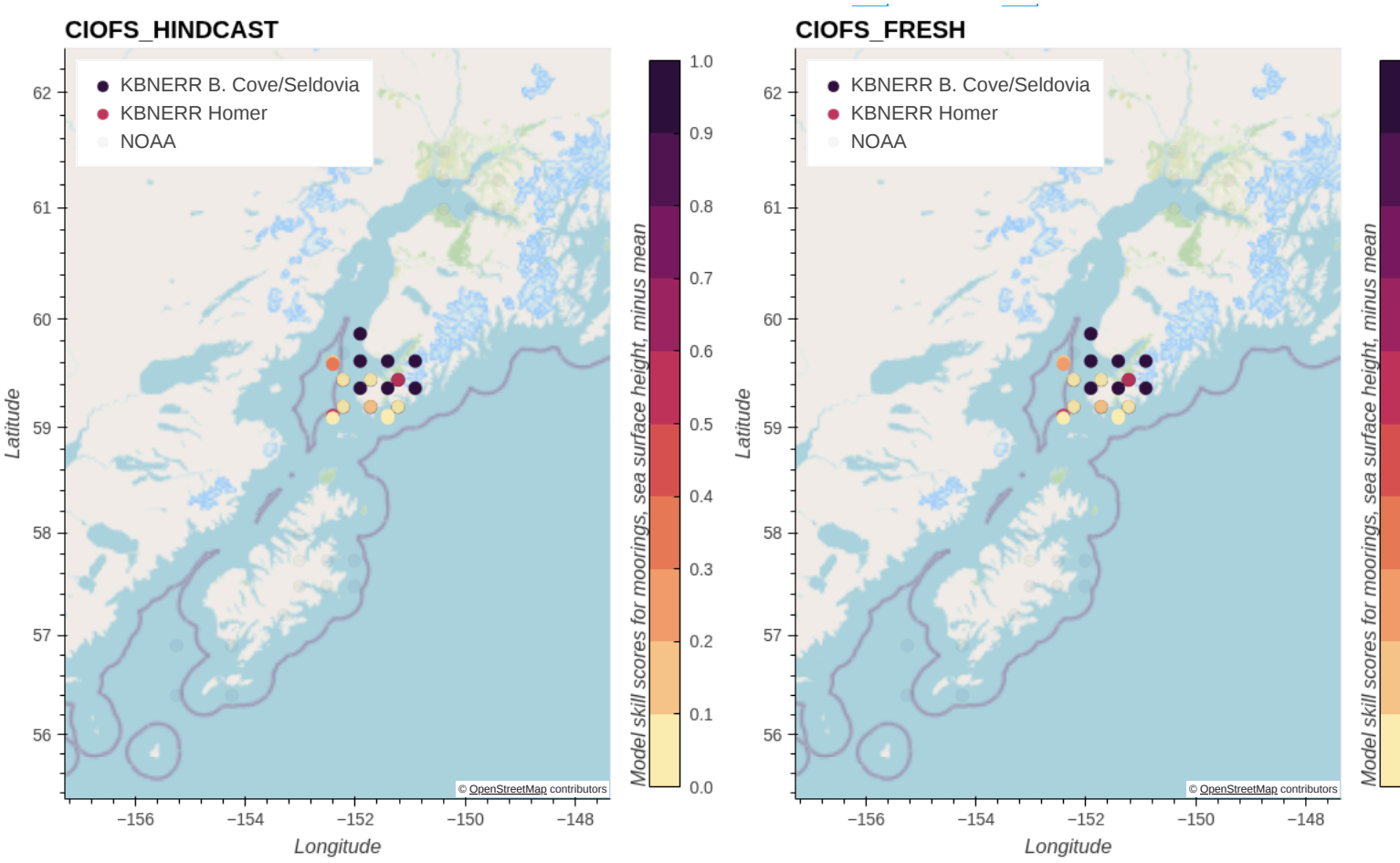

Fig. 7.6 Skill scores for CIOFS Hindcast (left) and CIOFS Freshwater (right) with moorings for sea surface height with mean subtracted, by project. Click on a legend entry to toggle the transparency. (HTML plot, won't show up correctly in PDF.)

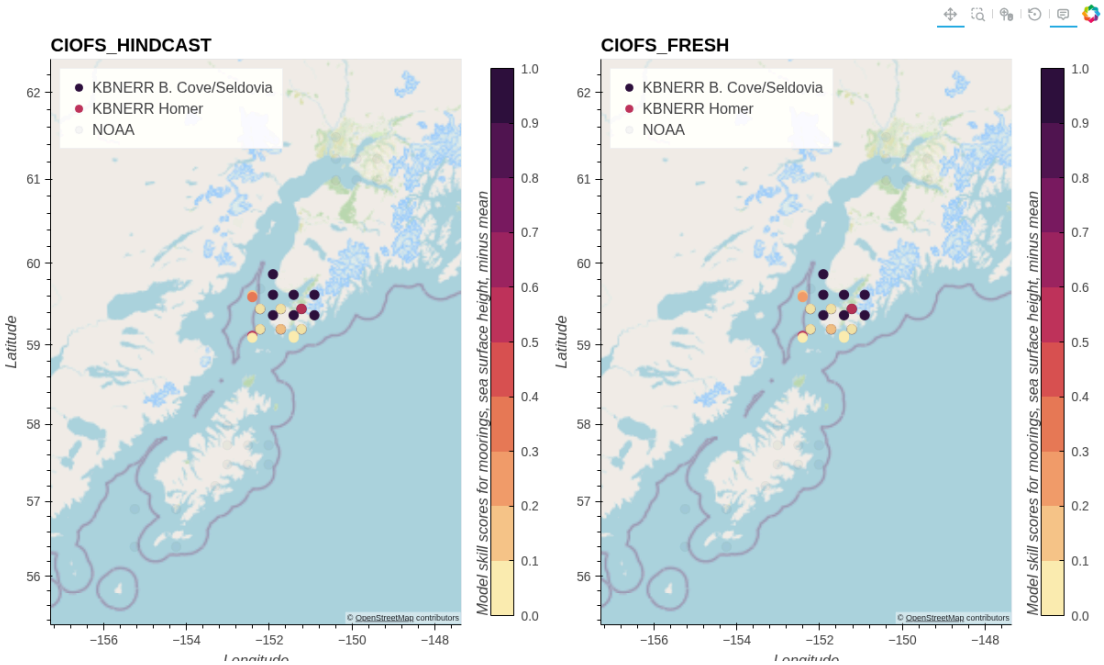

Fig. 7.7 Skill scores for CIOFS Hindcast (left) and CIOFS Freshwater (right) with moorings for sea surface height with mean subtracted, by project. (PNG screenshot, available for PDF and for saving image.)

7.3.2. Subtidal, mean subtracted

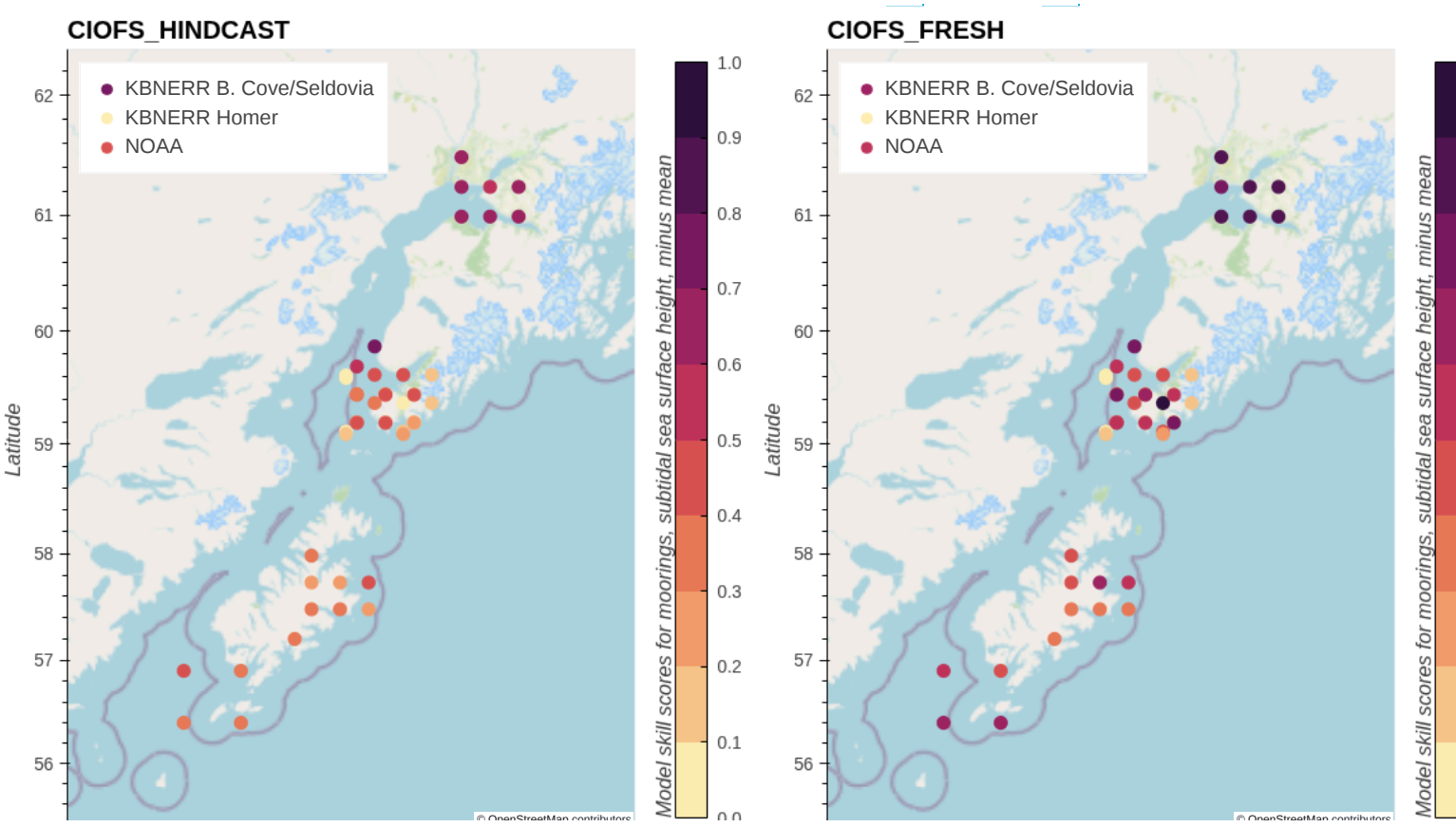

Fig. 7.8 Skill scores for CIOFS Hindcast (left) and CIOFS Freshwater (right) with moorings for subtidal sea surface height with mean subtracted, by project. Click on a legend entry to toggle the transparency. (HTML plot, won't show up correctly in PDF.)

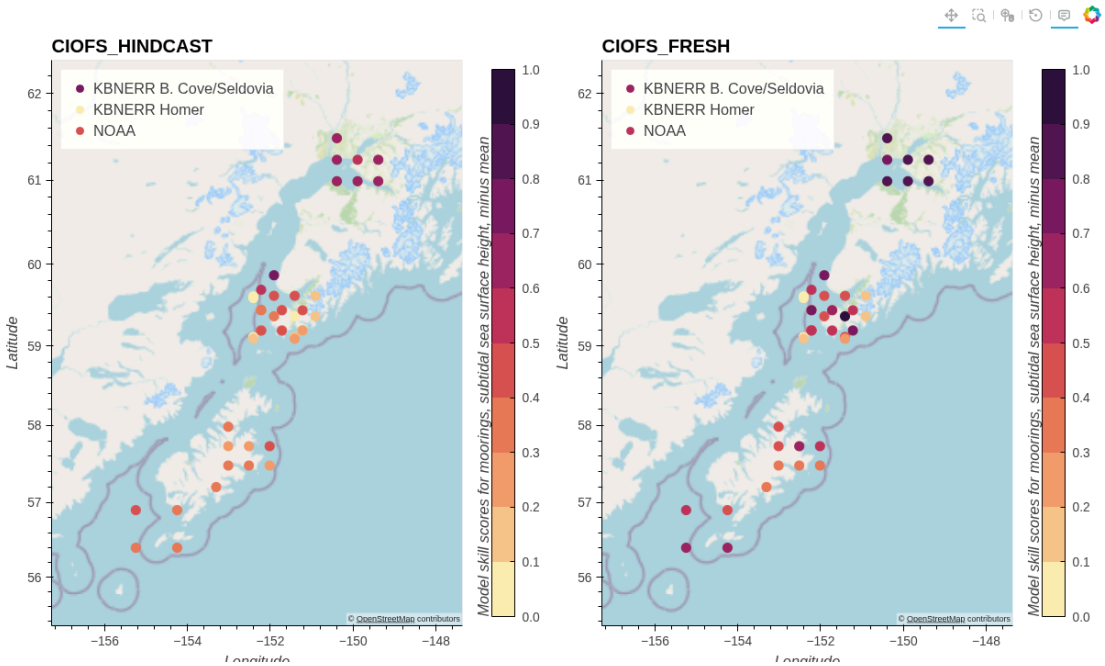

Fig. 7.9 Skill scores for CIOFS Hindcast (left) and CIOFS Freshwater (right) with moorings for subtidal sea surface height with mean subtracted, by project. (PNG screenshot, available for PDF and for saving image.)

7.4. Temperature

7.4.1. Full signal

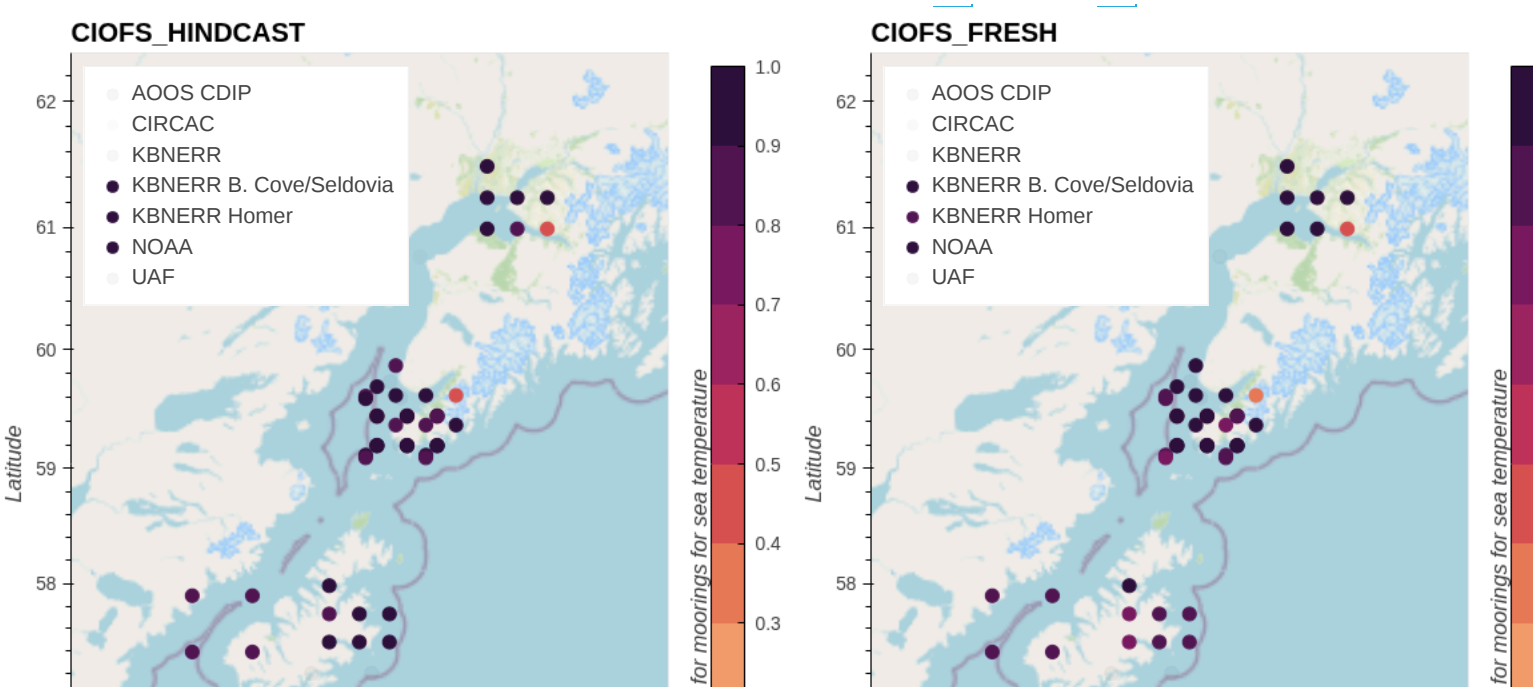

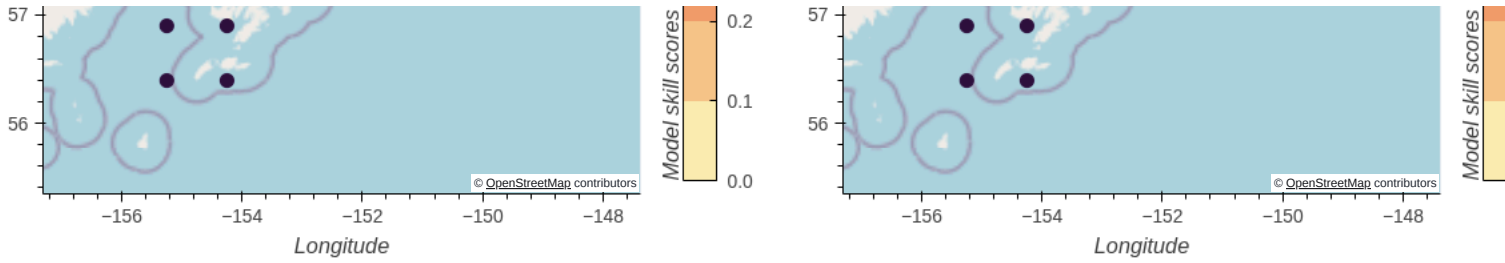

Fig. 7.10 Skill scores for CIOFS Hindcast (left) and CIOFS Freshwater (right) with moorings for temperature, by project. Click on a legend entry to toggle the transparency. (HTML plot, won't show up correctly in PDF.)

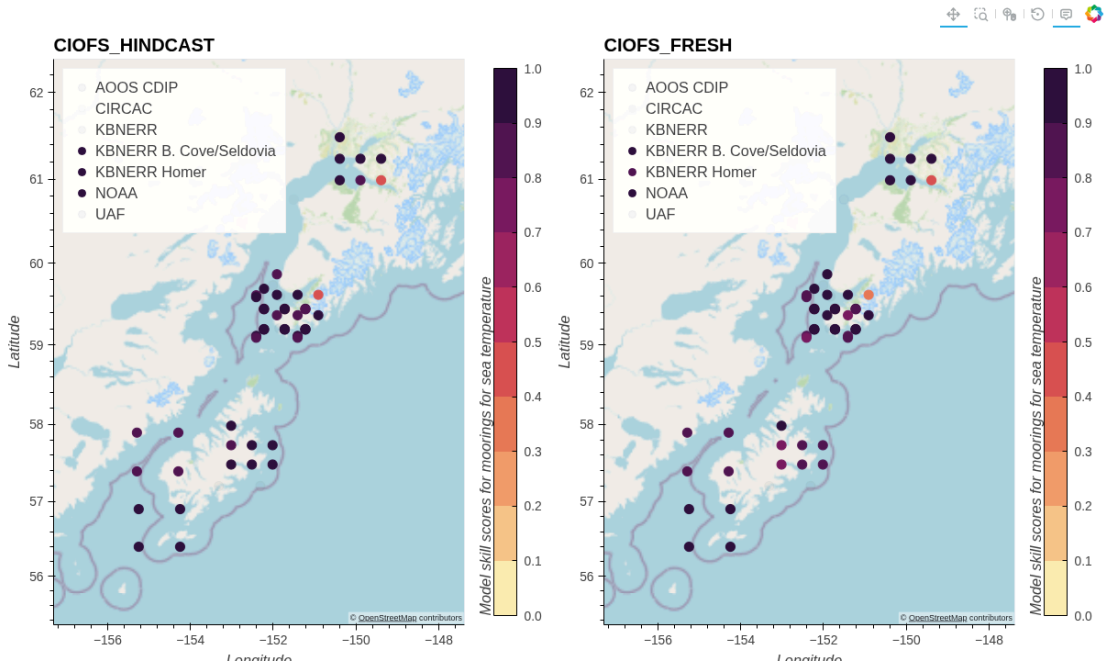

Fig. 7.11 Skill scores for CIOFS Hindcast (left) and CIOFS Freshwater (right) with moorings for subtidal sea surface height with mean subtracted, by project. (PNG screenshot, available for PDF and for saving image.)

7.4.2. Subtidal

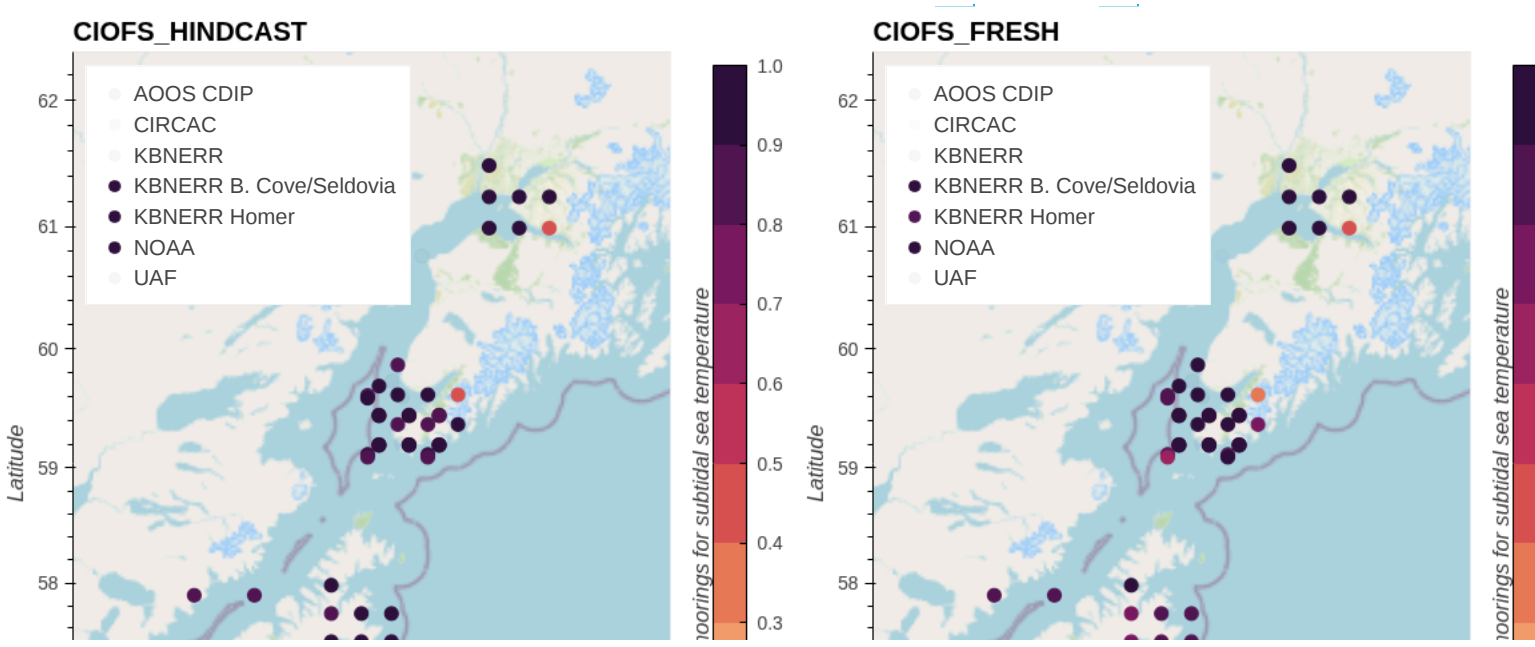

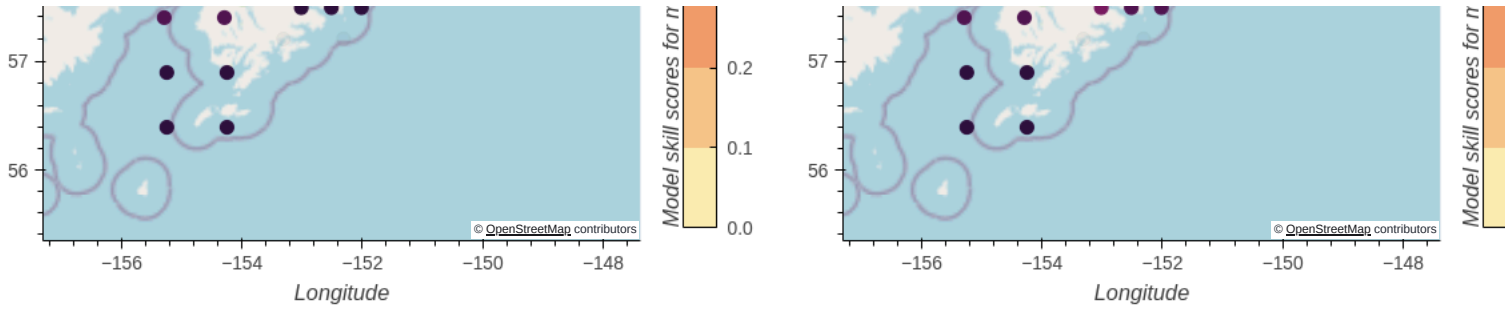

Fig. 7.12 Skill scores for CIOFS Hindcast (left) and CIOFS Freshwater (right) with moorings for subtidal temperature, by project. Click on a legend entry to toggle the transparency. (HTML plot, won't show up correctly in PDF.)

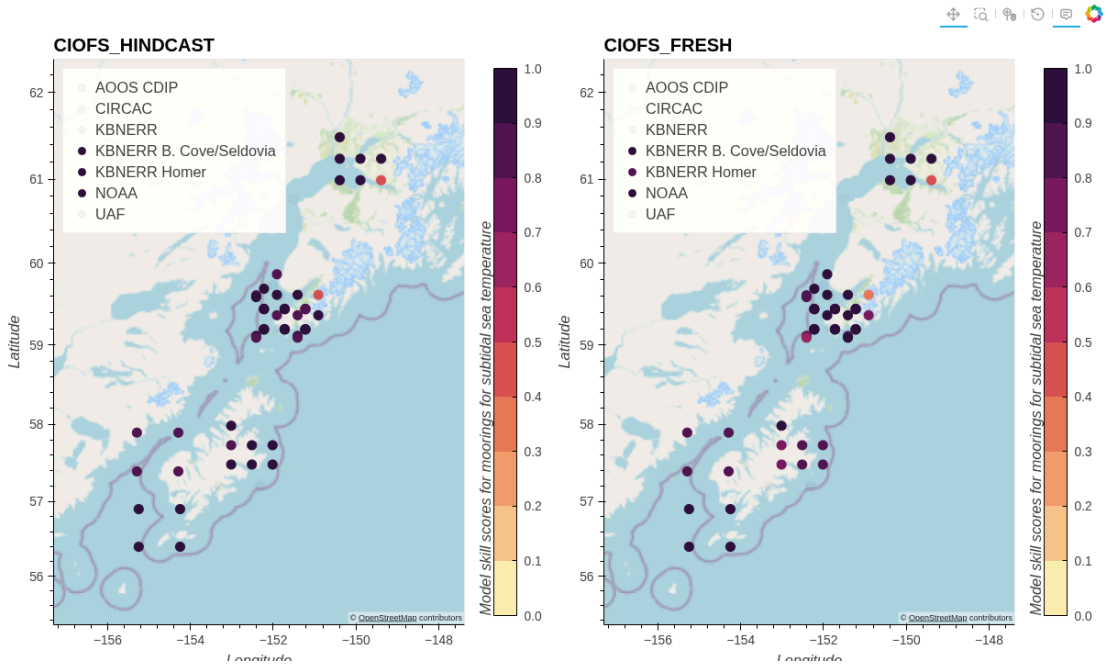

Fig. 7.13 Skill scores for CIOFS Hindcast (left) and CIOFS Freshwater (right) with moorings for subtidal temperature, by project. (PNG screenshot, available for PDF and for saving image.)

7.4.3. Subtidal with monthly-averaged climatology subtracted

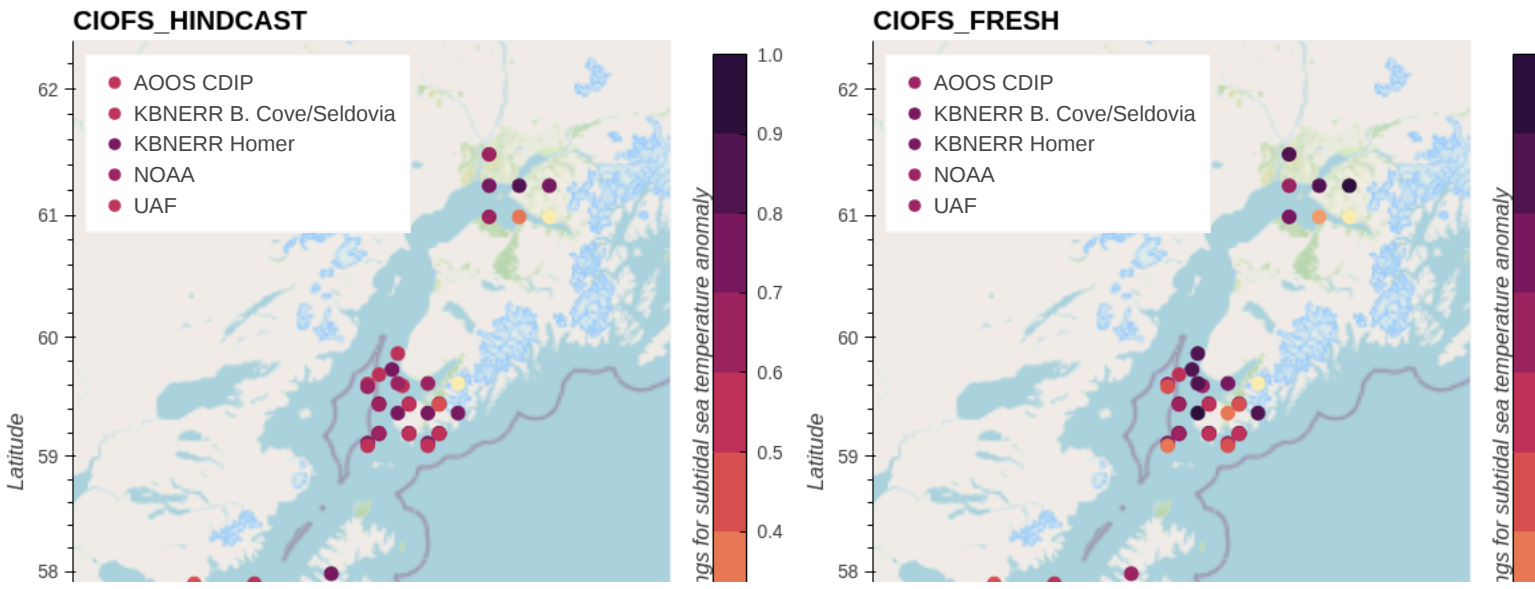

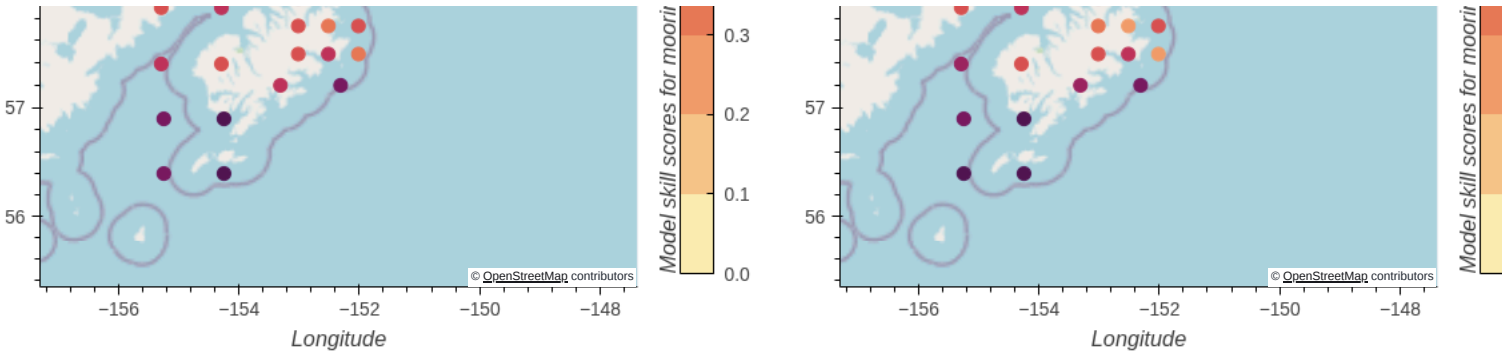

Fig. 7.14 Skill scores for CIOFS Hindcast (left) and CIOFS Freshwater (right) with moorings for subtidal temperature anomaly, by project. Click on a legend entry to toggle the transparency. (HTML plot, won't show up correctly in PDF.)

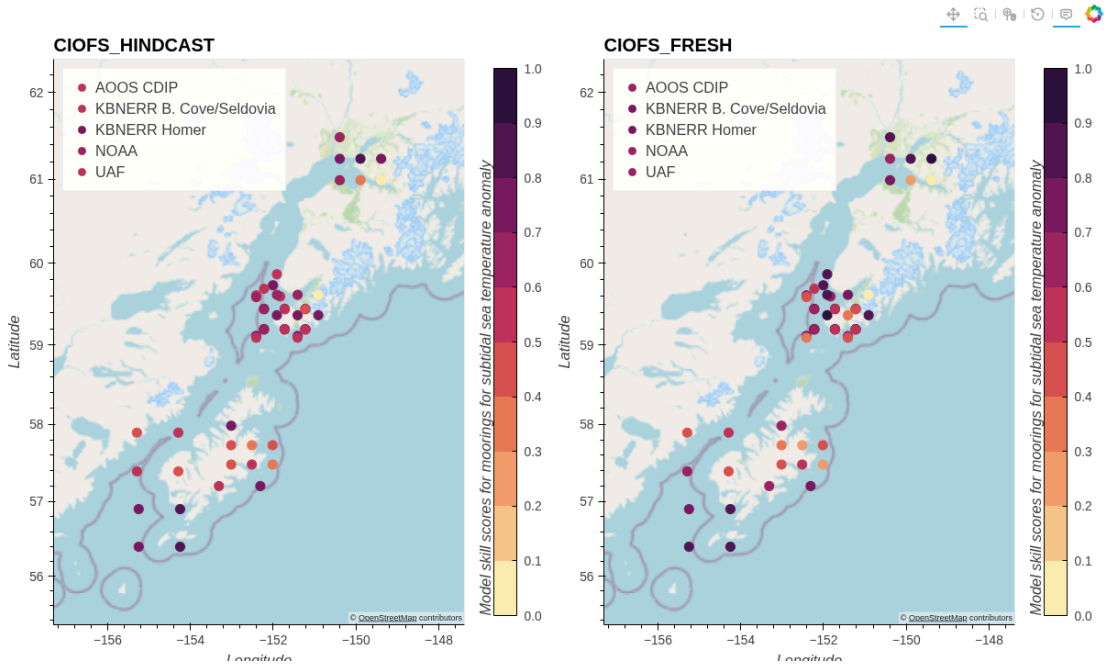

Fig. 7.15 Skill scores for CIOFS Hindcast (left) and CIOFS Freshwater (right) with moorings for subtidal temperature anomaly, by project. (PNG screenshot, available for PDF and for saving image.)

7.5. Salinity

7.5.1. Full signal

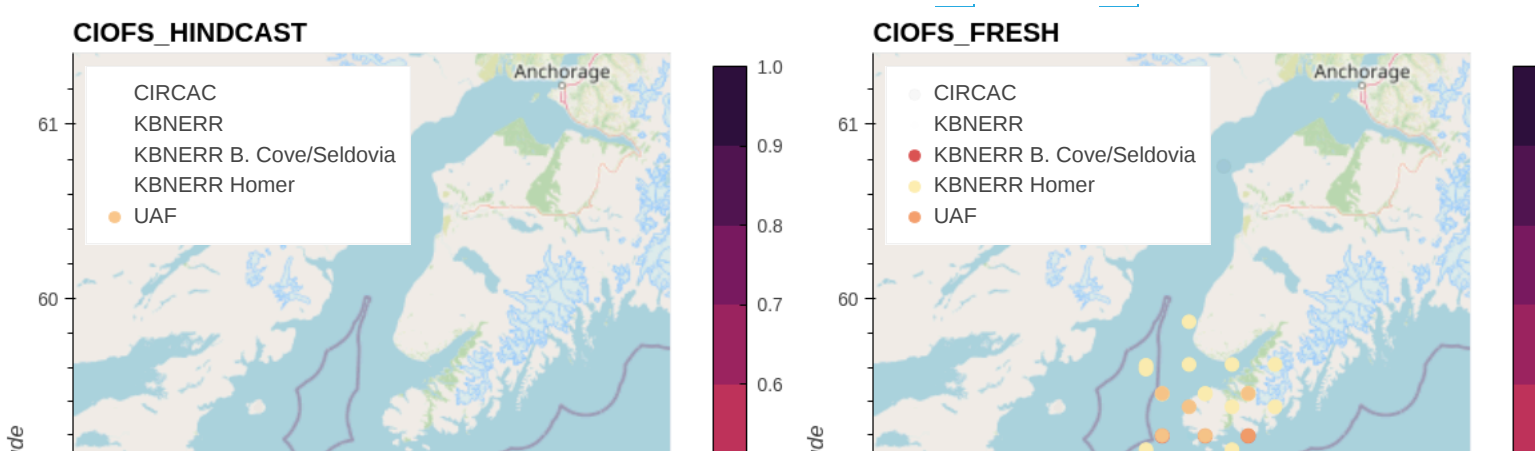

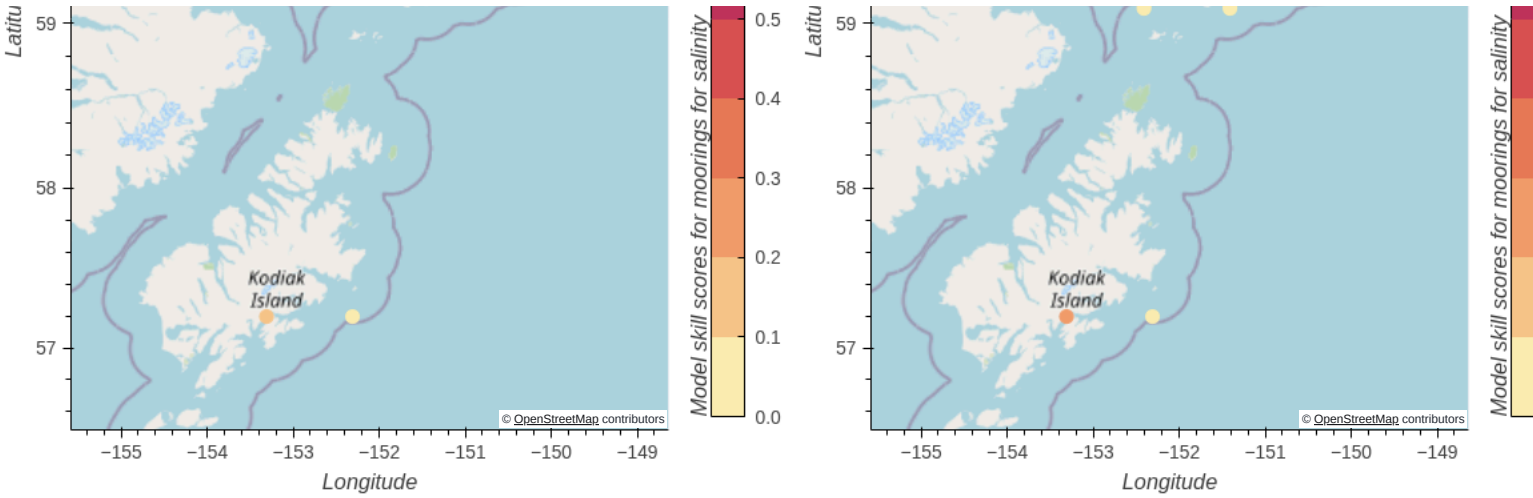

Fig. 7.16 Skill scores for CIOFS Hindcast (left) and CIOFS Freshwater (right) with moorings for salinity, by project. Click on a legend entry to toggle the transparency. (HTML plot, won't show up correctly in PDF.)

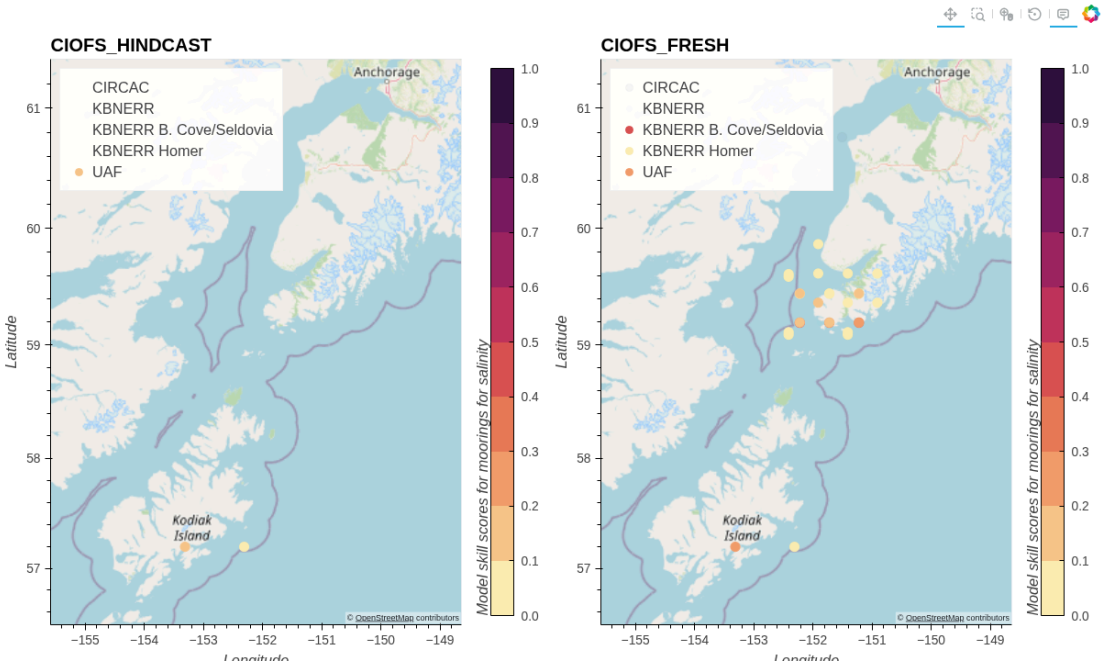

Fig. 7.17 Skill scores for CIOFS Hindcast (left) and CIOFS Freshwater (right) with moorings for salinity, by project. (PNG screenshot, available for PDF and for saving image.)

7.5.2. Subtidal

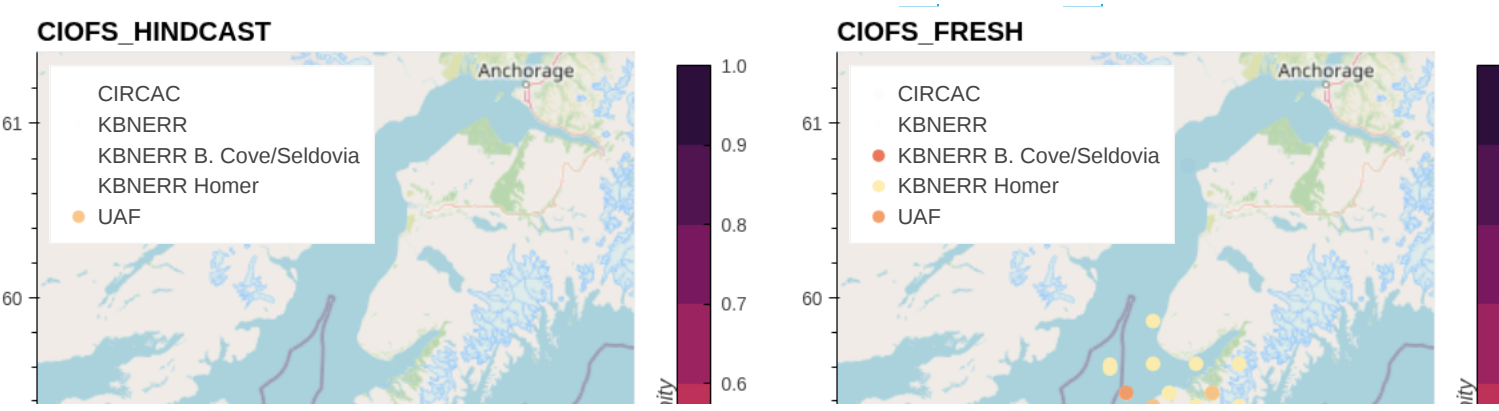

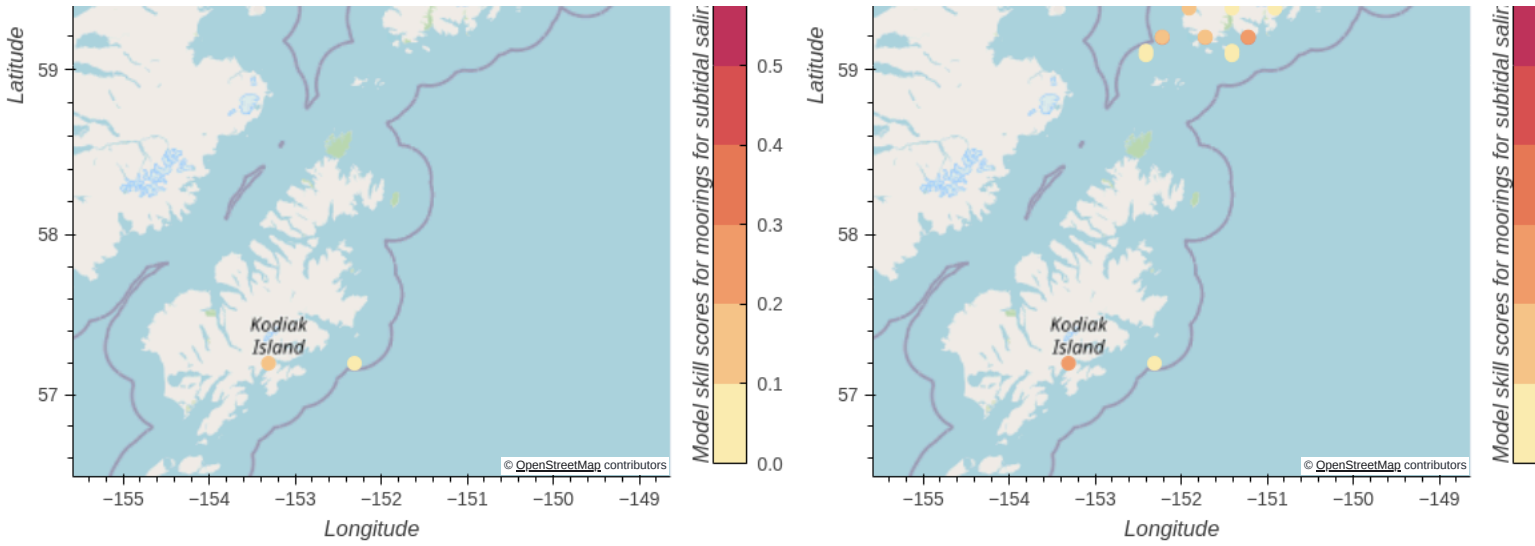

Fig. 7.18 Skill scores for CIOFS Hindcast (left) and CIOFS Freshwater (right) with moorings for subtidal salinity, by project. Click on a legend entry to toggle the transparency. (HTML plot, won't show up correctly in PDF.)

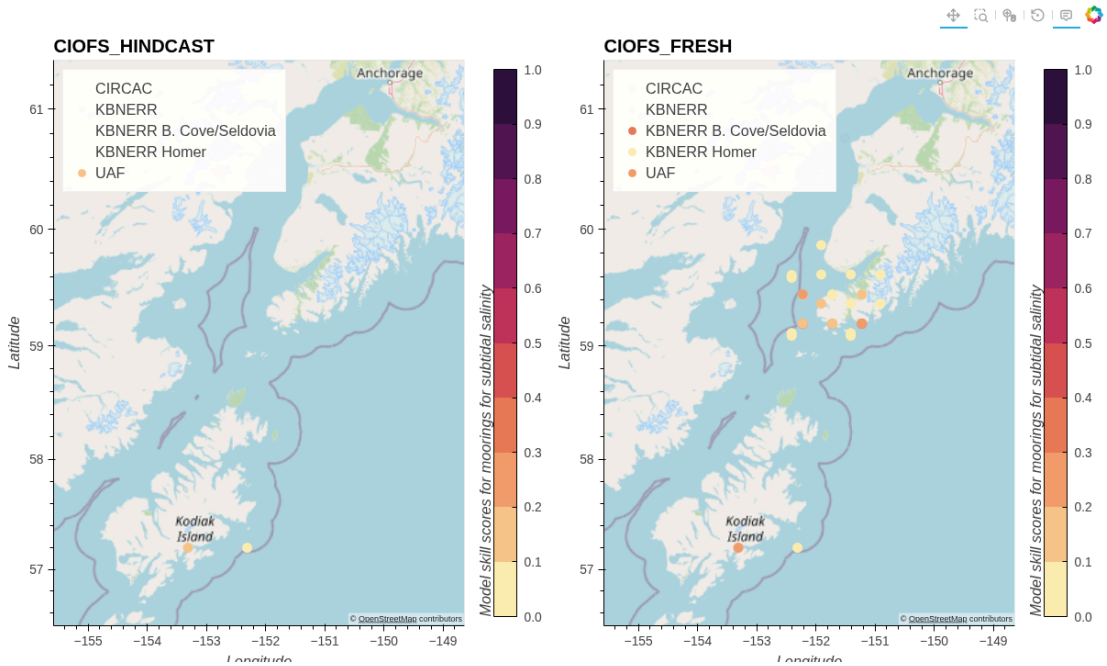

Fig. 7.19 Skill scores for CIOFS Hindcast (left) and CIOFS Freshwater (right) with moorings for subtidal salinity, by project. (PNG screenshot, available for PDF and for saving image.)

7.5.3. Subtidal with monthly-averaged climatology subtracted

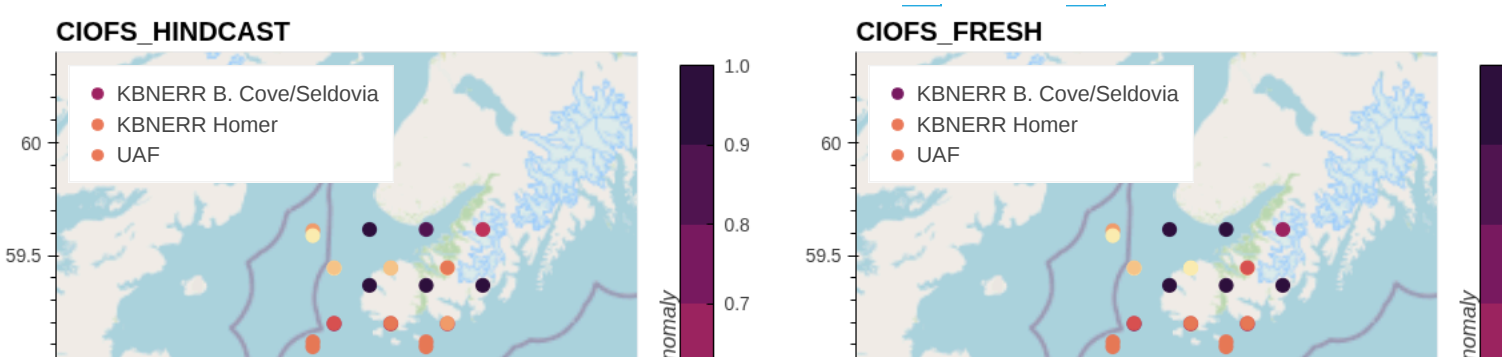

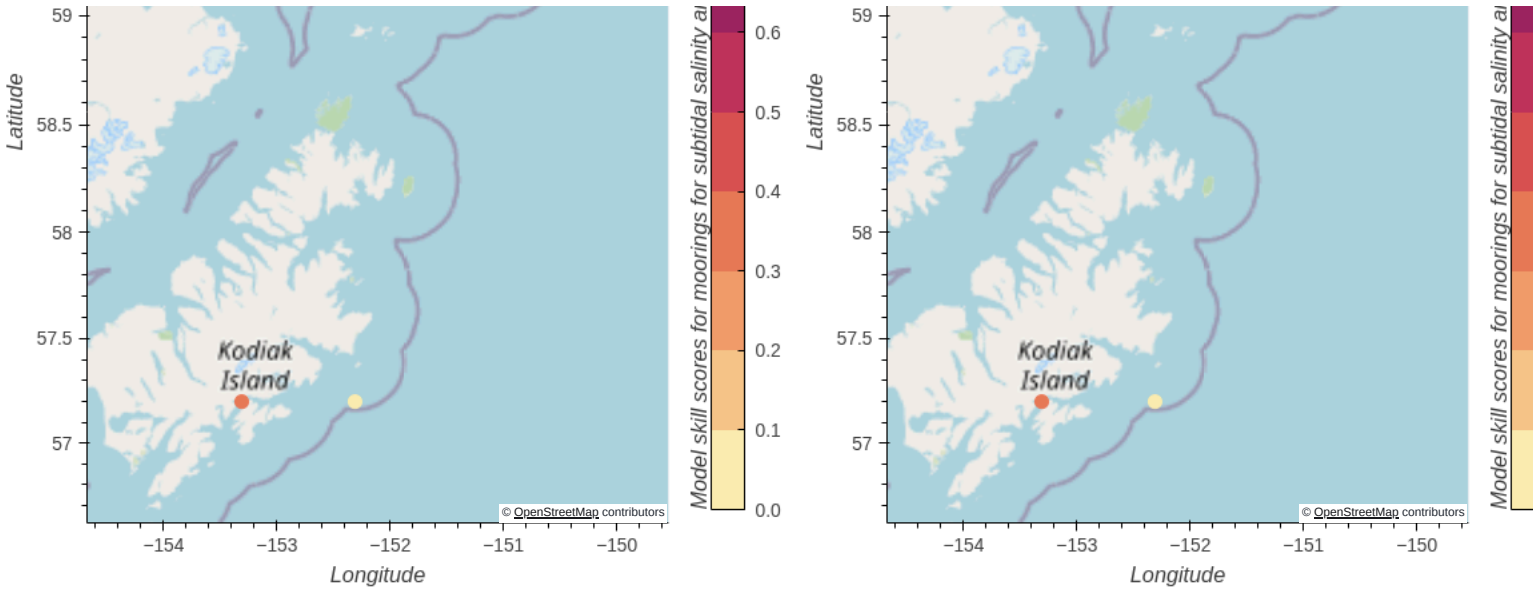

Fig. 7.20 Skill scores for CIOFS Hindcast (left) and CIOFS Freshwater (right) with moorings for subtidal salinity anomaly, by project. Click on a legend entry to toggle the transparency. (HTML plot, won't show up correctly in PDF.)

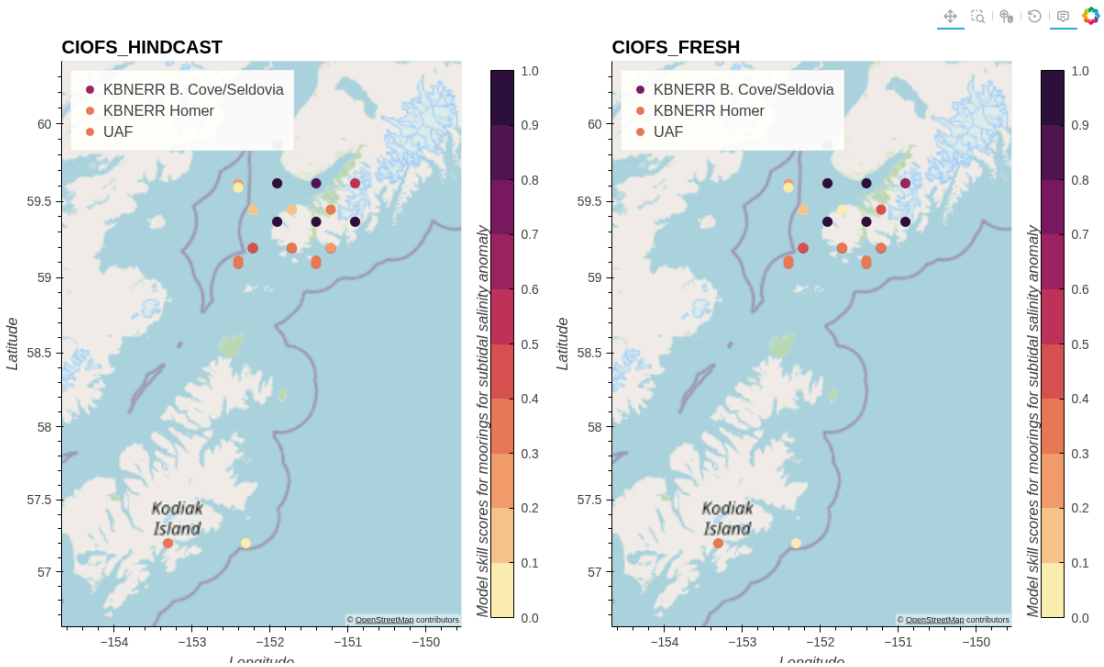

Fig. 7.21 Skill scores for CIOFS Hindcast (left) and CIOFS Freshwater (right) with moorings for subtidal salinity anomaly, by project. (PNG screenshot, available for PDF and for saving image.)

8. Overview CTD Transects

Shown here are plots to summarize the skill of the models in representing the data. First are Taylor Diagrams summarize the overall skill of the models. Subsequently, in the next overview plots, each colored square marker represents the skill score for the model compared with the data for a visit to the transect. The length of each transect was split into the number of visits with a square for each visit; if there were many repeat visits there are a lot of squares along a transect and only one for a single visit.

Results show similar but slightly improved skill for CIOFS fresh over CIOFS Hindcast for temperature and clearly improved skill for salinity.

226MB zipfile of plots and stats files

[164MB zipfile of CTD profile plots from CTD transects]

8.1. Map of Stations

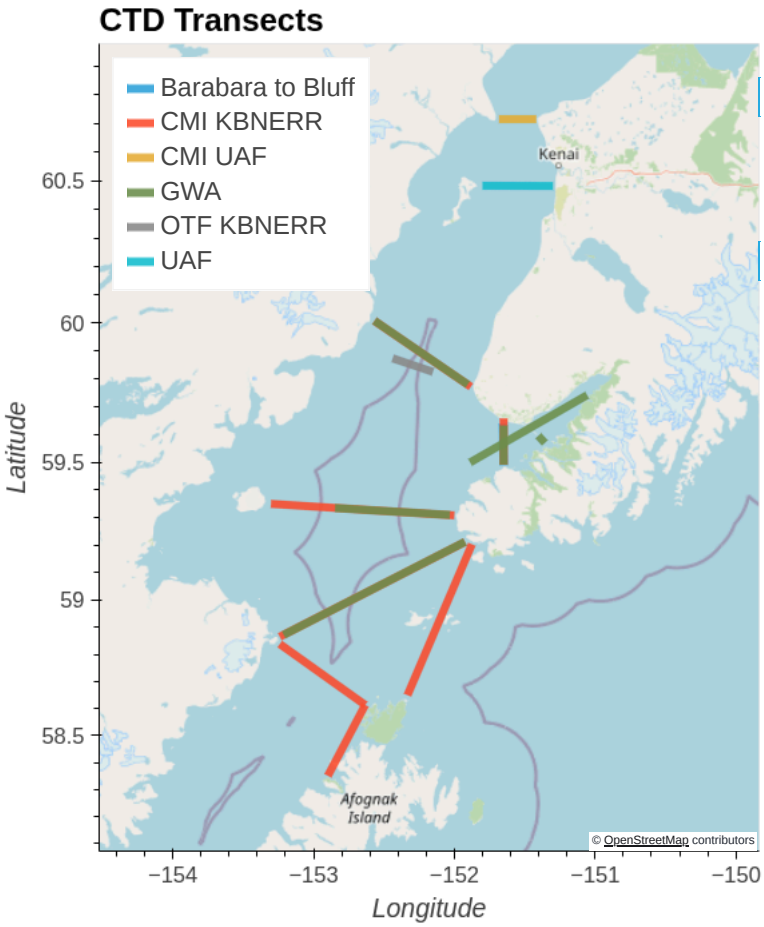

Fig. 8.1 All CTD transects (repeats indicated but not plotted), by project. Click on a legend entry to toggle the transparency.

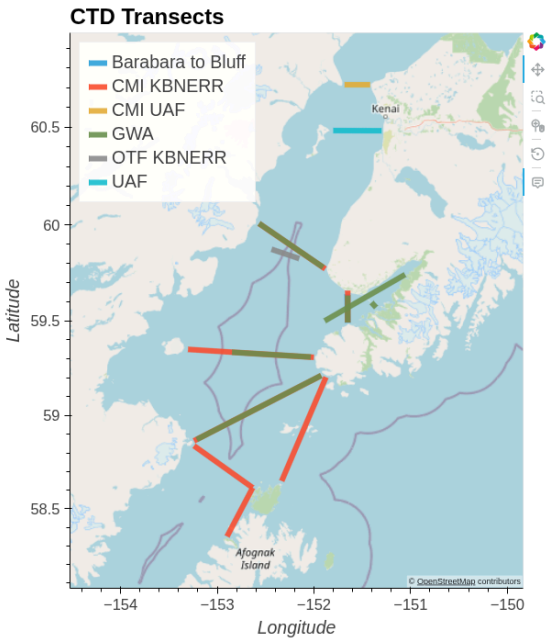

Fig. 8.2 All CTD transects, by project. (PNG screenshot, available for PDF and for saving image.)

8.2. Taylor Diagrams

Taylor diagrams summarize the skill of the two models in capturing the CTD transect datasets. The data has been grouped by region (Fig. 8.3) and season (Fig. 8.4). The results show that CIOFS fresh performs slightly better than CIOFS hindcast for temperature across different groupings, and much better for salinity. Skill scores are shown in the next plots for each dataset.

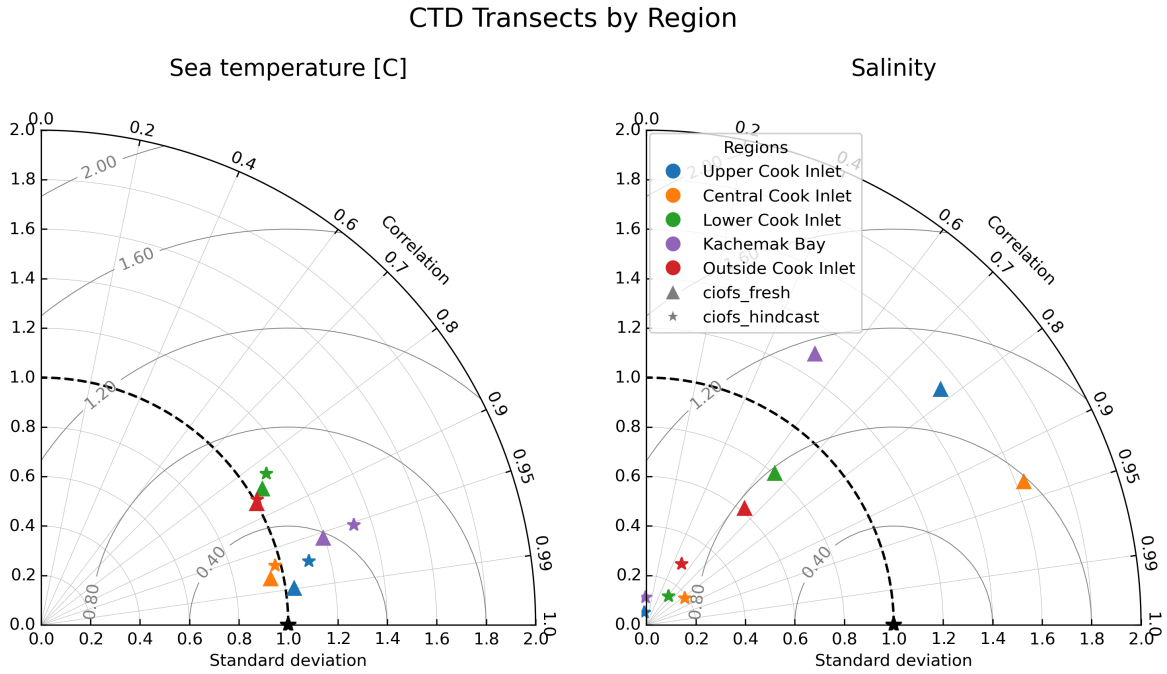

Fig. 8.3 Taylor Diagram summarizing skill of CIOFS Hindcast (stars) and CIOFS Fresh (triangles) for temperature (left) and salinity (right), grouped by region of Cook Inlet, for CTD transects datasets.

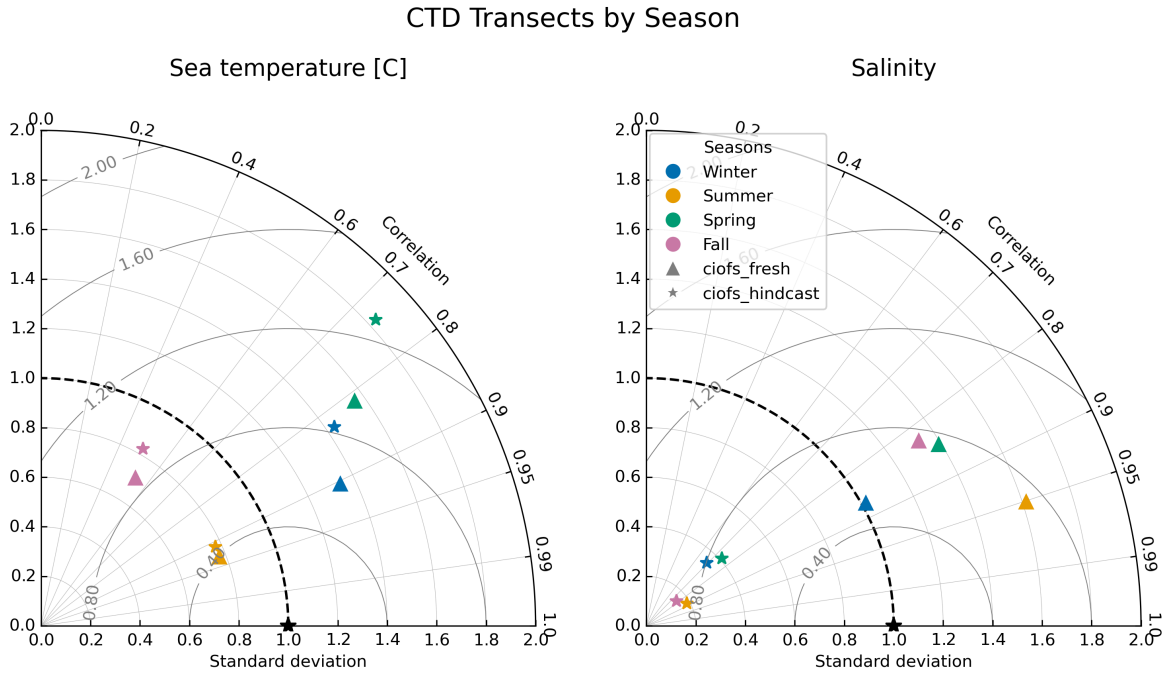

Fig. 8.4 Taylor Diagram summarizing skill of CIOFS Hindcast (stars) and CIOFS Fresh (triangles) for temperature (left) and salinity (right), grouped by season, for CTD transects datasets.

8.3. Sea Temperature

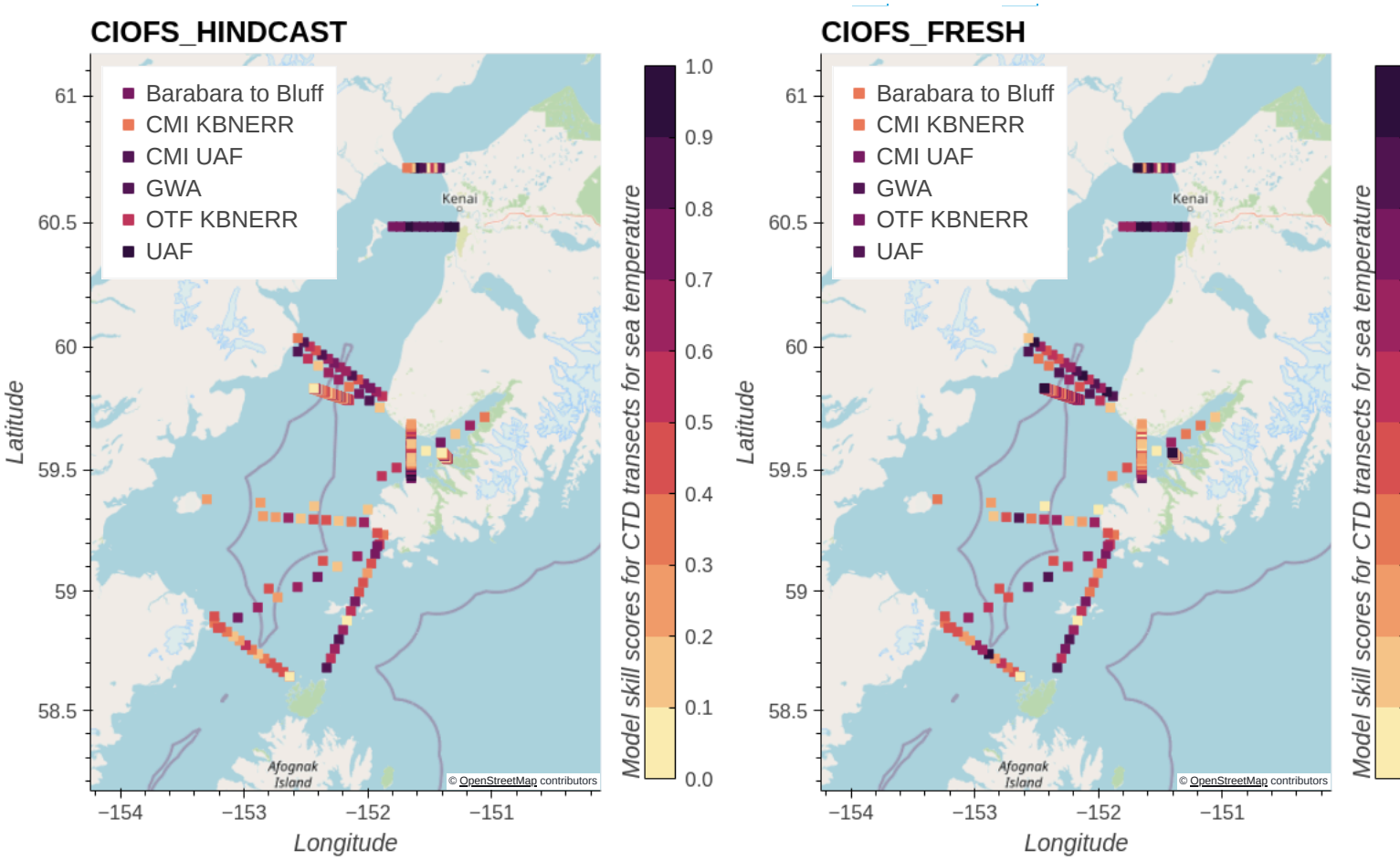

Fig. 8.5 Skill scores for CIOFS Hindcast (left) and CIOFS Freshwater (right) with CTD transects for sea temperature, by project. Click on a legend entry to toggle the transparency. (HTML plot, won't show up correctly in PDF.)

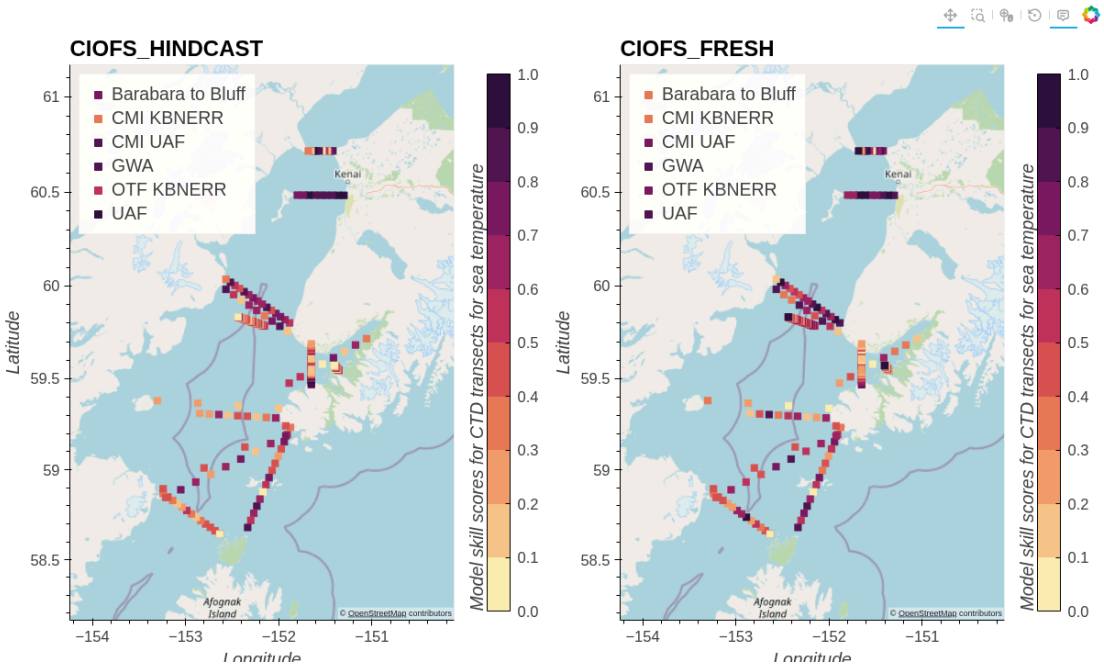

Fig. 8.6 Skill scores for CIOFS Hindcast (left) and CIOFS Freshwater (right) with CTD transects for sea temperature, by project. (PNG screenshot, available for PDF and for saving image.)

8.4. Salinity

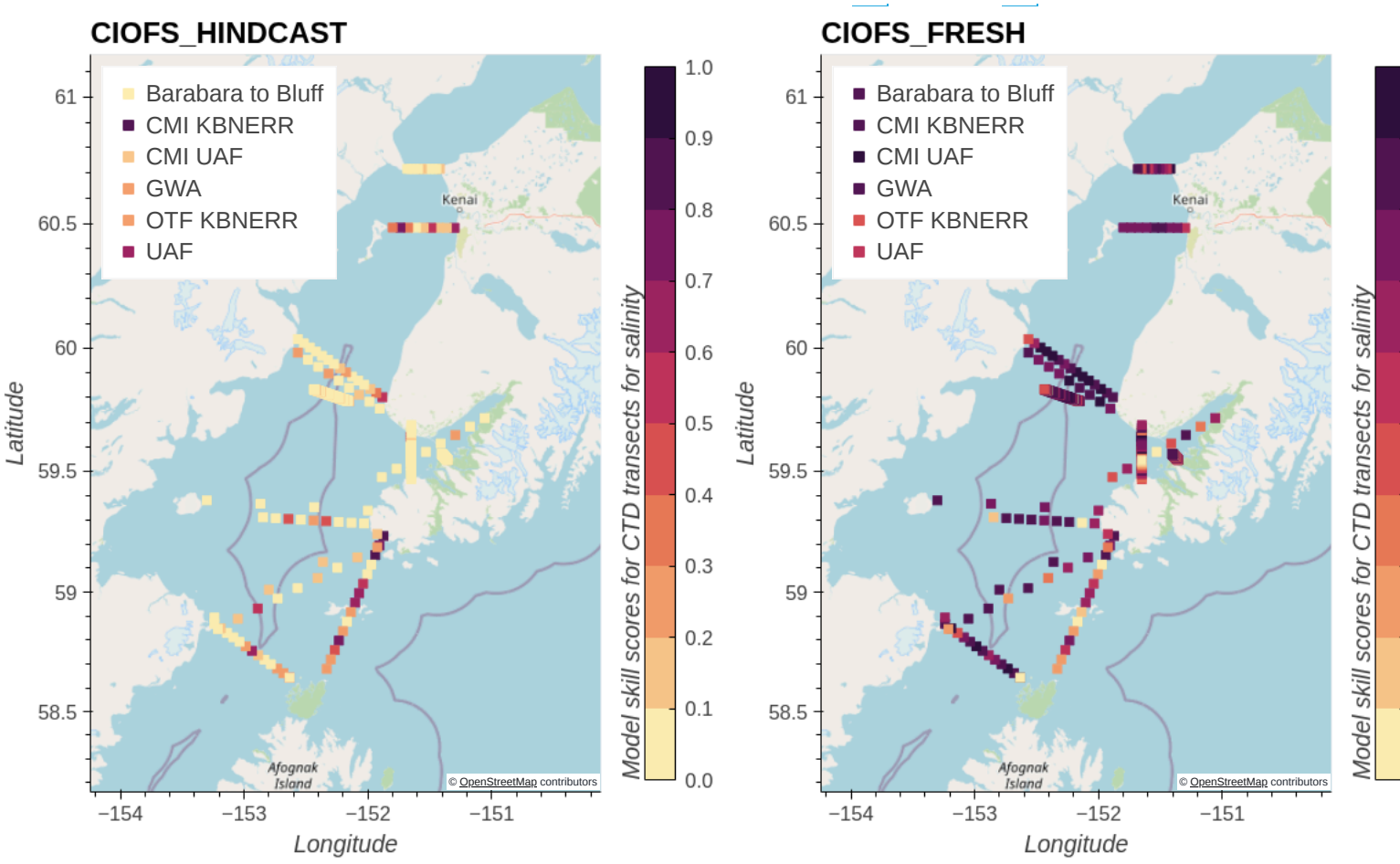

Fig. 8.7 Skill scores for CIOFS Hindcast (left) and CIOFS Freshwater (right) with CTD transects for salinity, by project. Click on a legend entry to toggle the transparency. (HTML plot, won't show up correctly in PDF.)

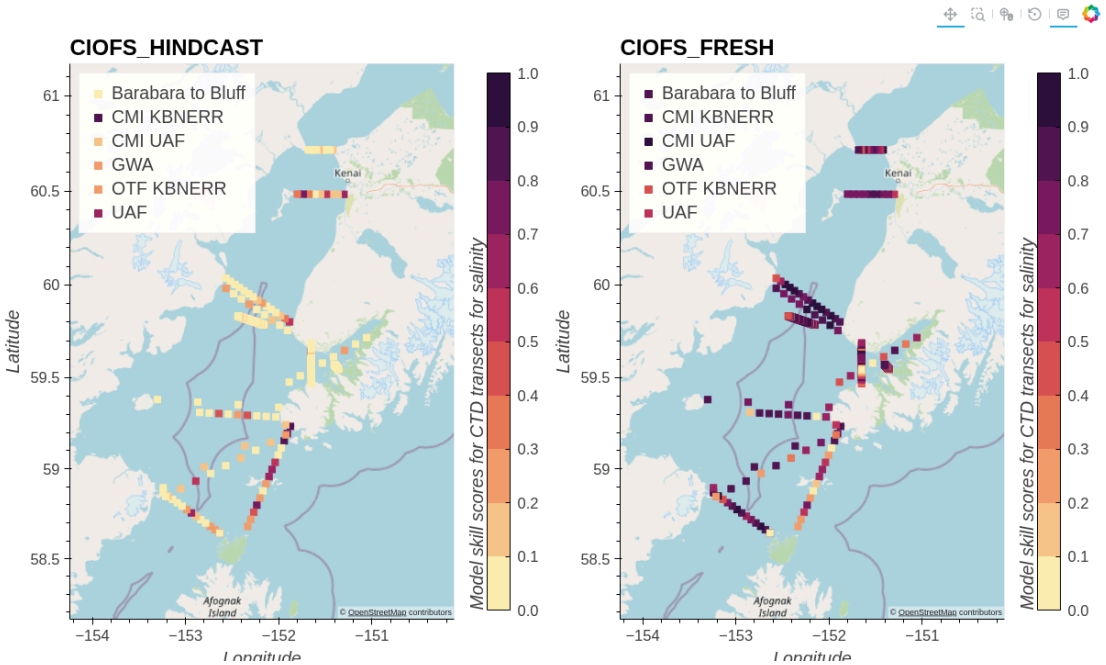

Fig. 8.8 Skill scores for CIOFS Hindcast (left) and CIOFS Freshwater (right) with CTD transects for salinity, by project. (PNG screenshot, available for PDF and for saving image.)

9. Overview CTD Profiles

CTD profiles are compared between data and each model and summarized on plots below by variable using the skill score. A higher skill score is better with 1 giving perfect skill.

Results show that CIOFS hindcast and CIOFS fresh have similar skill for temperature, but CIOFS fresh has better skill than CIOFS hindcast for salinity.

122MB zipfile of plots and stats files

9.1. Map of Stations

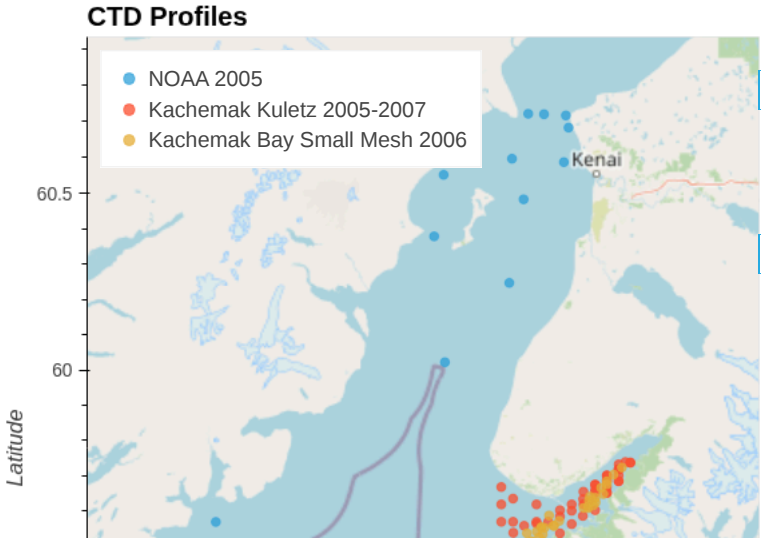

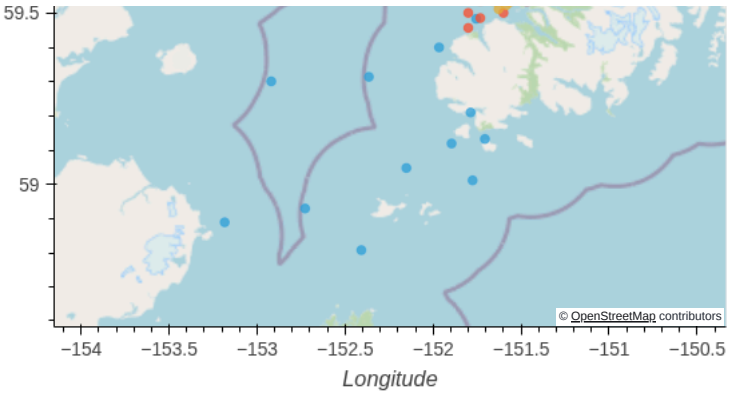

Fig. 9.1 All CTD profiles, by project. Click on a legend entry to toggle the transparency. (HTML plot, won't show up correctly in PDF.)

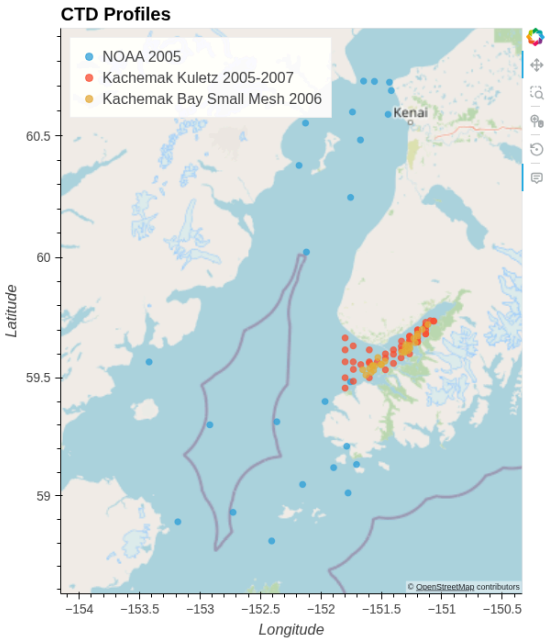

Fig. 9.2 All CTD profiles, by project. (PNG screenshot, available for PDF and for saving image.)

9.2. Taylor Diagrams

Taylor diagrams summarize the skill of the two models in capturing the CTD profile datasets. The data has been grouped by region (Fig. 9.3) and season (Fig. 9.4). By region for temperature, CIOFS Fresh has higher skill than CIOFS Hindcast, either by a little or a lot, except CIOFS Hindcast performs much better for Upper Cook Inlet. By region for salinity, CIOFS Fresh has much too high of variability in Kachemak Bay and Upper Cook Inlet while CIOFS Hindcast has much too low variability. For other regions, CIOFS Fresh performs clearly better than CIOFS Hindcast except for outside of Cook Inlet, for which CIOFS Fresh actually performs similarly to CIOFS Hindcast and neither are good. By season, data is only available in spring and summer. CIOFS Fresh is better for temperature in spring but similar for summer. For salinity, CIOFS Fresh again has much too high variability and CIOFS Hindcast much too low.

Skill scores are shown in the next plots for each dataset.

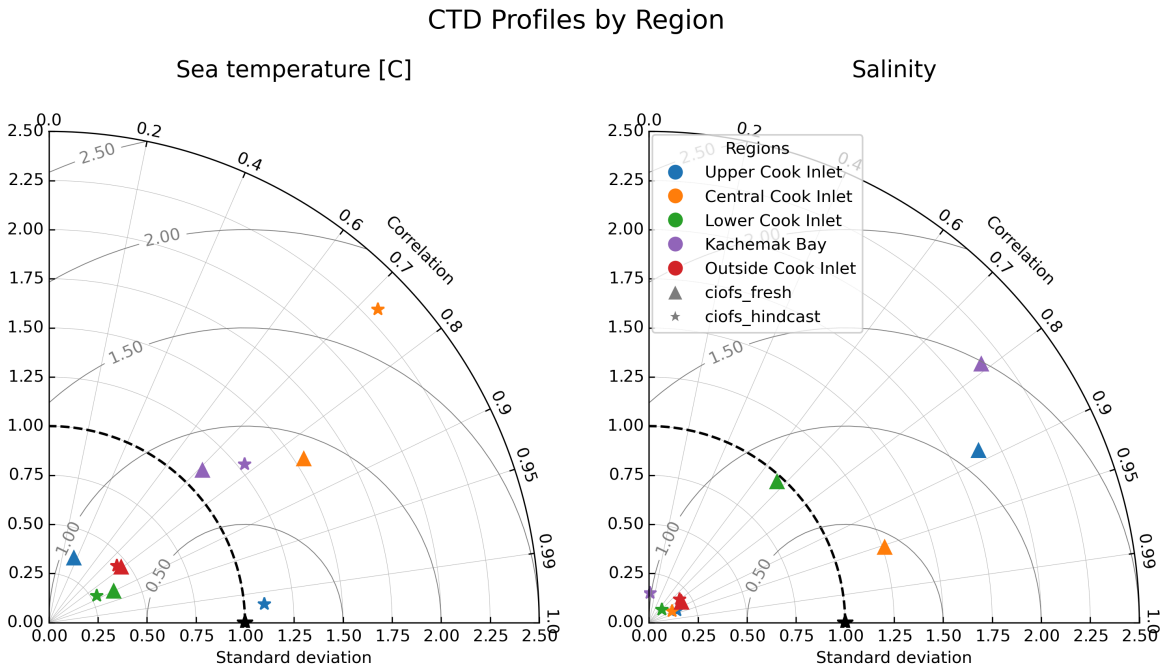

Fig. 9.3 Taylor Diagram summarizing skill of CIOFS Hindcast (stars) and CIOFS Fresh (triangles) for temperature (left) and salinity (right), grouped by region of Cook Inlet, for CTD profiles datasets.

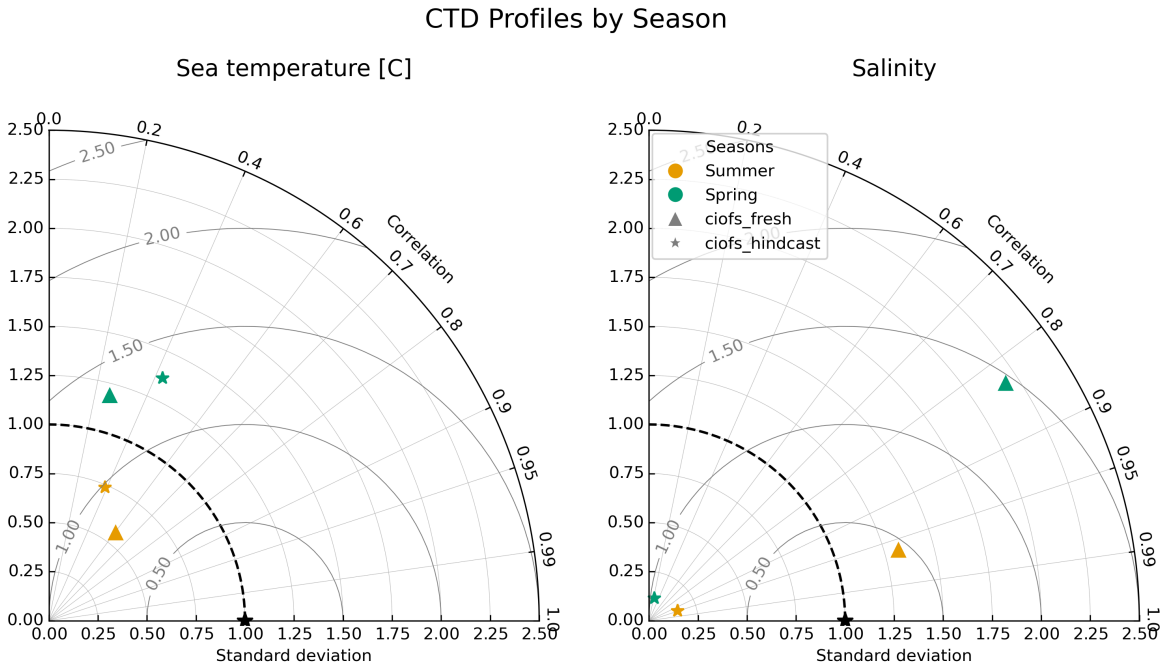

Fig. 9.4 Taylor Diagram summarizing skill of CIOFS Hindcast (stars) and CIOFS Fresh (triangles) for temperature (left) and salinity (right), grouped by season, for CTD profiles datasets.

9.3. Sea Temperature

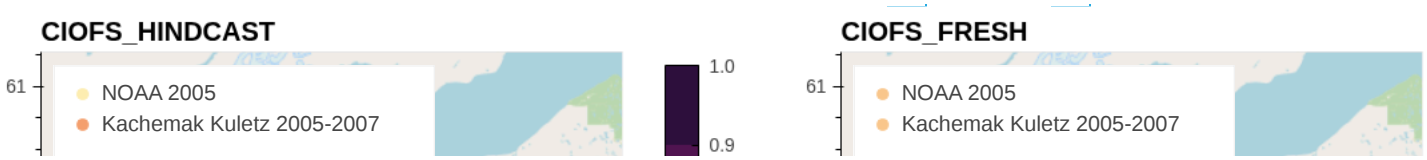

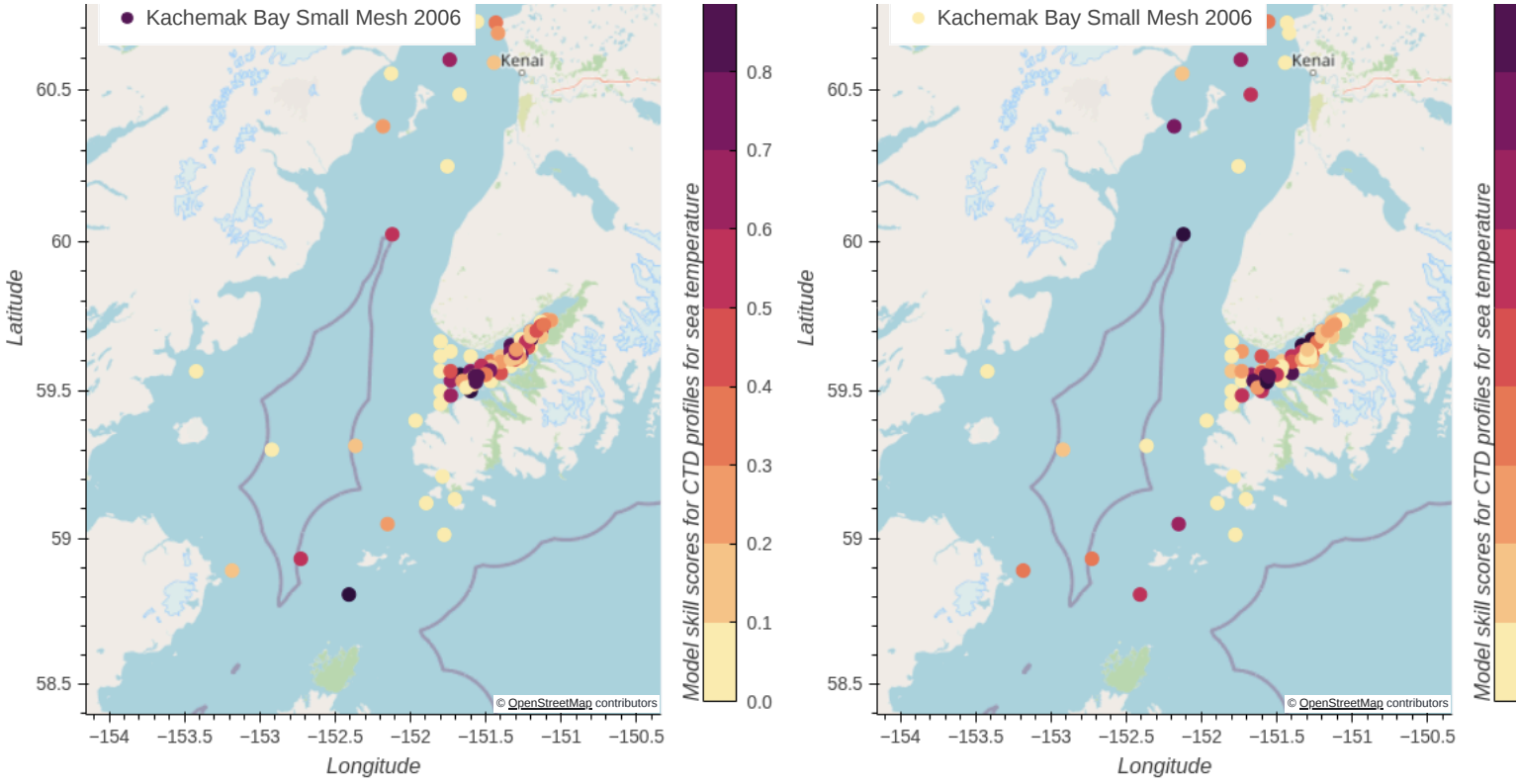

Fig. 9.5 Skill scores for CIOFS Hindcast (left) and CIOFS Freshwater (right) with CTD profiles for sea temperature, by project. Click on a legend entry to toggle the transparency. (HTML plot, won't show up correctly in PDF.)

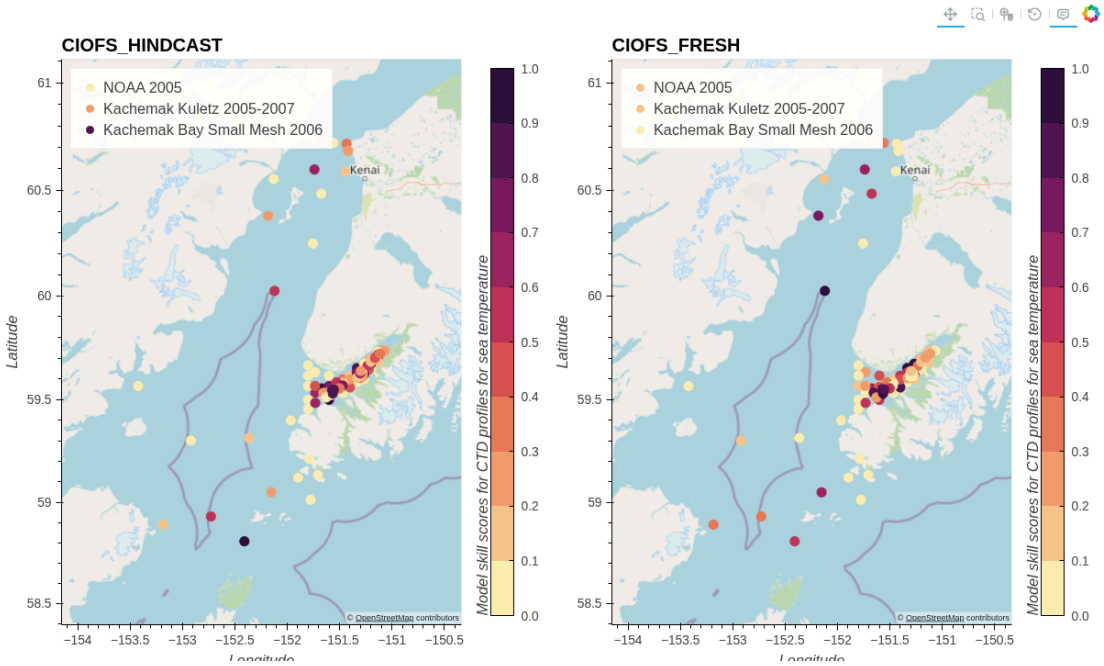

Fig. 9.6 Skill scores for CIOFS Hindcast (left) and CIOFS Freshwater (right) with CTD profiles for sea temperature, by project. (PNG screenshot, available for PDF and for saving image.)

9.4. Salinity

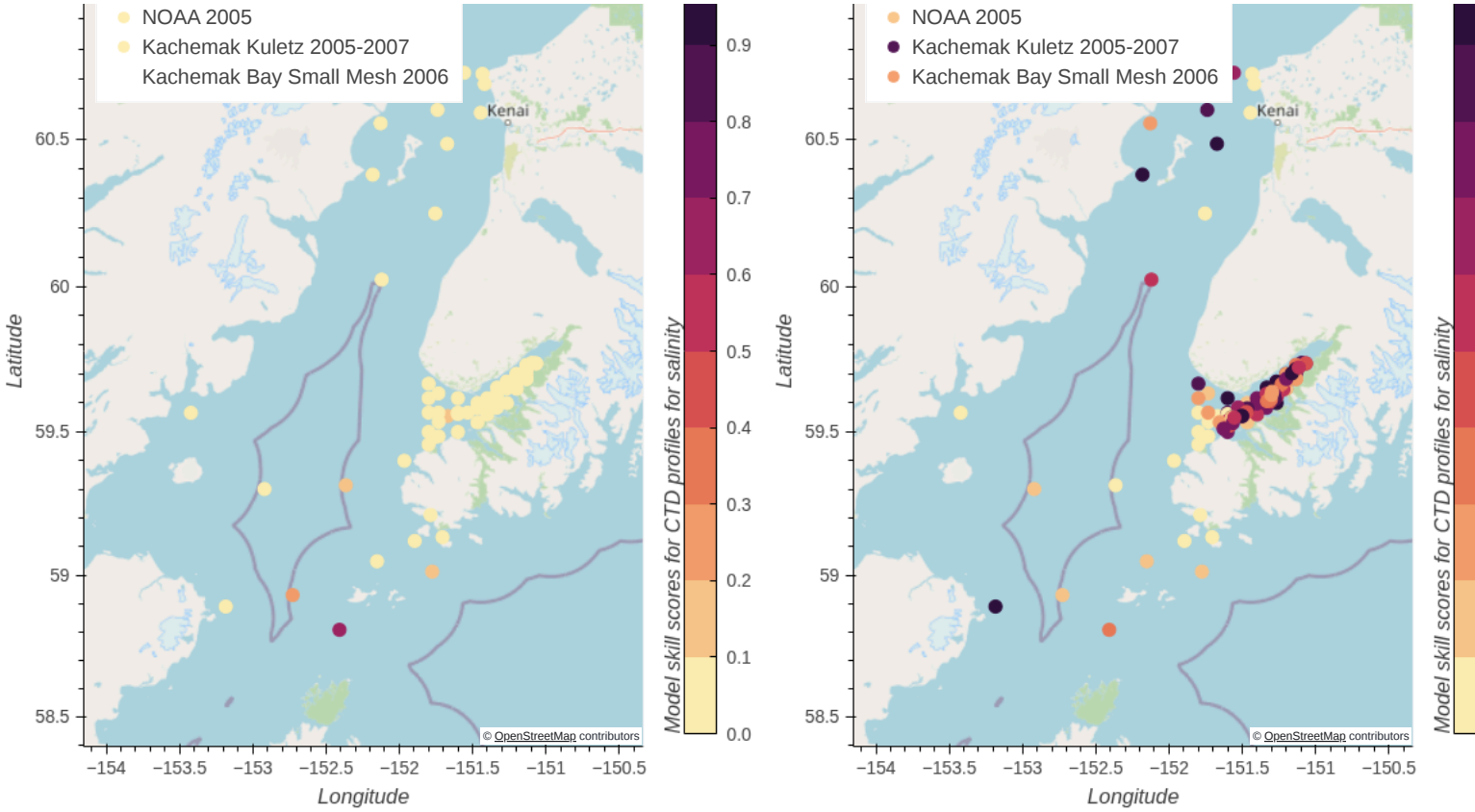

Fig. 9.7 Skill scores for CIOFS Hindcast (left) and CIOFS Freshwater (right) with CTD profiles for salinity, by project. Click on a legend entry to toggle the transparency. (HTML plot, won't show up correctly in PDF.)

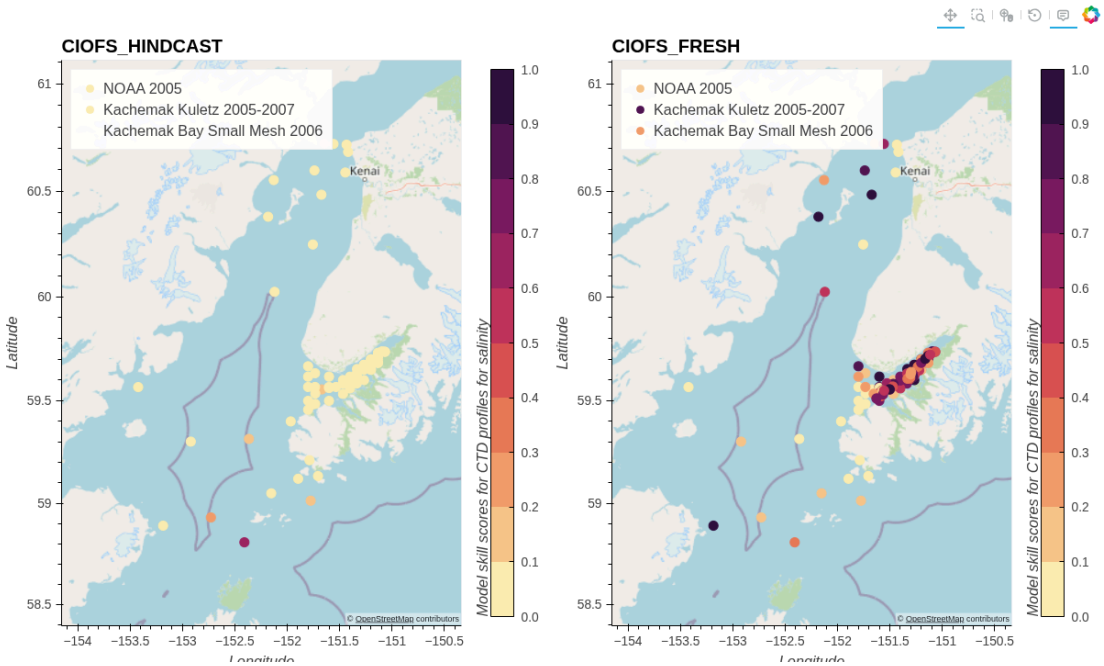

Fig. 9.8 Skill scores for CIOFS Hindcast (left) and CIOFS Freshwater (right) with CTD profiles for salinity, by project. (PNG screenshot, available for PDF and for saving image.)

10. Overview HF Radar Data

Detailed model-data comparison page: HF Radar model-data comparison page

See the original full dataset description page in the original report for more information or the new catalog page.

Note that the map shows all datasets from the catalog; it is not limited to the current report time periods.

8MB zipfile of plots

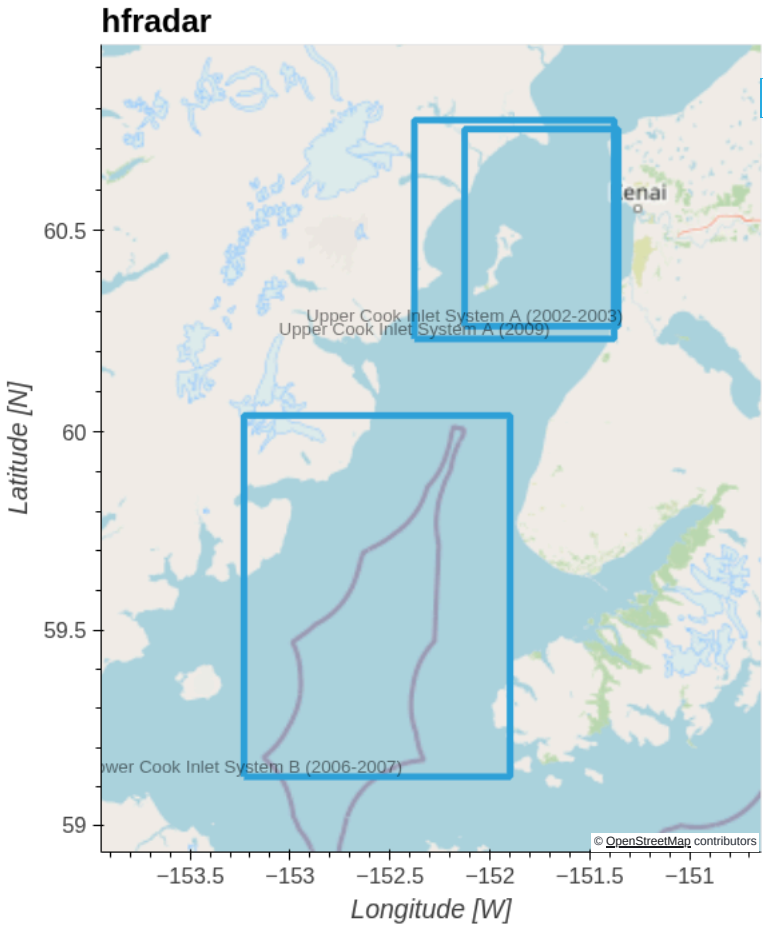

10.1. Taylor Diagrams

Taylor diagrams summarize the skill of the two models in capturing the HF Radar datasets. The data has been grouped by region (Figs. 10.1 and 10.2). Correlations are higher for the northward tidal component of velocity, which is most along-channel oriented for the HF Radar areas, than for the eastward component, and CIOFS Hindcast and Fresh perform similarly. The subtidal components are poorly captured by both models: low correlations for the eastward component and even lower and negative (not shown on plot) for the northward component. Skill scores are shown in the next plots for each dataset.

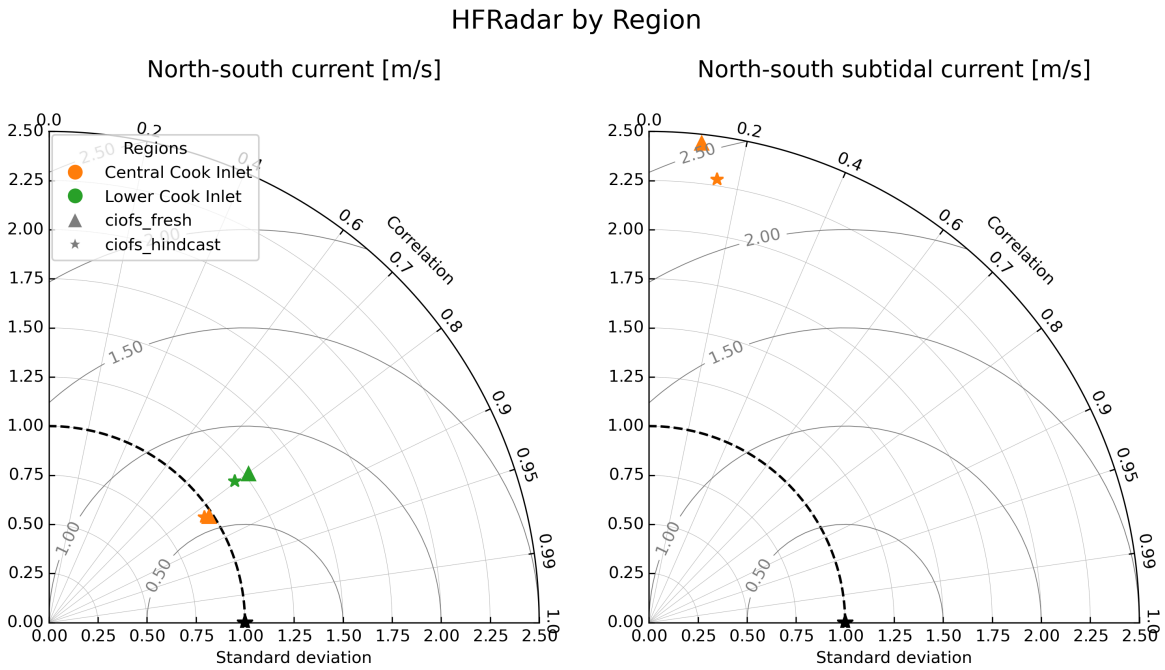

Fig. 10.1 Taylor Diagram summarizing skill of CIOFS Hindcast (stars) and CIOFS Fresh (triangles) for north-south velocity component for the full tidal signal (left) and subtidal signal (right), grouped by region of Cook Inlet, for HF Radar data.

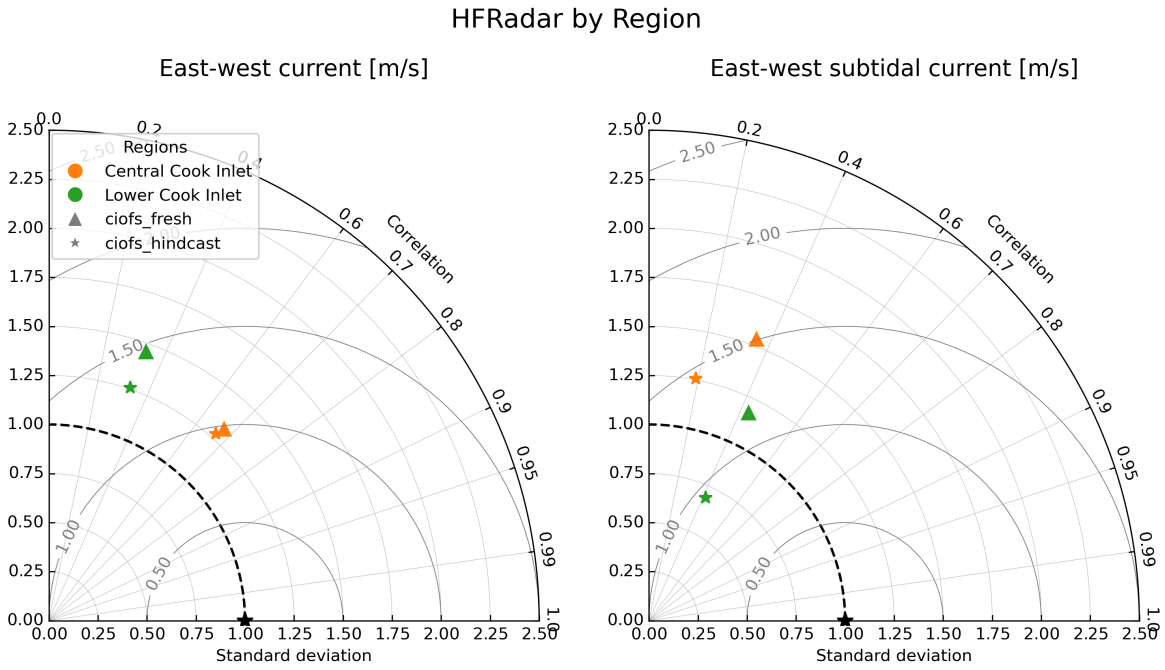

Fig. 10.2 Taylor Diagram summarizing skill of CIOFS Hindcast (stars) and CIOFS Fresh (triangles) for east-west velocity component for the full tidal signal (left) and subtidal signal (right), grouped by region of Cook Inlet, for HF Radar data.

10.2. CIOFS_HINDCAST

10.2.1. lower-ci_system-B_2006

10.2.1.1. Tidal

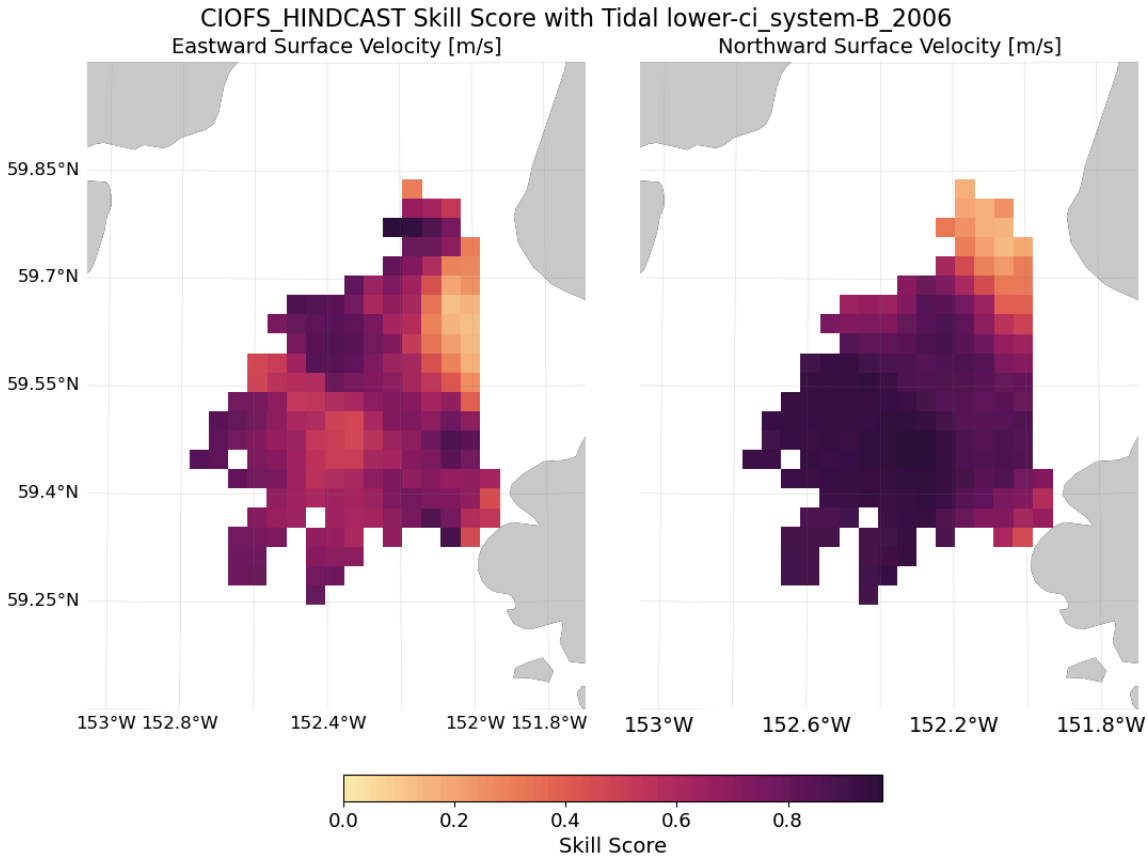

Fig. 10.3 Tidal surface currents skill score for CIOFS_HINDCAST and dataset lower-ci_system-B_2006

10.2.1.2. Subtidal

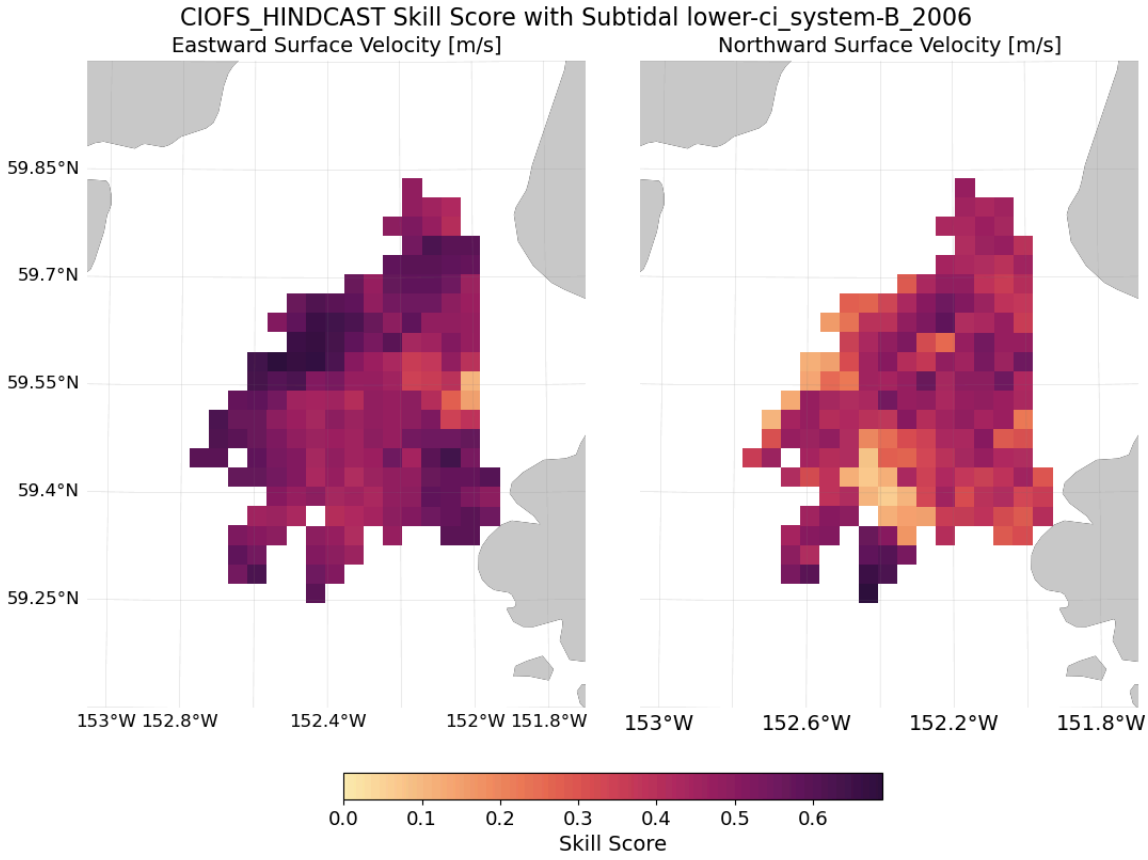

Fig. 10.4 Subtidal surface currents skill score for CIOFS_HINDCAST and dataset lower-ci_system-B_2006

10.2.2. upper-ci_system-A_2003

10.2.2.1. Tidal

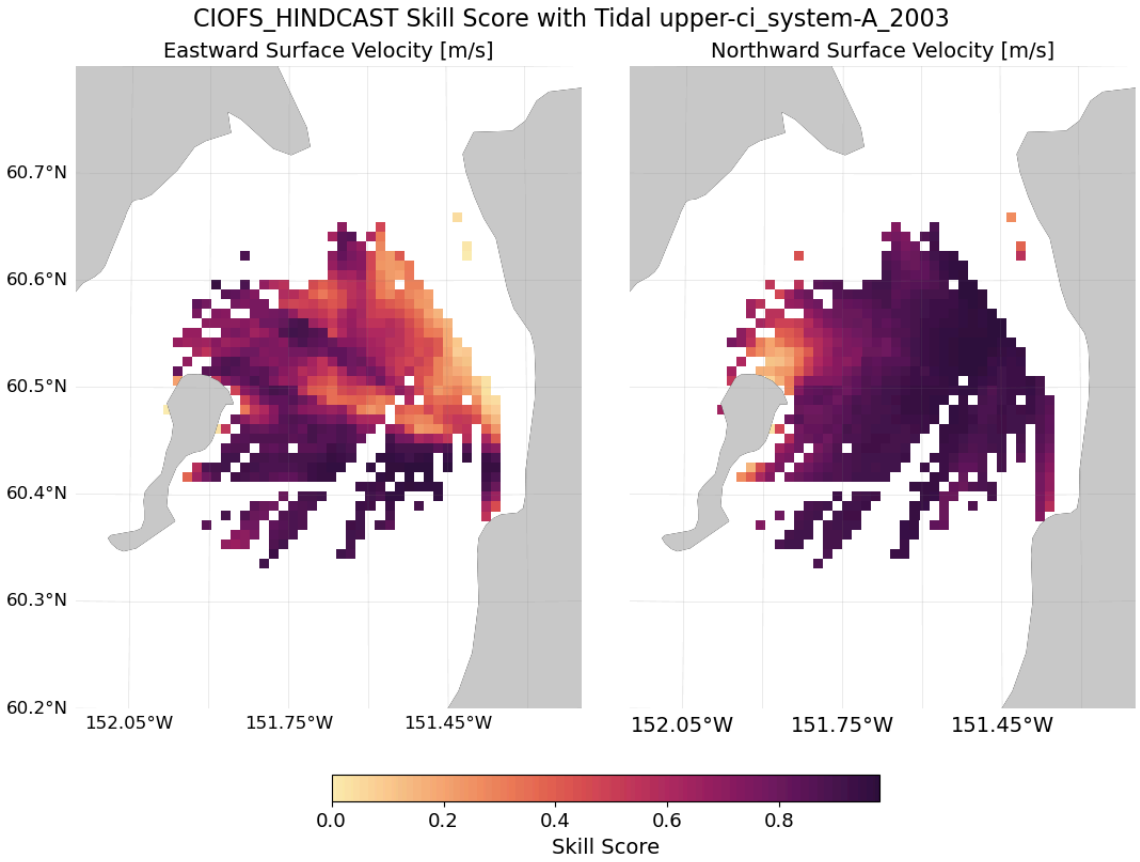

Fig. 10.5 Tidal surface currents skill score for CIOFS_HINDCAST and dataset upper-ci_system-A_2003

10.2.2.2. Subtidal

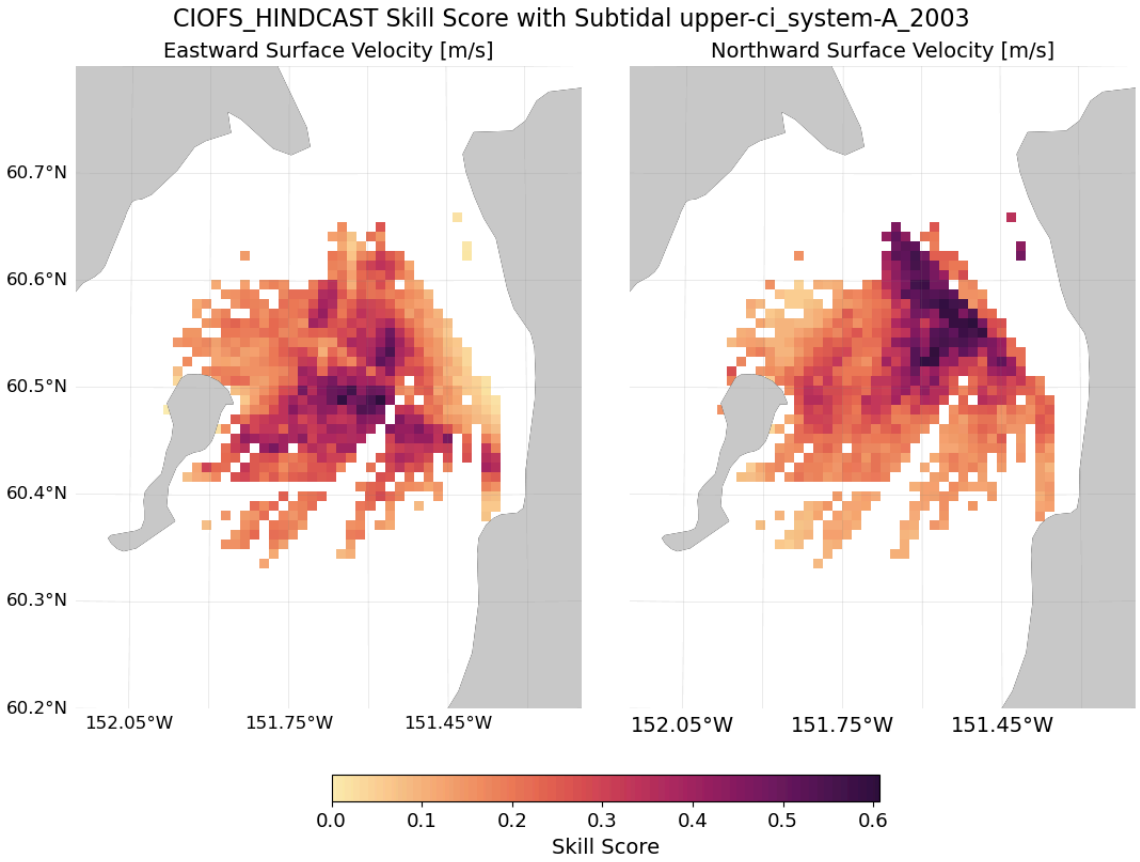

Fig. 10.6 Subtidal surface currents skill score for CIOFS_HINDCAST and dataset upper-ci_system-A_2003

10.3. CIOFS_FRESH

10.3.1. lower-ci_system-B_2006

10.3.1.1. Tidal

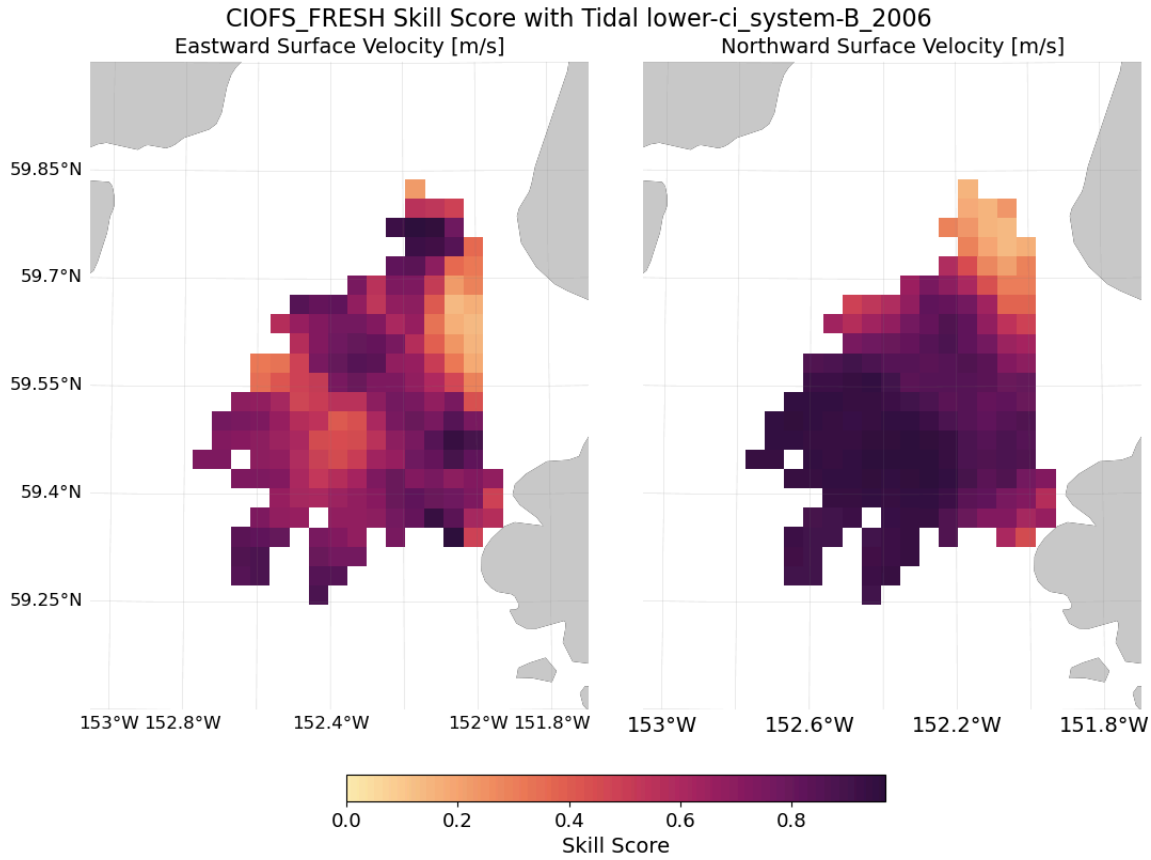

Fig. 10.7 Tidal surface currents skill score for CIOFS_FRESH and dataset lower-ci_system-B_2006

10.3.1.2. Subtidal

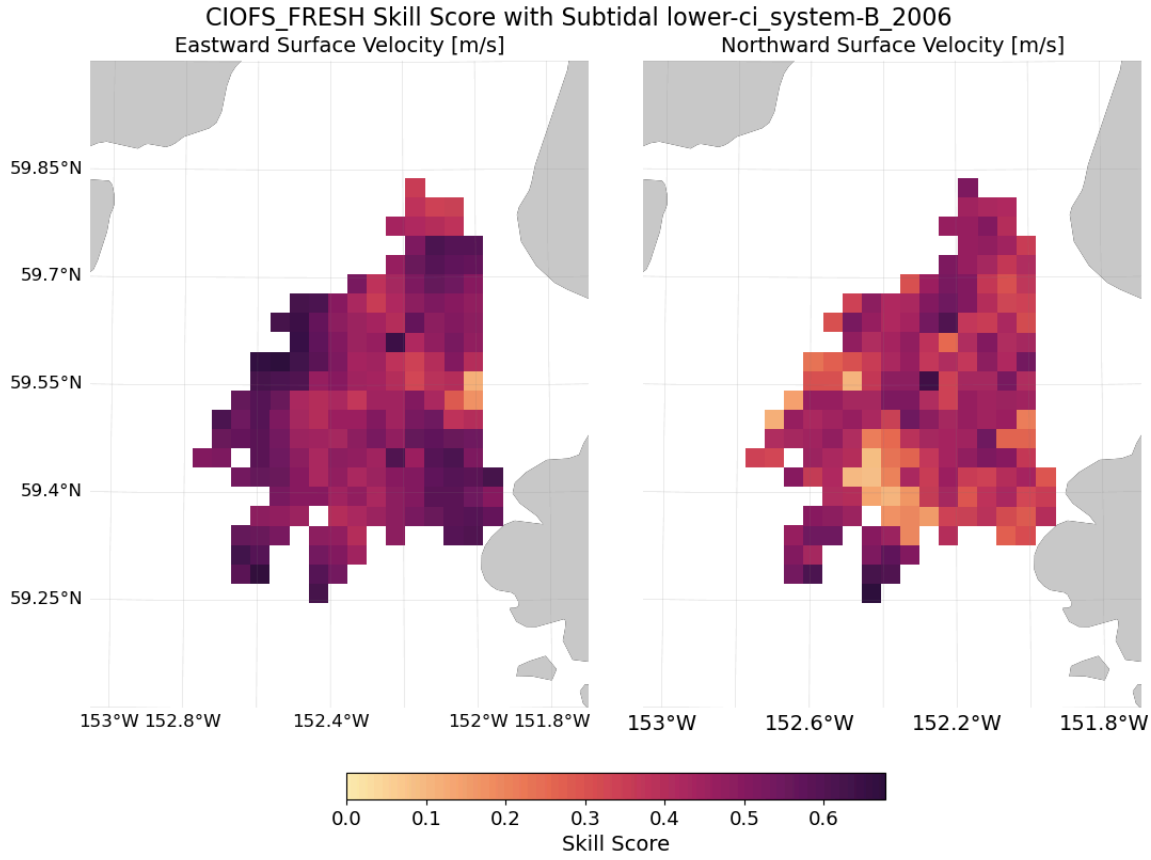

Fig. 10.8 Subtidal surface currents skill score for CIOFS_FRESH and dataset lower-ci_system-B_2006

10.3.2. upper-ci_system-A_2003

10.3.2.1. Tidal

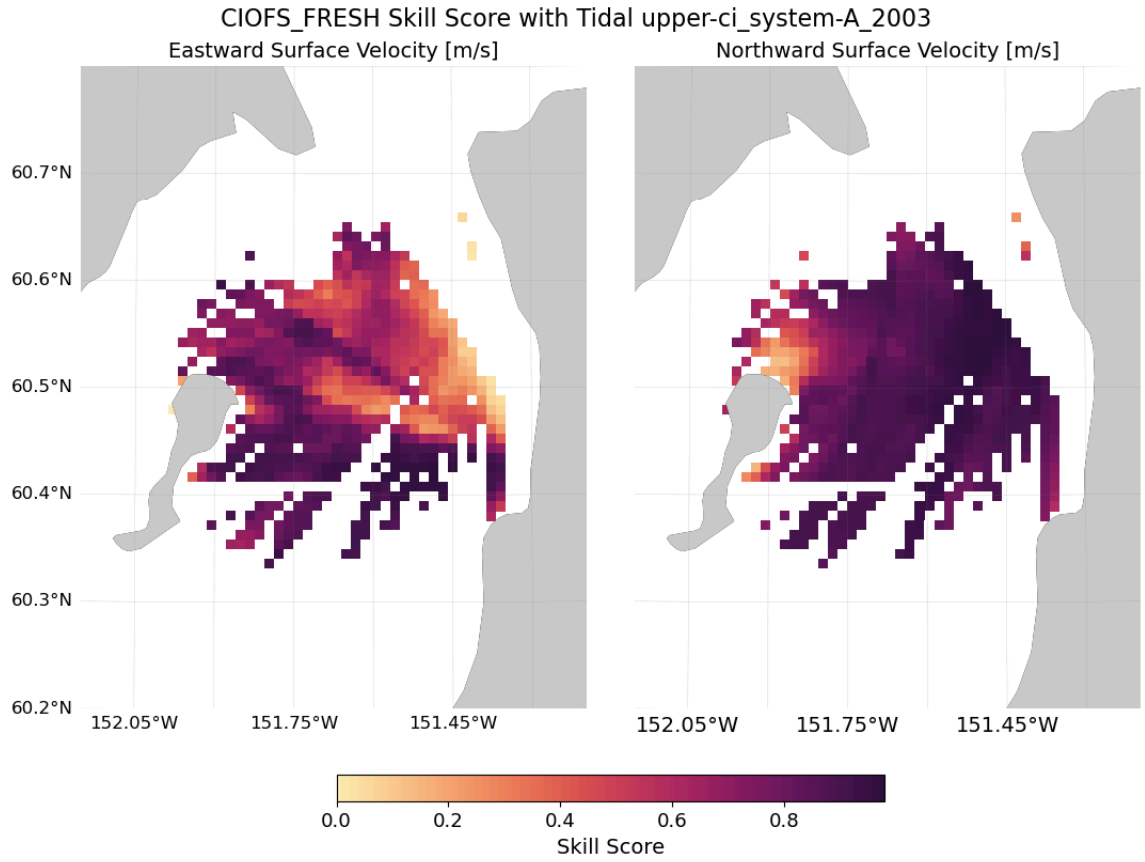

Fig. 10.9 Tidal surface currents skill score for CIOFS_FRESH and dataset upper-ci_system-A_2003

10.3.2.2. Subtidal

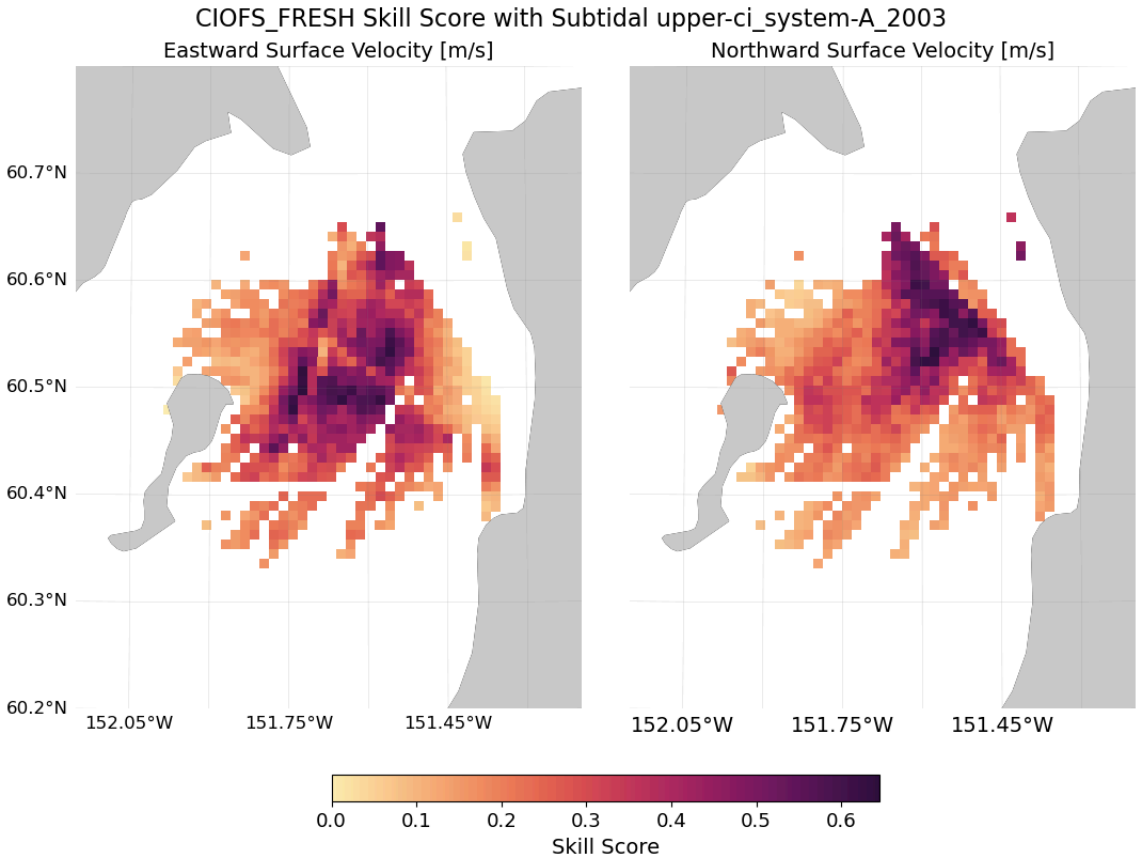

Fig. 10.10 Subtidal surface currents skill score for CIOFS_FRESH and dataset upper-ci_system-A_2003

11. Overview ADCP Data

Comparisons between each model and ADCP datasets are shown below, first in Taylor diagrams, then in maps of skill scores where each marker is colored to indicate the skill score of the comparison.

The two models perform similarly to each other with the exception of increased variance in CIOFS Fresh for subtidal variable comparisons. They both generally perform well for tidal time series and only moderately well for subtidal time series.

77MB zipfile of plots and stats files

11.1. Map of Stations

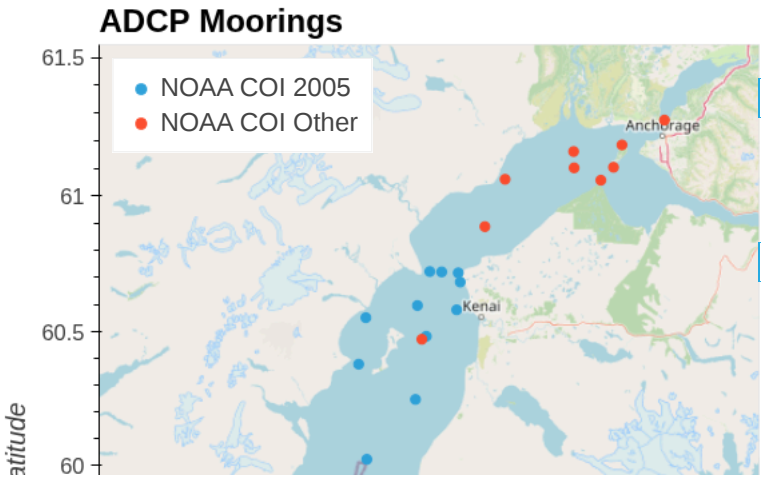

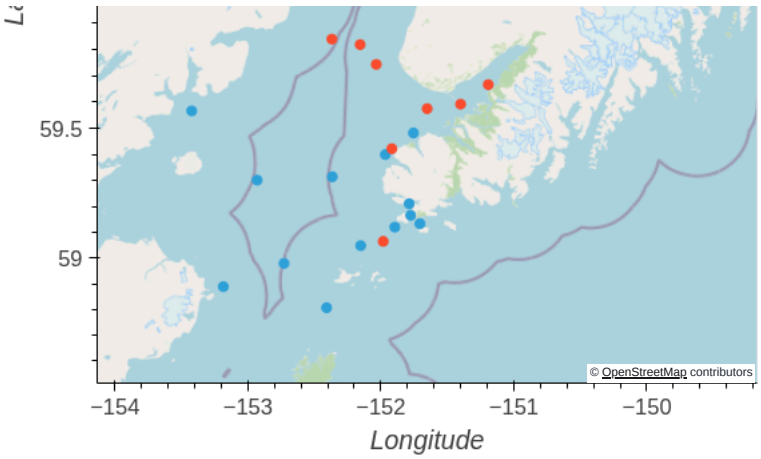

Fig. 11.1 All ADCP deployments, by project. Click on a legend entry to toggle the transparency. (HTML plot, won't show up correctly in PDF.)

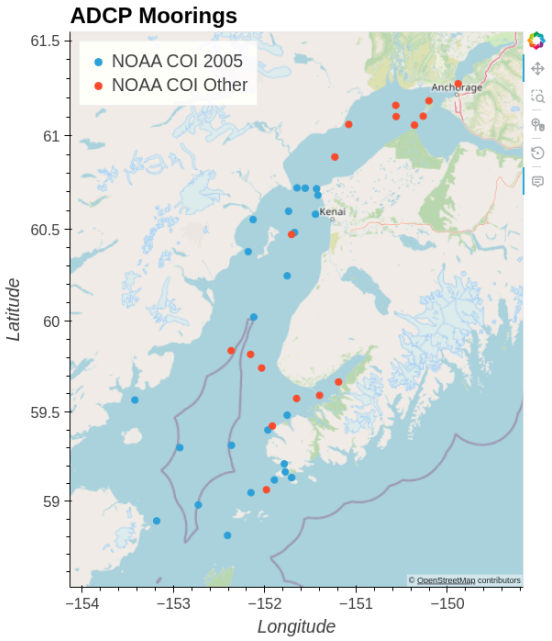

Fig. 11.2 All ADCP deployments, by project. (PNG screenshot, available for PDF and for saving image.)

11.2. Taylor Diagrams

Taylor diagrams summarize the skill of the two models in capturing the ADCP moorings. The data has been grouped by region (Figs. 11.3, 11.4, 11.5) and season (Figs. 11.6, 11.7, 11.8). The results show that CIOFS fresh and CIOFS hindcast perform similarly for tidal results. For the subtidal along-channel velocity component by region, CIOFS Hindcast and CIOFS Fresh have mostly similar correlation coefficients, but CIOFS Fresh has more accurate variance. By season, CIOFS Fresh has more accurate variance again though in the spring both models have too high of variance. For the across-channel subtidal component, the two models again have similar correlation coefficients but CIOFS Fresh has more accurate variance in Upper Cook Inlet; in Kachemak Bay and Central Cook Inlet CIOFS Hindcast is more accurate. When considering subtidal speed, we see that the two models perform similarly to each other. Skill scores are shown in the next plots for each dataset.

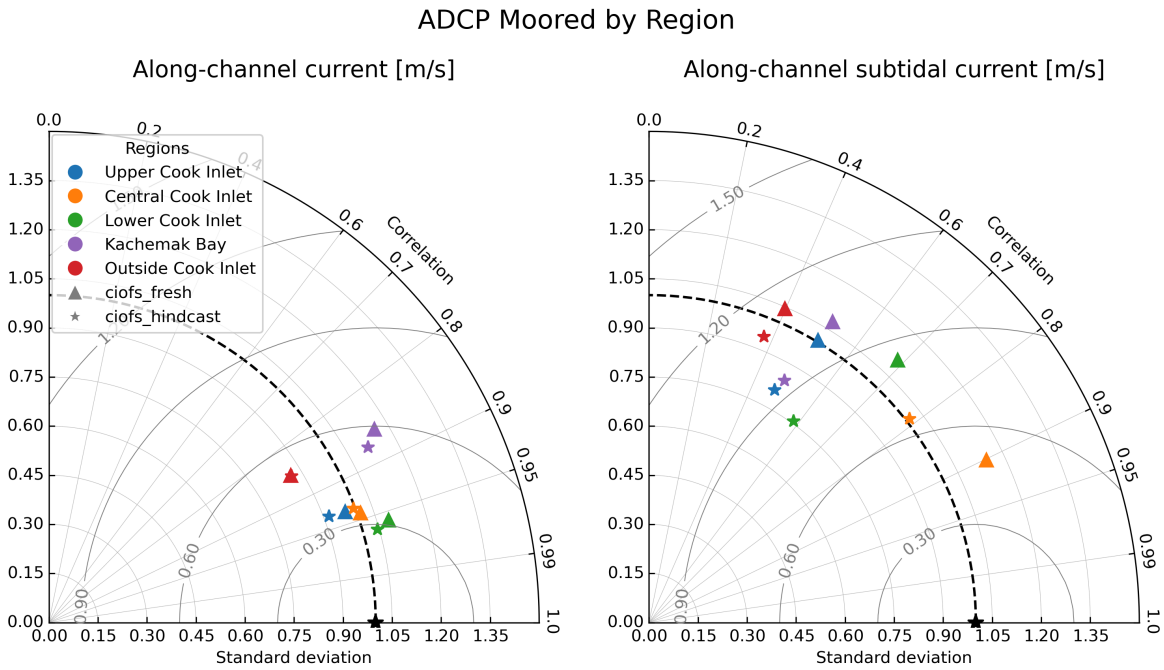

Fig. 11.3 Taylor Diagram summarizing skill of CIOFS Hindcast (stars) and CIOFS Fresh (triangles) for the along-channel component of velocity with tides (left) and subtidal (right), grouped by region of Cook Inlet, for moored ADCP datasets.

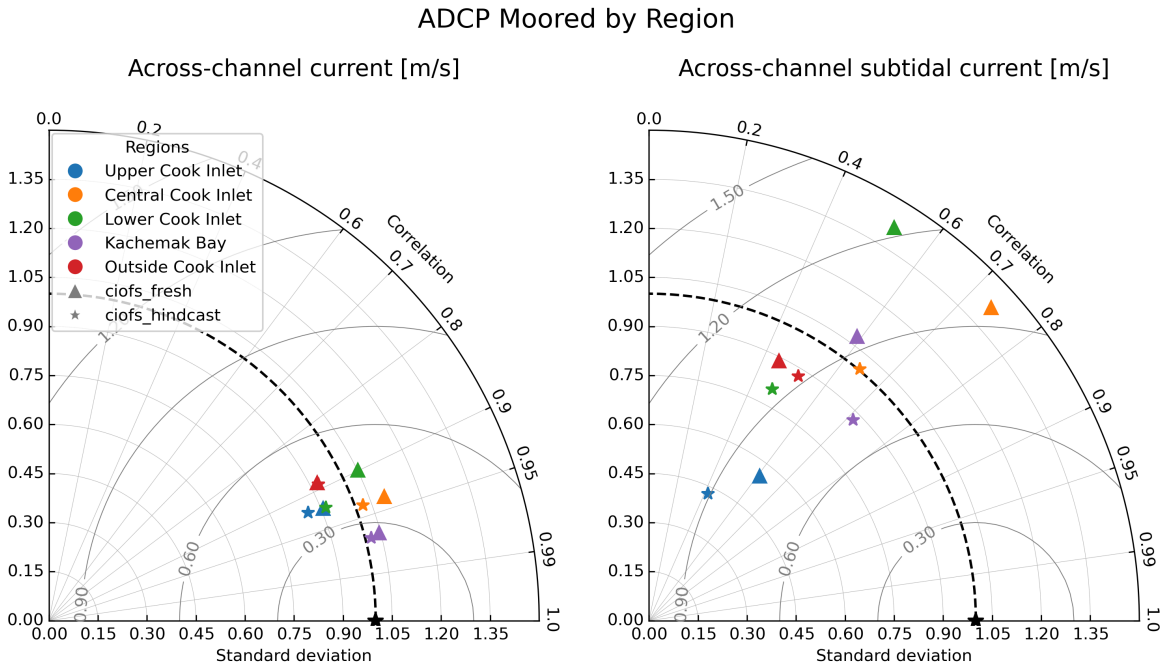

Fig. 11.4 Taylor Diagram summarizing skill of CIOFS Hindcast (stars) and CIOFS Fresh (triangles) for the across-channel component of velocity with tides (left) and subtidal (right), grouped by region of Cook Inlet, for moored ADCP datasets.

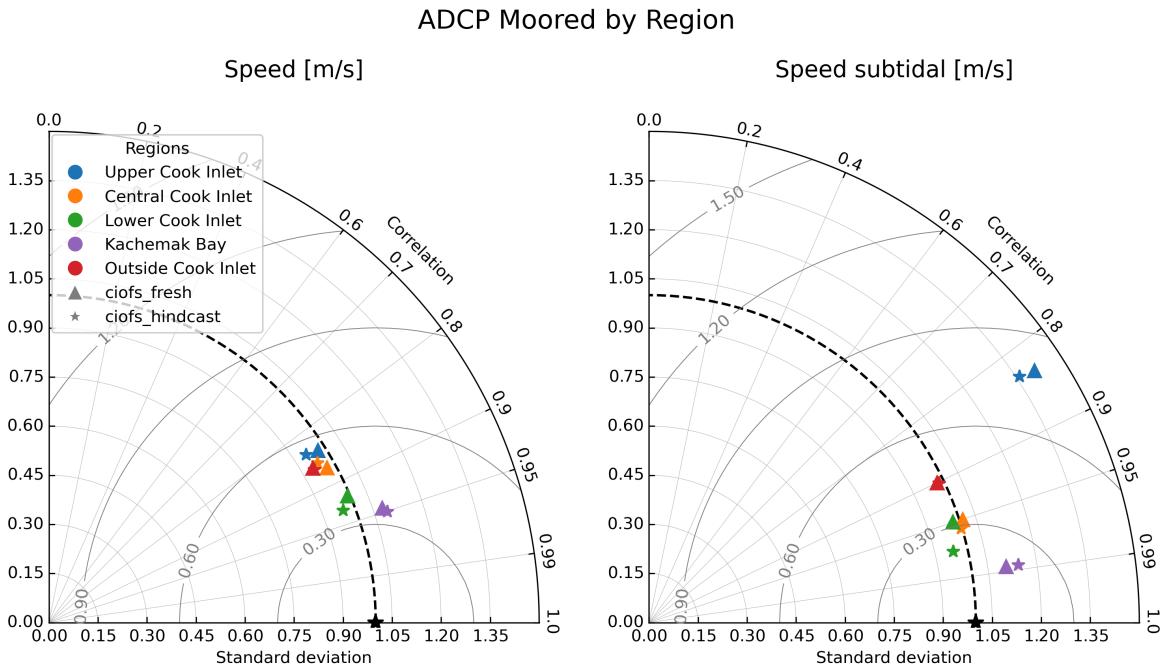

Fig. 11.5 Taylor Diagram summarizing skill of CIOFS Hindcast (stars) and CIOFS Fresh (triangles) for the magnitude of velocity with tides (left) and subtidal (right), grouped by region of Cook Inlet, for moored ADCP datasets.

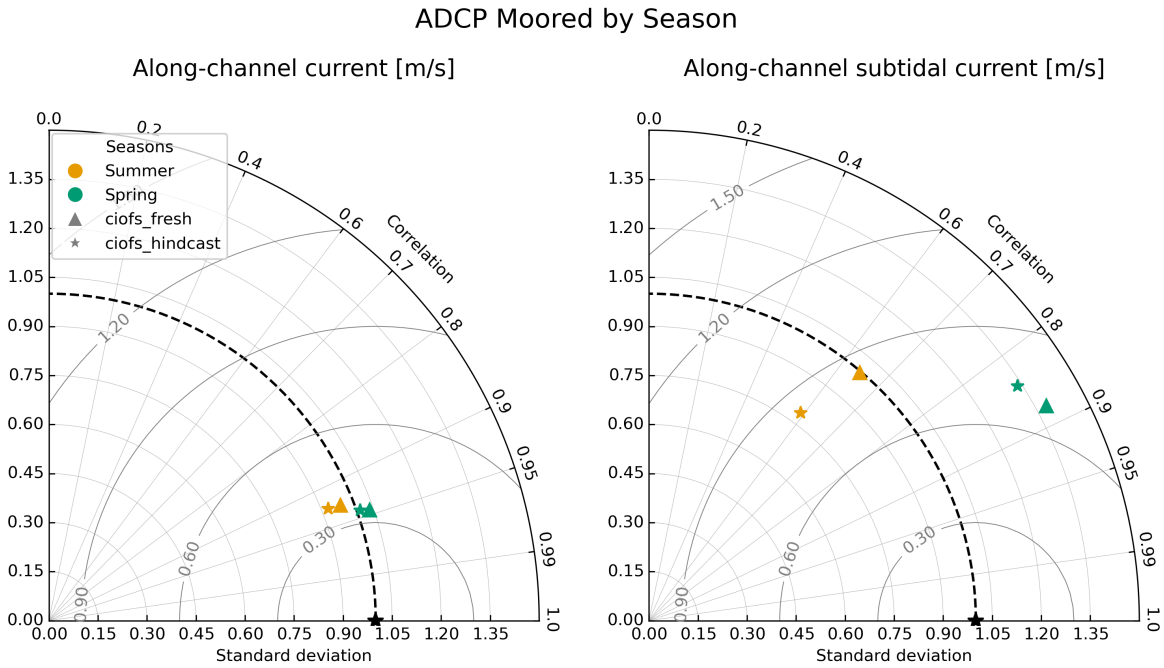

Fig. 11.6 Taylor Diagram summarizing skill of CIOFS Hindcast (stars) and CIOFS Fresh (triangles) for the along-channel component of velocity with tides (left) and subtidal (right), grouped by season, for moored ADCP datasets.

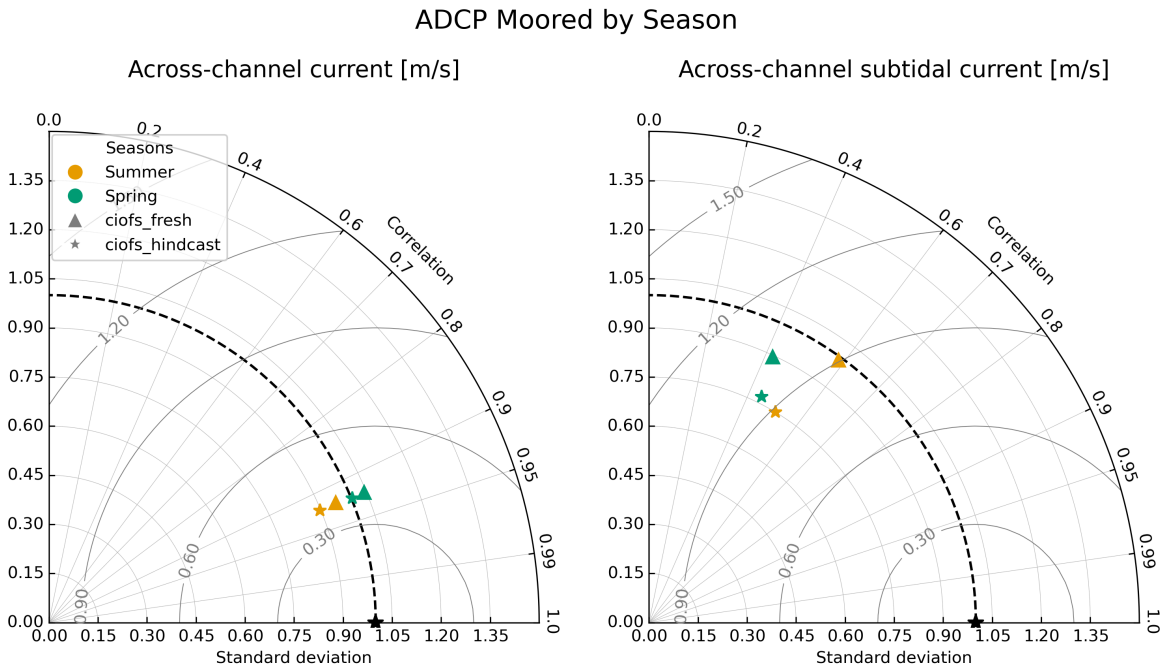

Fig. 11.7 Taylor Diagram summarizing skill of CIOFS Hindcast (stars) and CIOFS Fresh (triangles) for the across-channel component of velocity with tides (left) and subtidal (right), grouped by season, for moored ADCP datasets.

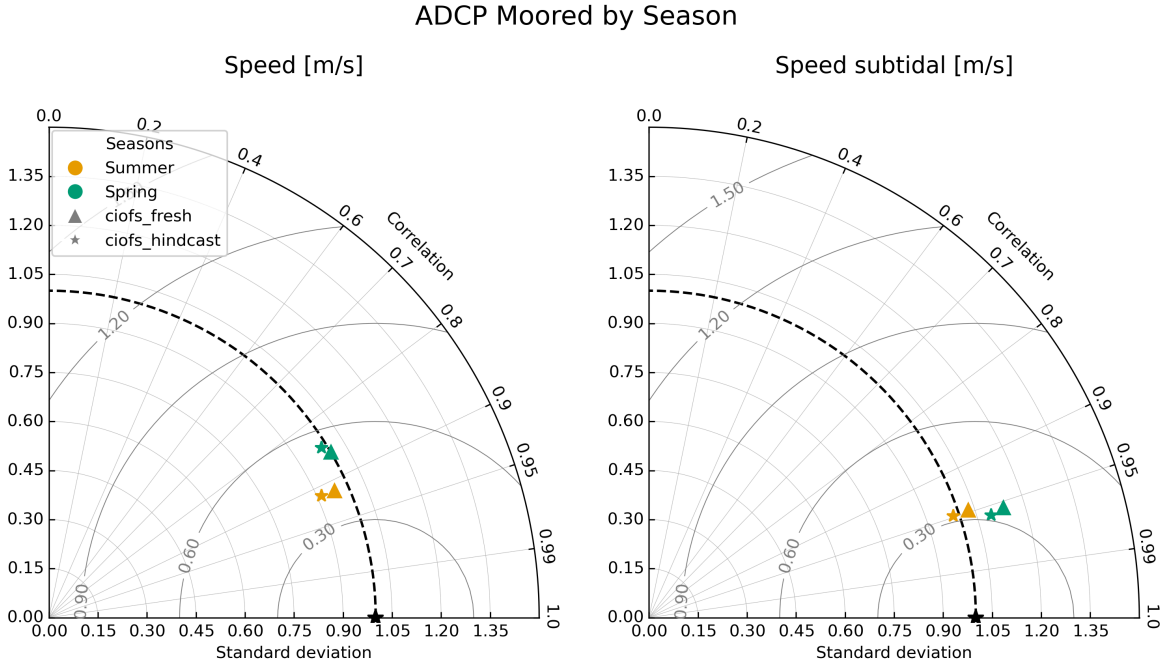

Fig. 11.8 Taylor Diagram summarizing skill of CIOFS Hindcast (stars) and CIOFS Fresh (triangles) for the magnitude of velocity with tides (left) and subtidal (right), grouped by season, for moored ADCP datasets.

11.3. Tidal

11.3.1. Horizontal Speed

CIOFS_HINDCAST CIOFS_FRESH

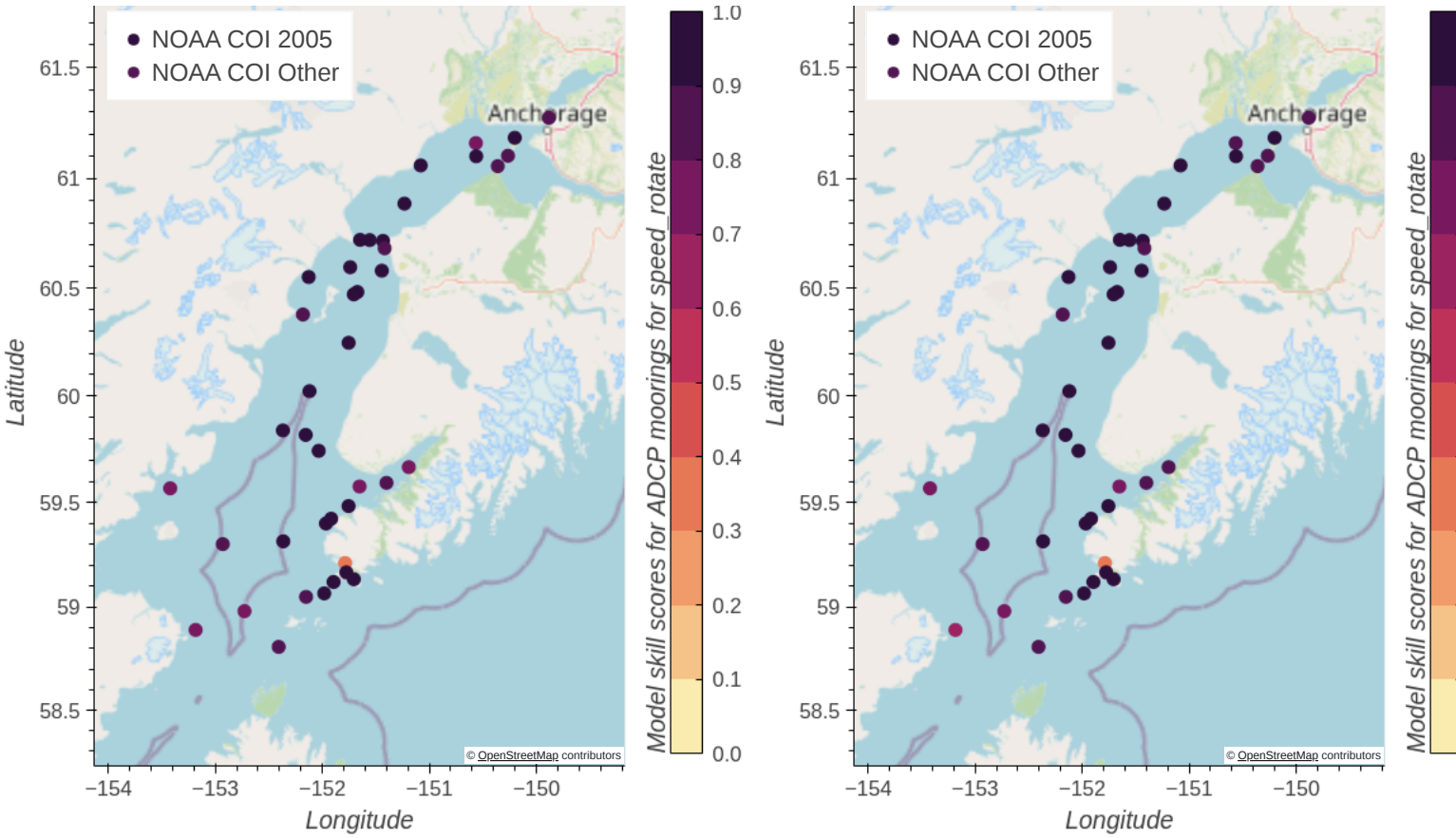

Fig. 11.9 Skill scores for CIOFS Hindcast (left) and CIOFS Freshwater (right) with ADCP moorings for horizontal speed, by project. Click on a legend entry to toggle the transparency. (HTML plot, won't show up correctly in PDF.)

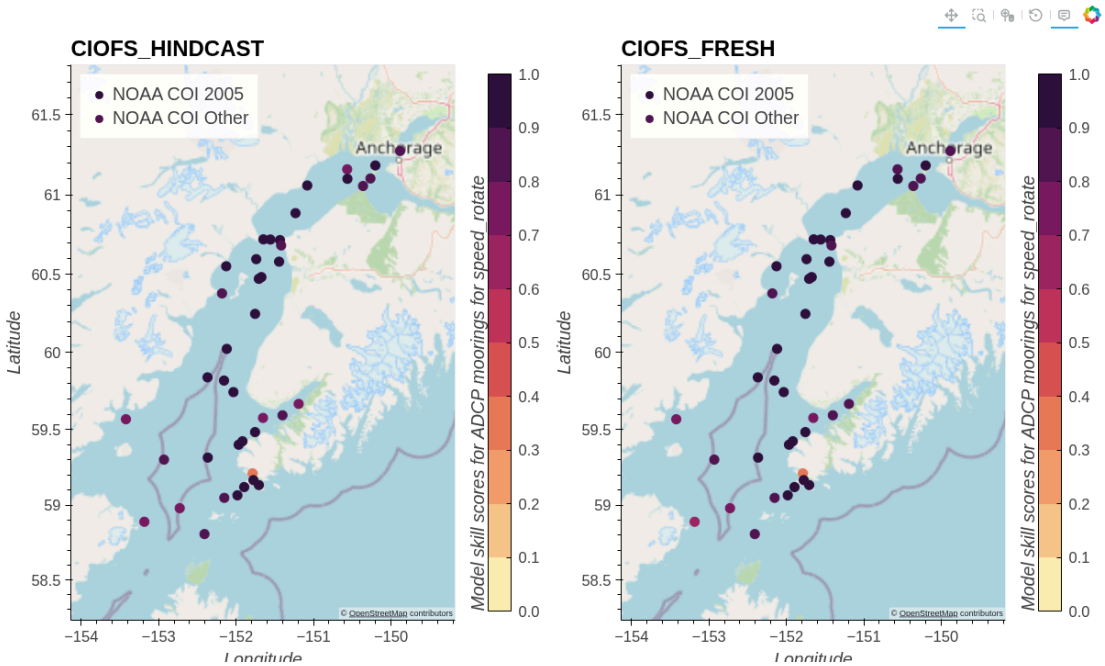

Fig. 11.10 Skill scores for CIOFS Hindcast (left) and CIOFS Freshwater (right) with ADCP moorings for horizontal speed, by project. (PNG screenshot, available for PDF and for saving image.)

11.3.2. Along-Channel Velocity

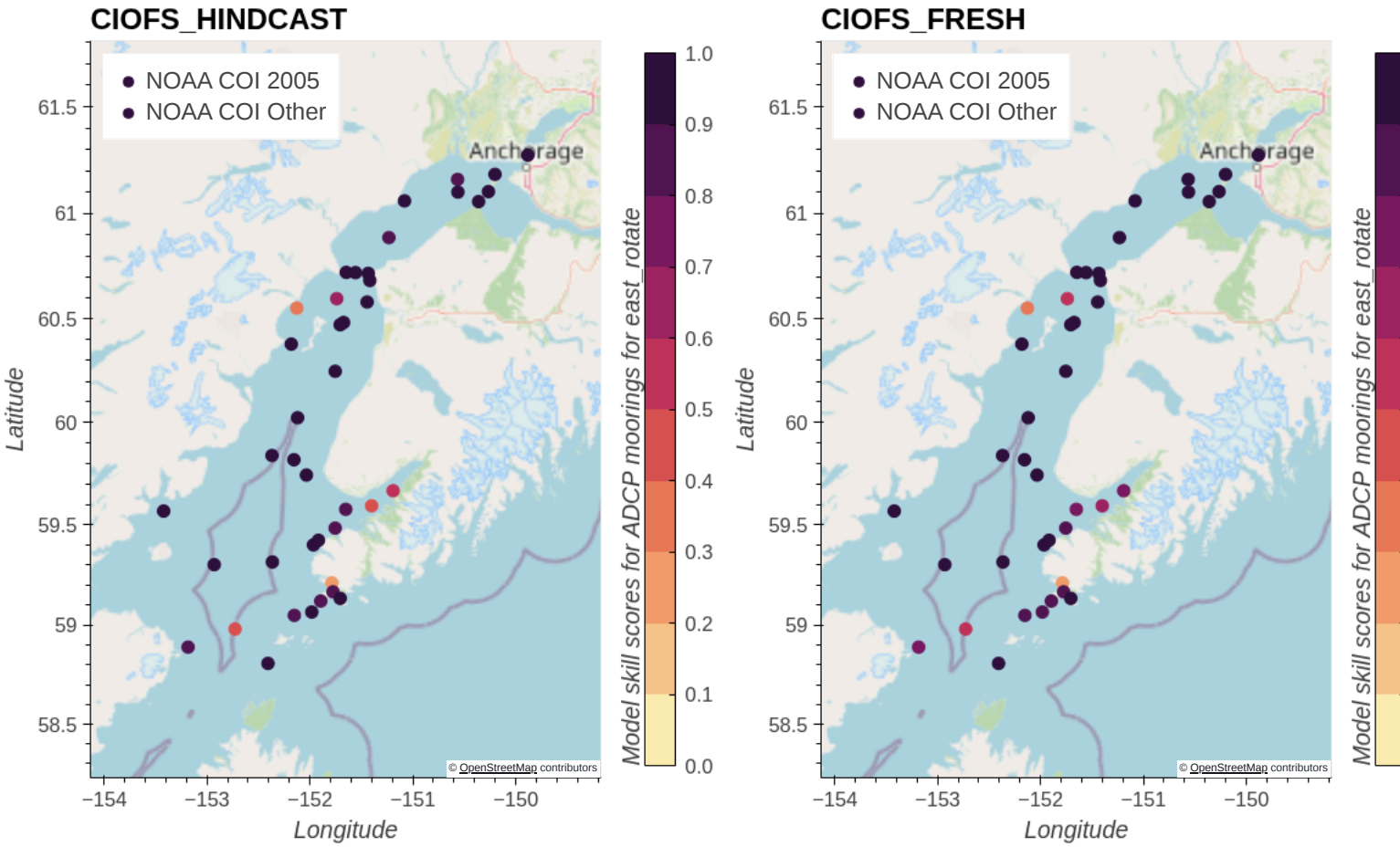

Fig. 11.11 Skill scores for CIOFS Hindcast (left) and CIOFS Freshwater (right) with ADCP moorings for along-channel velocity, by project. Click on a legend entry to toggle the transparency. (HTML plot, won't show up correctly in PDF.)

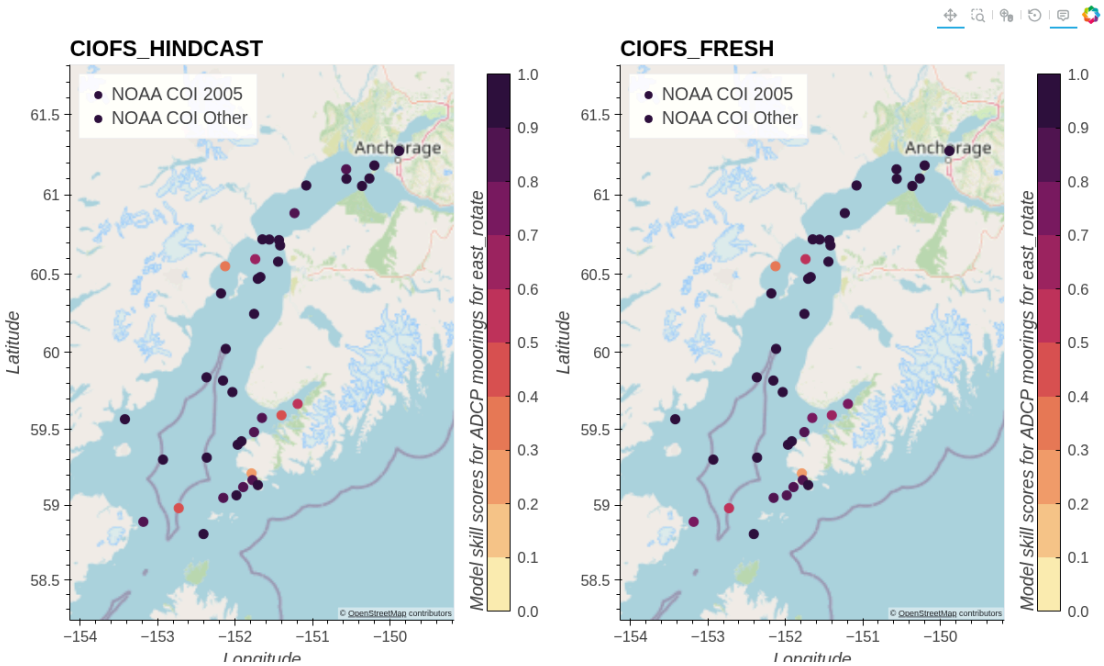

Fig. 11.12 Skill scores for CIOFS Hindcast (left) and CIOFS Freshwater (right) with ADCP moorings for along-channel velocity, by project. (PNG screenshot, available for PDF and for saving image.)

11.3.3. Across-Channel Velocity

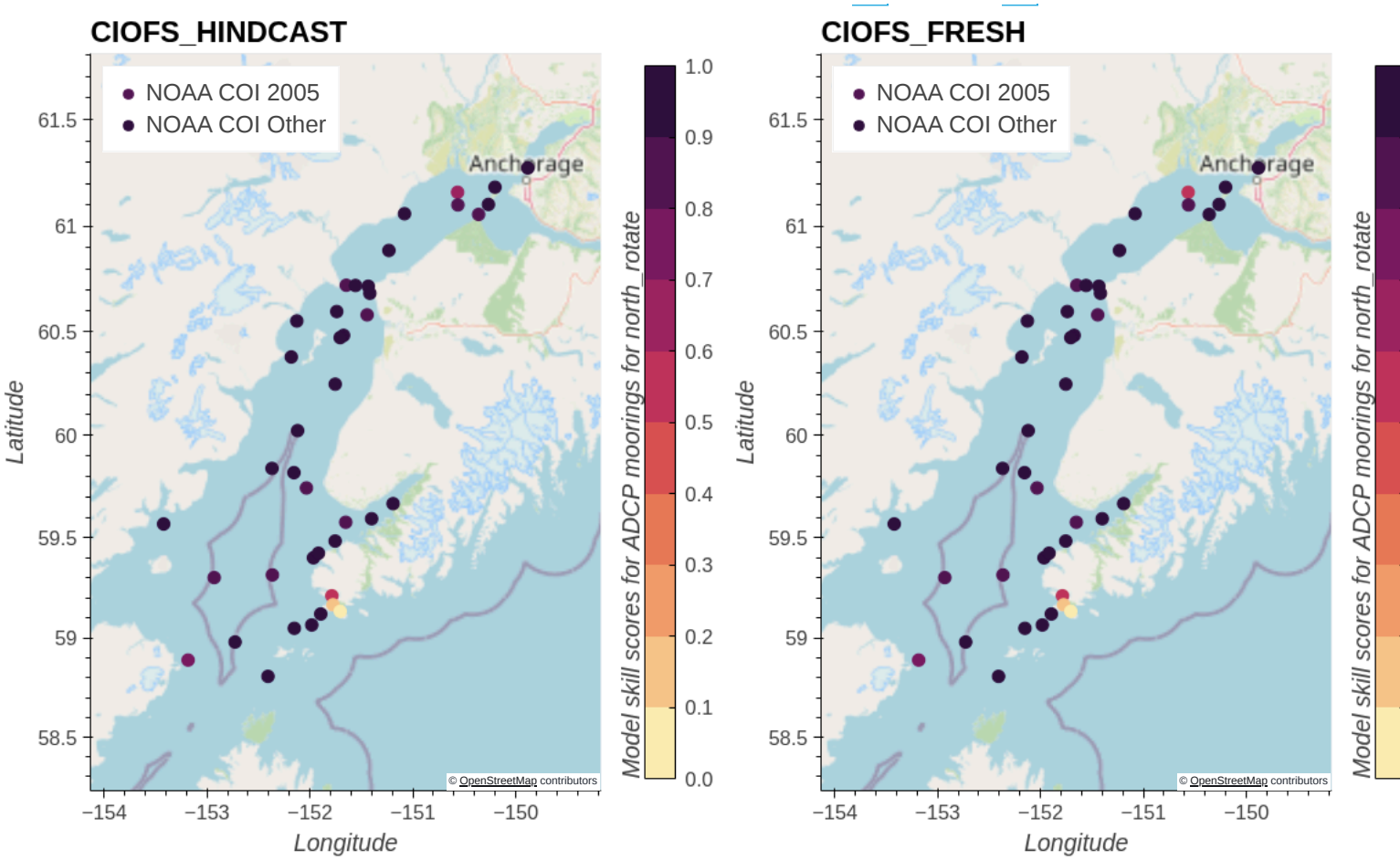

Fig. 11.13 Skill scores for CIOFS Hindcast (left) and CIOFS Freshwater (right) with ADCP moorings for across-channel velocity, by project. Click on a legend entry to toggle the transparency. (HTML plot, won't show up correctly in PDF.)

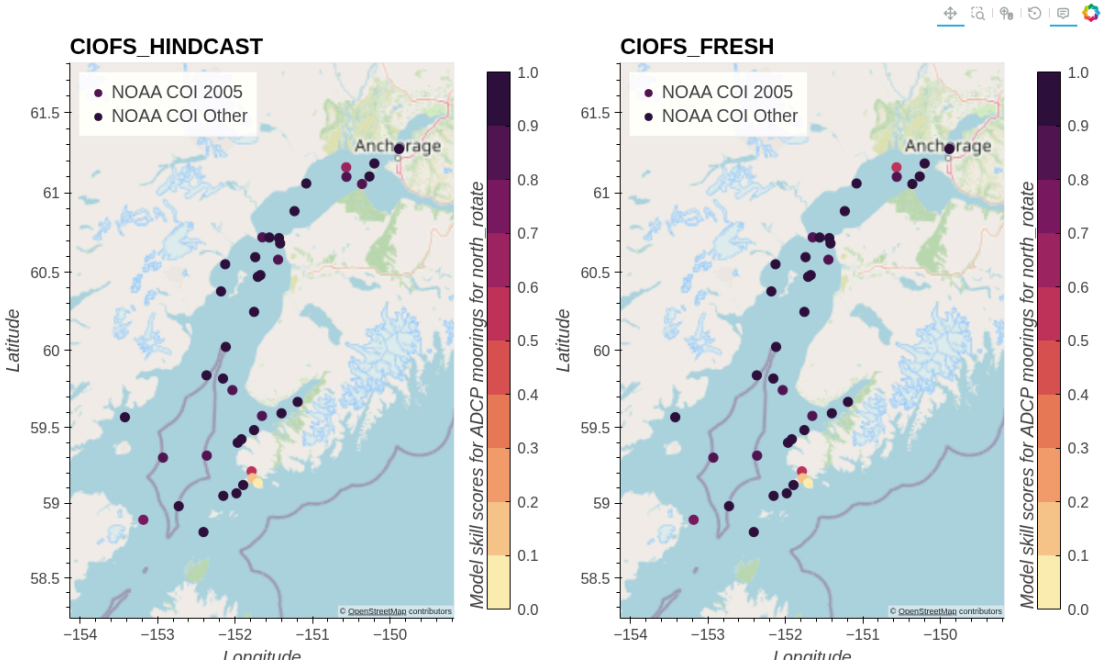

Fig. 11.14 Skill scores for CIOFS Hindcast (left) and CIOFS Freshwater (right) with ADCP moorings for across-channel velocity, by project. (PNG screenshot, available for PDF and for saving image.)

11.4. Subtidal

11.4.1. Horizontal Speed

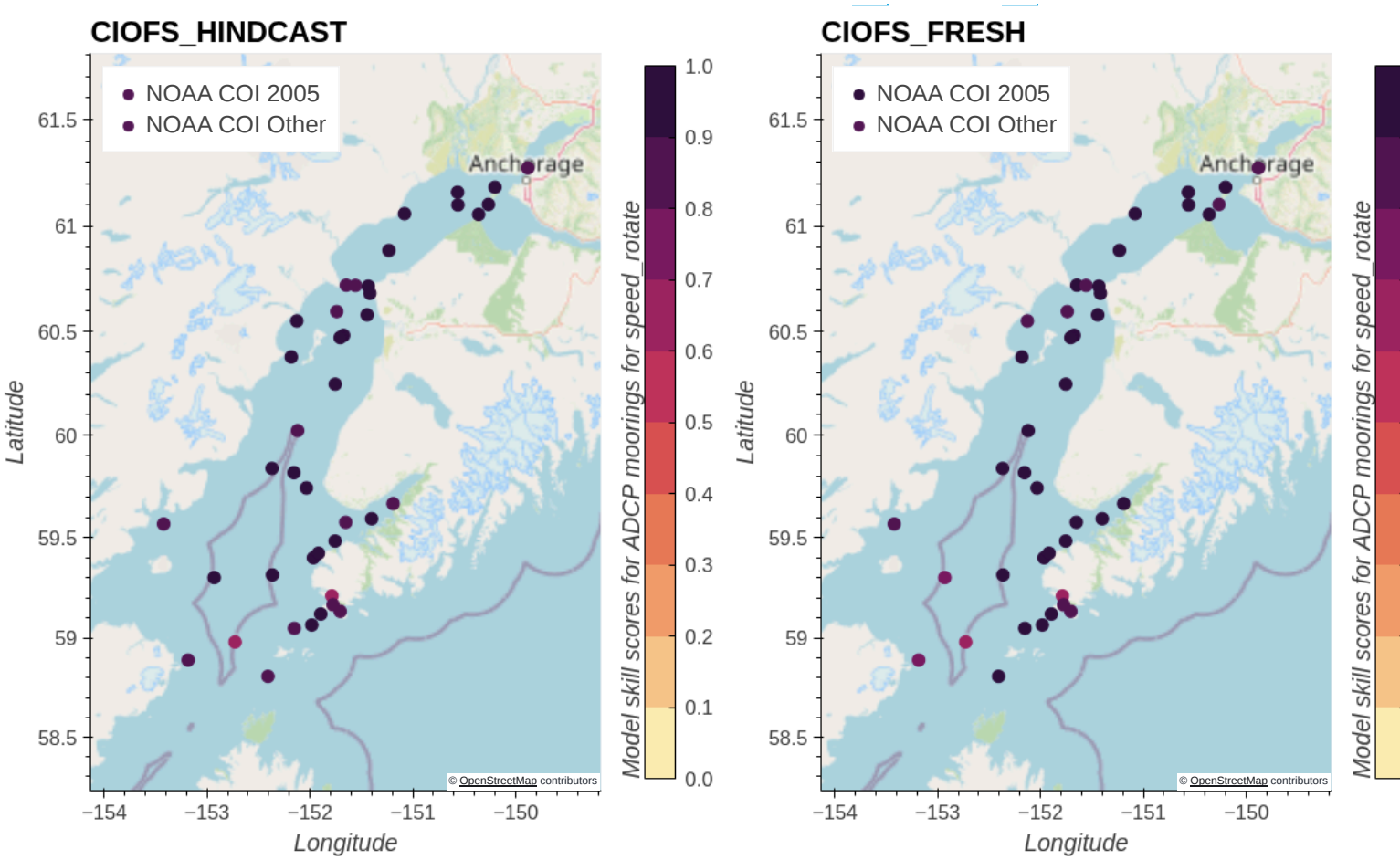

Fig. 11.15 Skill scores for CIOFS Hindcast (left) and CIOFS Freshwater (right) with ADCP moorings for subtidal horizontal speed, by project. Click on a legend entry to toggle the transparency. (HTML plot, won't show up correctly in PDF.)

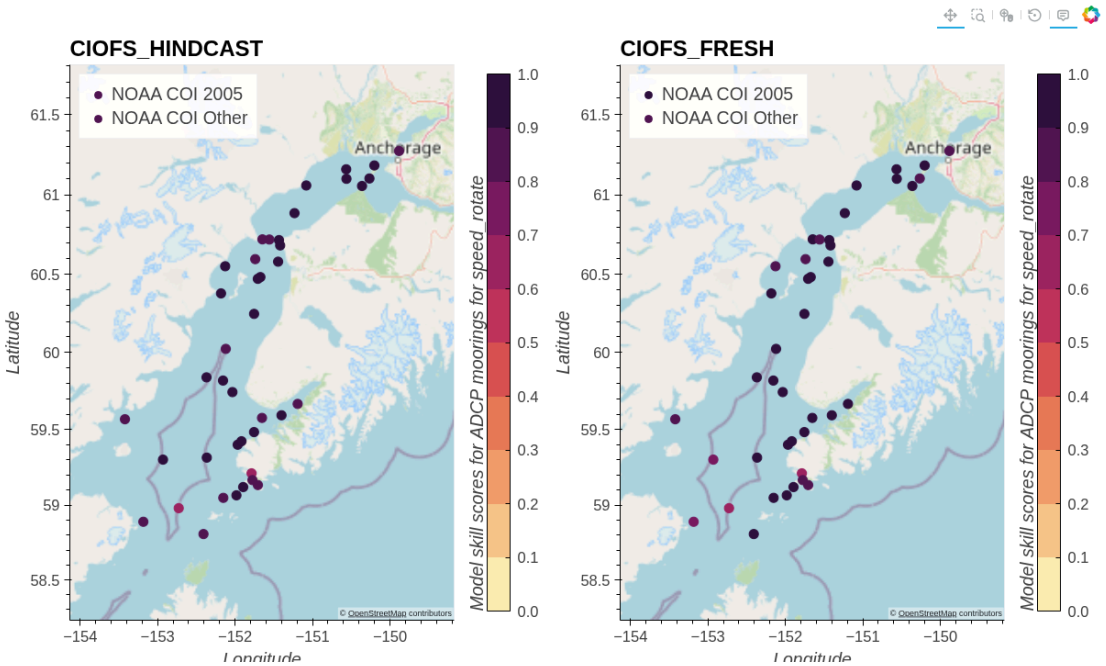

Fig. 11.16 Skill scores for CIOFS Hindcast (left) and CIOFS Freshwater (right) with ADCP moorings for subtidal horizontal speed, by project. (PNG screenshot, available for PDF and for saving image.)

11.4.2. Along-Channel Velocity

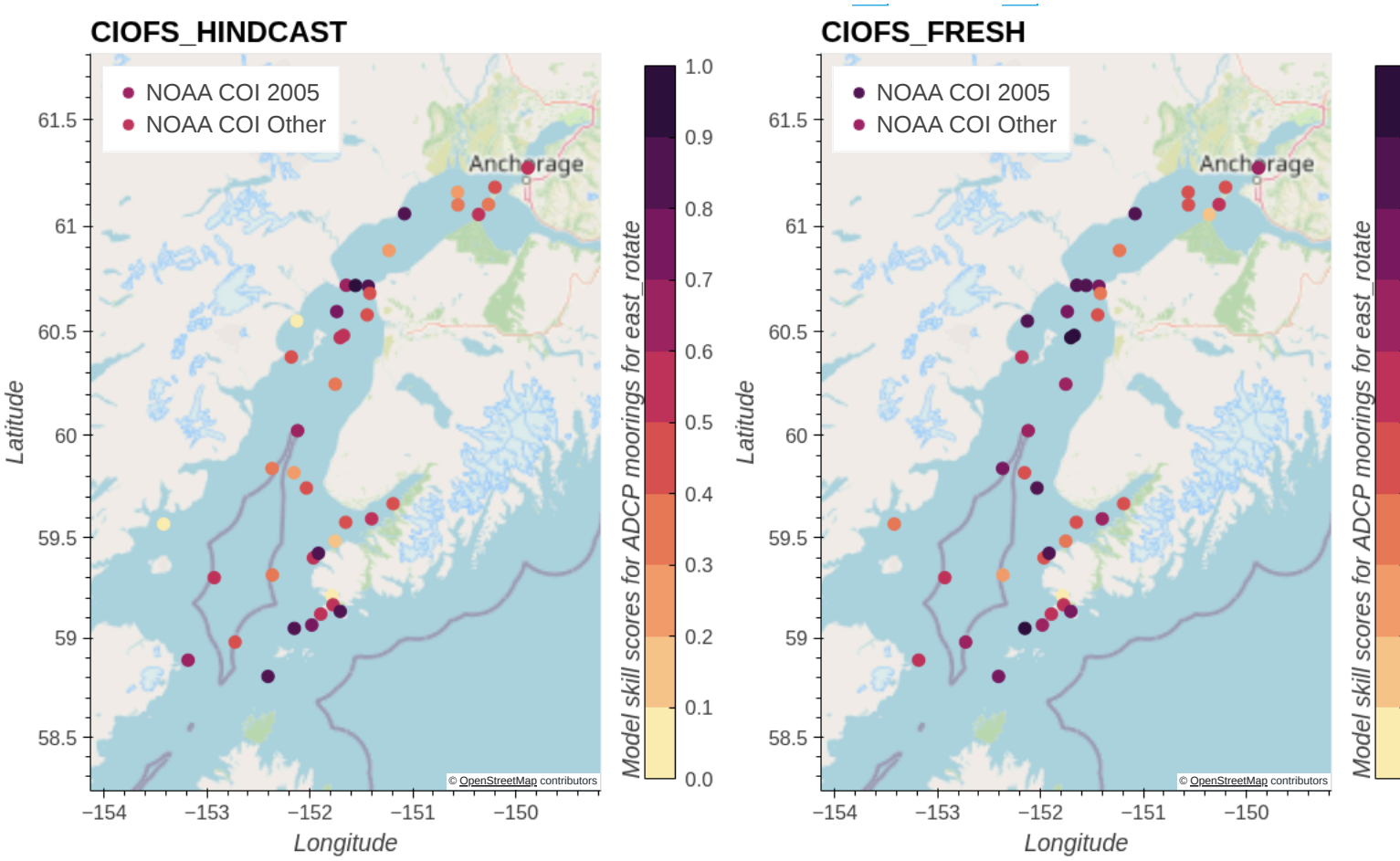

Fig. 11.17 Skill scores for CIOFS Hindcast (left) and CIOFS Freshwater (right) with ADCP moorings for subtidal along-channel velocity, by project. Click on a legend entry to toggle the transparency. (HTML plot, won't show up correctly in PDF.)

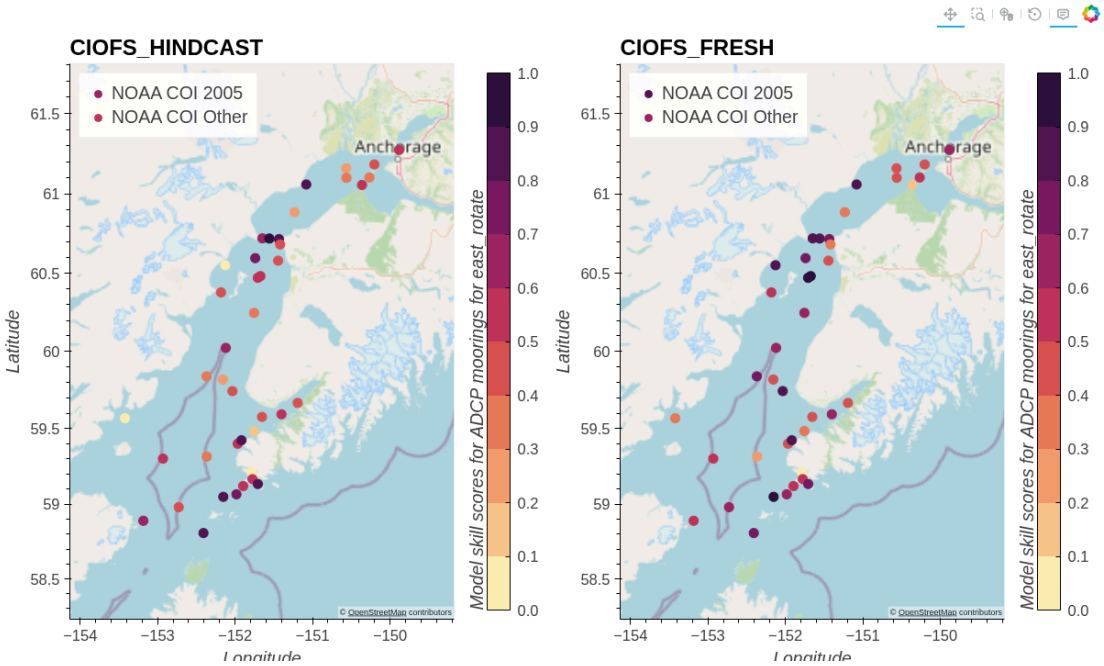

Fig. 11.18 Skill scores for CIOFS Hindcast (left) and CIOFS Freshwater (right) with ADCP moorings for subtidal along-channel velocity, by project. (PNG screenshot, available for PDF and for saving image.)

11.4.3. Across-Channel Velocity

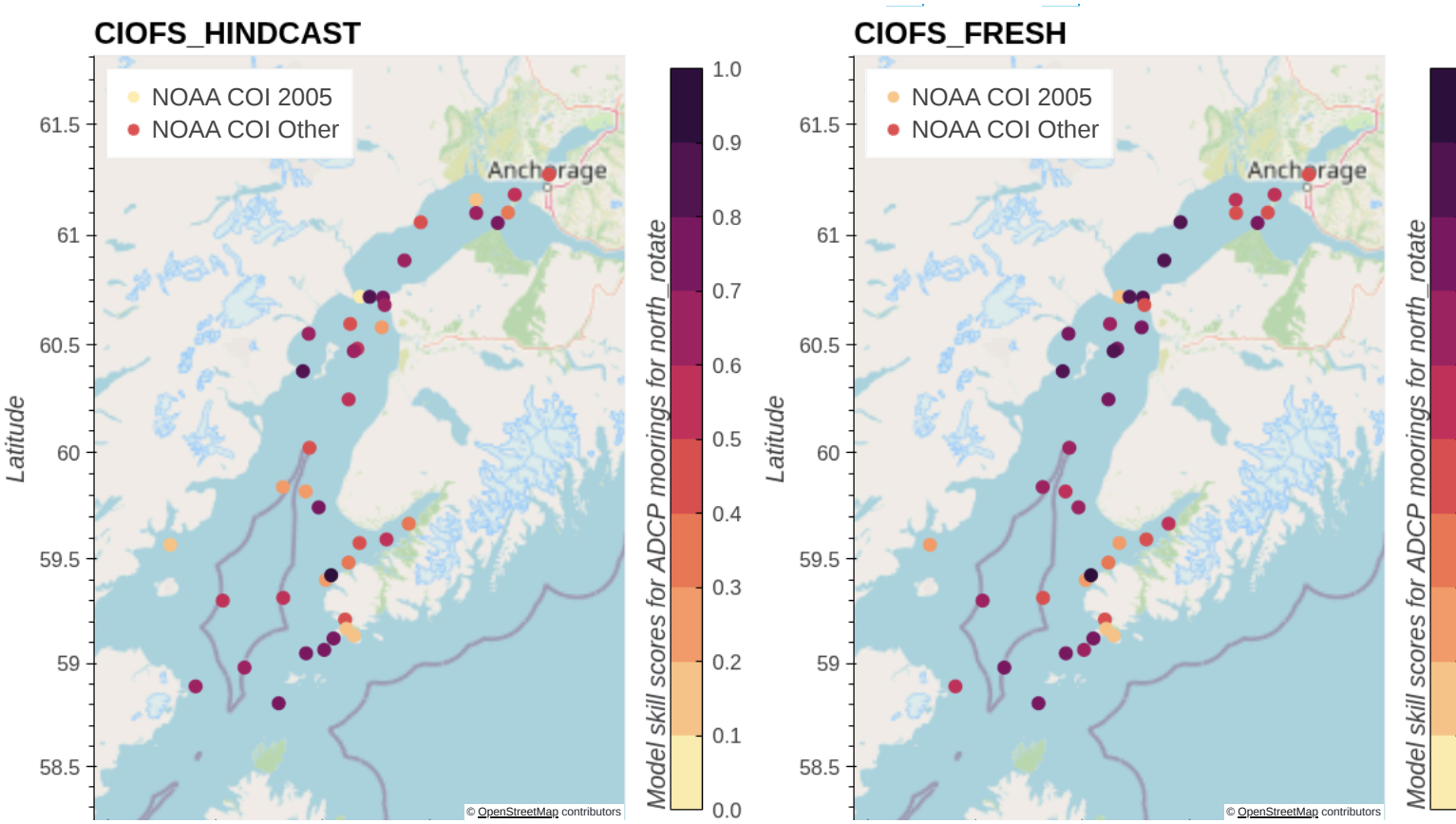

Fig. 11.19 Skill scores for CIOFS Hindcast (left) and CIOFS Freshwater (right) with ADCP moorings for subtidal across-channel velocity, by project. Click on a legend entry to toggle the transparency. (HTML plot, won't show up correctly in PDF.)

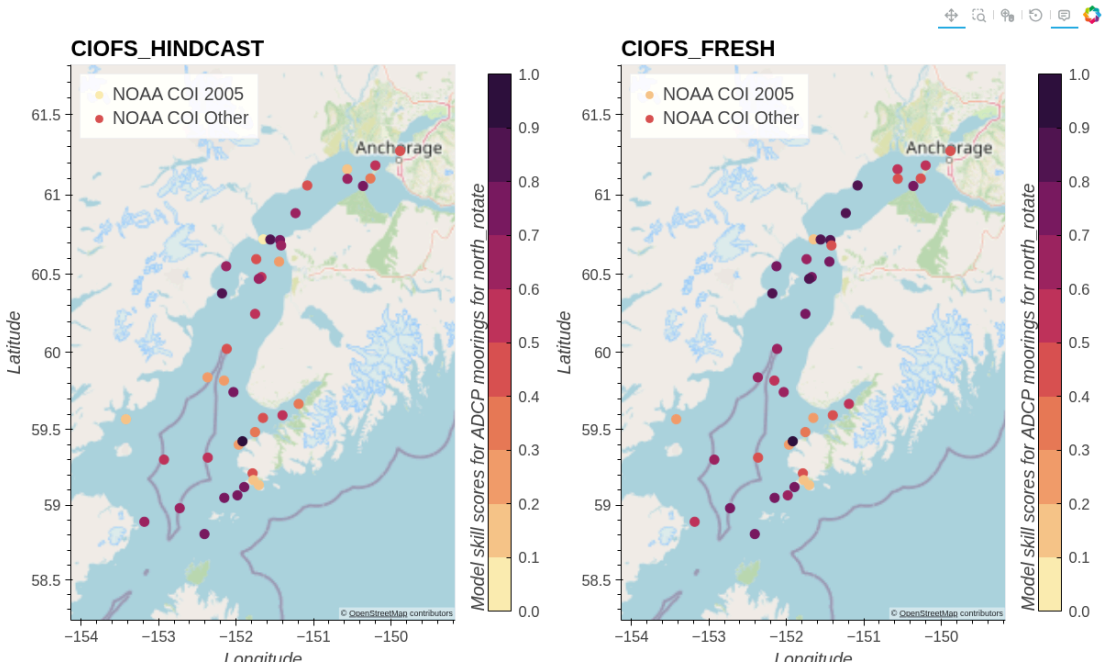

Fig. 11.20 Skill scores for CIOFS Hindcast (left) and CIOFS Freshwater (right) with ADCP moorings for subtidal across-channel velocity, by project. (PNG screenshot, available for PDF and for saving image.)

12. Overview of Drifter Simulations

Particle simulations are run to match each available drifter dataset: `drifters_ecofoci` and `drifters_uaf`.

12.1. Simulation Setup

The simulated particle simulations are run with the following conditions:

- Start the simulated particles at the *in situ* drifter location in the CIOFS domain and in a radius 500m around that location.
- Start the simulated particles at the time the drifter is at that location in the CIOFS domain, but starting 40 minutes before and every time step through 40 minutes after. See immediately below for details.
- Start the simulated particles at the same depth that the *in situ* drifter is drogued, and run them fixed to that depth.
- Run 1000 simulated particles.
- Use time-varying masks from ROMS if the drifter is shallower than the tidal flats ($5m$), otherwise use static versions to save time.
- Use estimate of horizontal diffusivity in `particle-tracking-manager` which is calculated as $0.1m/s$ sub-gridscale velocity that is missing from the model output and multiplied by an estimate of the horizontal grid resolution. The horizontal grid resolution is variable but is approximated as $100m$ so that the horizontal diffusivity is calculated as $0.1m/s$ * $100m$ = 10 m^2/s. This has not been tuned but instead is a theoretical calculation.

The timing of how out to extend the simulation timing before and after the *in situ* drifter was based on the HF Radar comparisons in the CIOFS Hindcast Report [TLFD23]. On the HF Radar comparison page, the tidal phase difference of the data minus the model is plotted on the far right side of each of the two figures, each for two different time periods for HF Radar data. The M_2 tide is the dominant tide in the region.

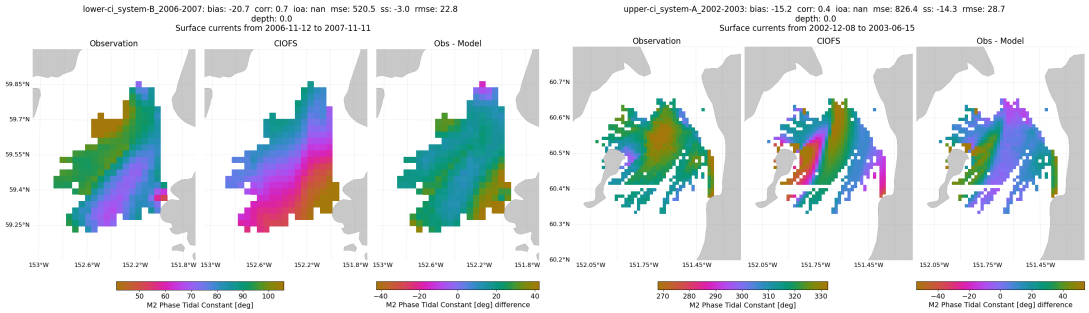

Taking the maximum phase difference seen in the plot of about 20 degrees, we use the relationship based on the fact that the M_2 tide repeats every 12 hours and 25 minutes:

$$\frac{360^\circ}{12hr25min} = \frac{20^\circ}{x}$$

This phase difference between the model and the data gives us a time difference of 41.4 minutes, or about 40 minutes. We use this time scale both backward and forward in time with our simulation start times.

12.2. Metrics

We use two metrics to assess the performance of the model in capturing the drifter movements: an area-based metric and a separation distance-based metric. We will use an example simulation shown here to explain each metric, where the gray lines show the 1000 simulated particles with the green circles showing their initial locations and blue circles showing their final locations, and the single red line shows the *in situ* drifter with the red circle showing its final location (at least in the domain, it may continue farther, outside the domain). The dashed black line shows an estimated model domain boundary.

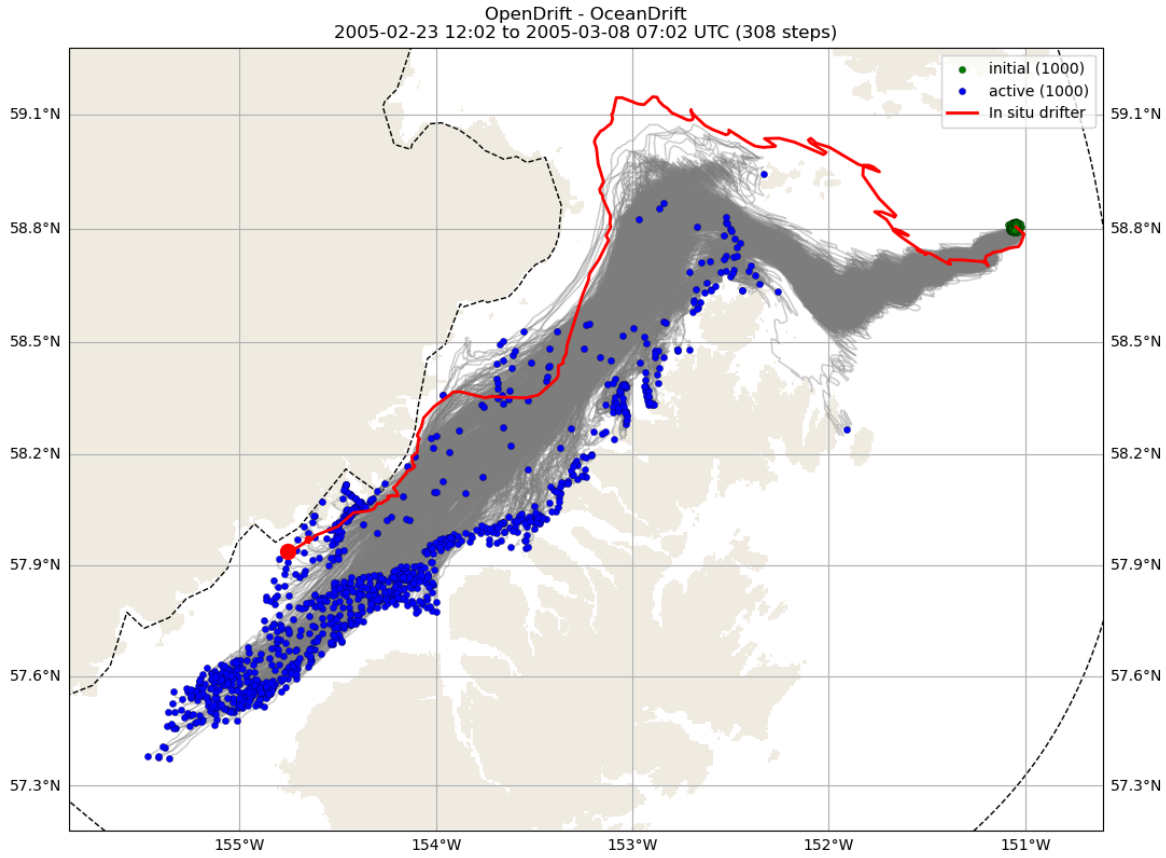

Fig. 12.1 Example particle simulation (EcoFOCI 53298_y2005).

12.2.1. Area-Based Length Scale

The normalized length-scale metric L compares the behavior of the group of simulated particles with the *in situ* drifter, with the idea that no single simulated drifter track is more representative than another. The distance from the drifter to the envelope of simulated particles represents how well the model captures the drifter's movement, and is 0 if the drifter is within the Qhull of the simulated particles. This length scale is normalized by the square root of the area of the same Qhull, which is the dispersion of the particles and therefore gives a lengthscale for the flowfield at the same time. In other words, this metric gives the difference between the *in situ* drifter location and the envelope of numerical particles, in time.

$$L_i = \frac{d_i^{Qhull}}{\sqrt{A_i^{Qhull}}}$$

for i from times 1 to N. For example, in the image we see how this is calculated at a particular time step overlaid on a representation of particle simulations. At the time shown, the drifter locations are in blue circles, and the envelope or Qhull they create is outlined in blue. The shortest distance from that polygon to the present *in situ* drifter location (red circle) is represented by a dashed blue line, which is the numerator of L. The square root of the area within the blue polygon is the denominator of L. This is calculated for each time step of the drifter simulation.

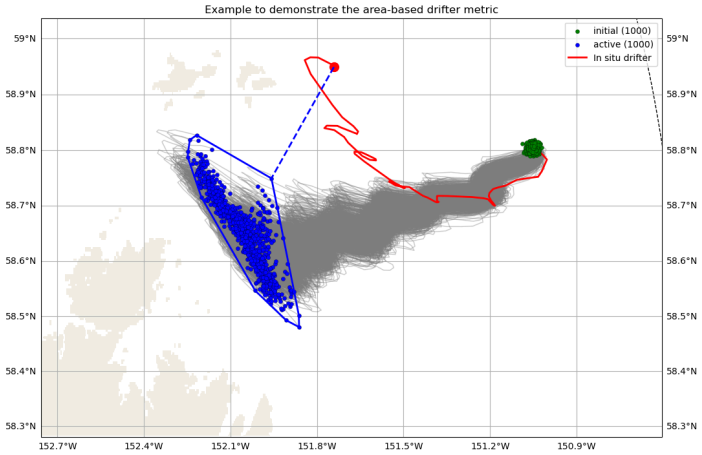

Fig. 12.2 Diagram explaining the area-based length scale (EcoFOCI 53298_y2005 as example).

For this example, the calculation of L for the full set of time are in the following image, with the time of comparison noted with the vertical dashed blue line. Comparing with the image of the full set of simulation tracks above, one can see that the time of comparison was chosen to be the time of maximal excursion of the simulated particles away from the *in situ* drifter. A horizontal line marks the value of $L = 1$ since that is when the length scale of the Qhull away from the drifter equals the length scale of the particle dispersion. When $L > 1$, the particle Qhull and drifter are farther apart than the dispersion length scale, and thus the model is performing worse compared to this measure.

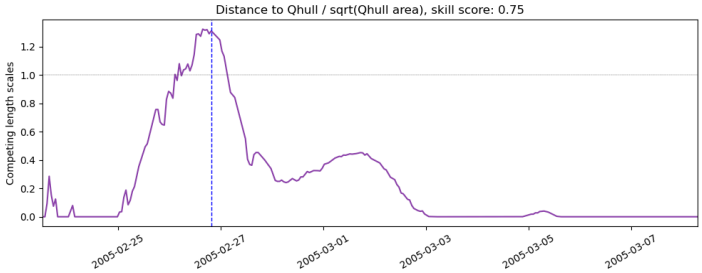

Fig. 12.3 Area-based length scale over time for example drifter and particle simulations EcoFOCI 53298_y2005.

The length scale metric L is converted into a skill score by adding over the time frame, dividing by the number of time steps to create a mean, and subtracting it from 1:

$$ss_L = 1 - \frac{1}{N}\Sigma_{i=1}^{N} L_i.$$

When $0 < ss_L \leq 1$, the simulated particle cloud is capturing the *in situ* drifter within the cloud with some skill, particularly if $0.5 \leq ss_L \leq 1$. There can be scenarios in which $ss_L < 0$ due to the way it is calculated, in which case, the model is not

demonstrating skill. Note that the skill score for this example is shown in the title of the image and in this case it is $ss_L = 0.75$.

12.2.2. Separation Distance

The separation distance is proposed in Liu and Weisberg [LW11] as a way to compare modeled particles against *in situ* drifters 1 to 1 and to be able to interpret the full time series without having separations early in the time series pollute the interpretation later in the time series. The way they manage this is by having both the numerator and the denominator be cumulative calculations. The separation distance s is calculated as:

$$s_i = \frac{\Sigma_{j=1}^{i} d_j}{\Sigma_{j=1}^{i} \ell_j}$$

for i from times 1 to N, and where d_j is the distance between a simulated particle and the *in situ* drifter at time j between 1 and i, and ℓ_j is the distance traveled along the *in situ* drifter trajectory at time j. To help understand the separation distance, two drifters are pulled out as examples in particular in the image: the *in situ* drifter in red and a simulated particle track in purple. At the time shown, they have each reached to an extent marked by circles, having traveled along the paths indicated by matching colors, and occasionally marked by circles to represent previous time steps, pretending that there were only a few time steps for demonstration purposes. The separation distance is calculated as the summation of the distance between the drifters at each time up to this point in time divided by the summation of the distance traveled by the *in situ* drifter from start up each time up to this point:

$$s_6 = \frac{d_1+d_2+d_3+d_4+d_5+d_6}{\ell_1+\ell_2+\ell_3+\ell_4+\ell_5+\ell_6},$$

but remember that ℓ_j are the total distance from the start of the drifter track to the time it is counting.

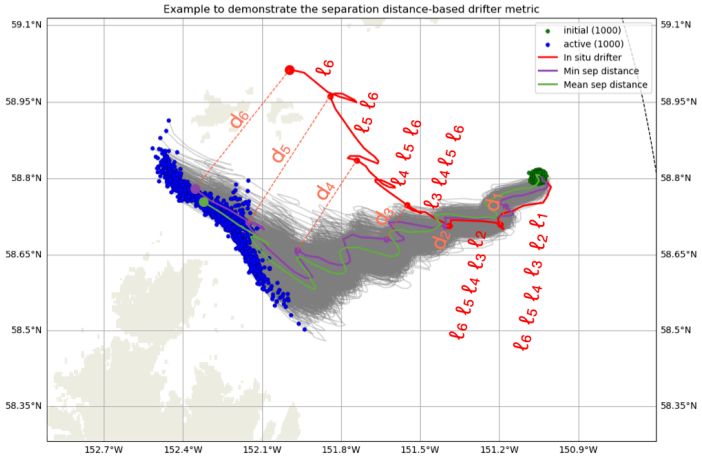

Fig. 12.4 Diagram explaining the separation distance (EcoFOCI 53298_y2005 as example).

The full time series of the separation distance for the example is shown in the following image. The time shown in the previous plot is noted with a vertical dashed line. The time shown is a time when the *in situ* drifter and comparison simulated particle were the farthest apart for the simulation. The separation distance can be converted into a skill score by taking the root mean square error over the times available as follows:

$$ss_s = 1 - \frac{1}{N}\Sigma_{i=1}^{N}\sqrt{s_i^2}.$$

The skill score can be negative but must be positive to display skill in recreating the drifter behavior; closer to 1 is better skill with 1 being perfect skill.

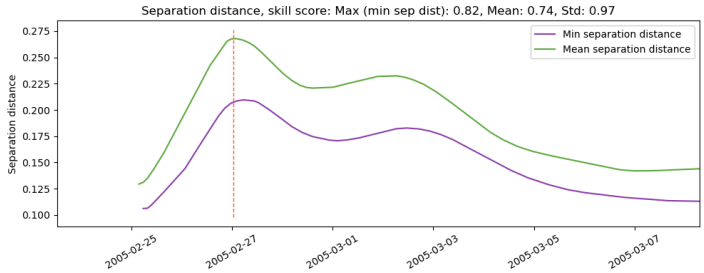

Fig. 12.5 Separation distance over time for example drifter and particle simulations EcoFOCI 53298_y2005.

The separation distance is calculated between each simulated drifter and the *in situ* drifter. We present two specific simulated particles: the minimum and the mean separation distance, as calculated from the root mean square. These are the two tracks highlighted in the example image, and the two skill scores given in the results. Note that the skill score is given in the image title and is $ss_s = 0.82$ for the minimum separation distance (which is the maximum skill score) and $ss_s = 0.74$ for the mean separation distance (which is the mean skill score).

13. Overview of Drifter Data

This page summarizes skill scores comparing simulated particles in the ocean models with *in situ* drifters. See details describing drifter simulations and metrics here.

The area-based skill score distinguishes between models much more than the separate distance skill score. For the area-based skill score, results show that model skill is similar for CIOFS hindcast and CIOFS fresh below the influence of freshwater (15m and 40m depth) but improved in CIOFS fresh above that (1m, 5m, 7.5m).

100MB zipfile of plots

13.1. Map of Drifters

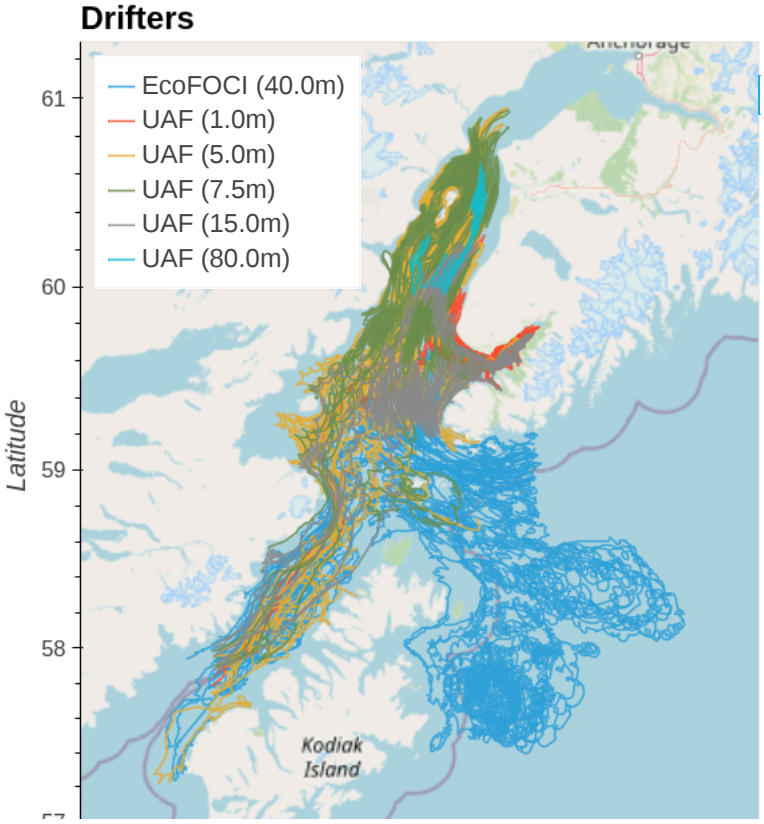

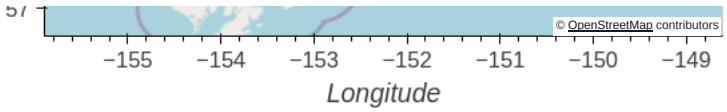

Fig. 13.1 All drifter deployments, by project. Click on a legend entry to toggle the transparency. (HTML plot, won't show up correctly in PDF.)

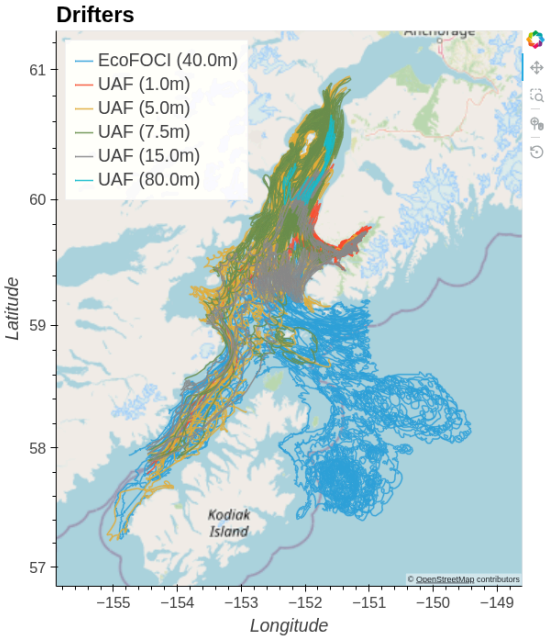

Fig. 13.2 All drifter deployments, by project. (PNG screenshot, available for PDF and for saving image.)

13.2. Results

13.2.1. Skill Score: Area-Based Length Scale

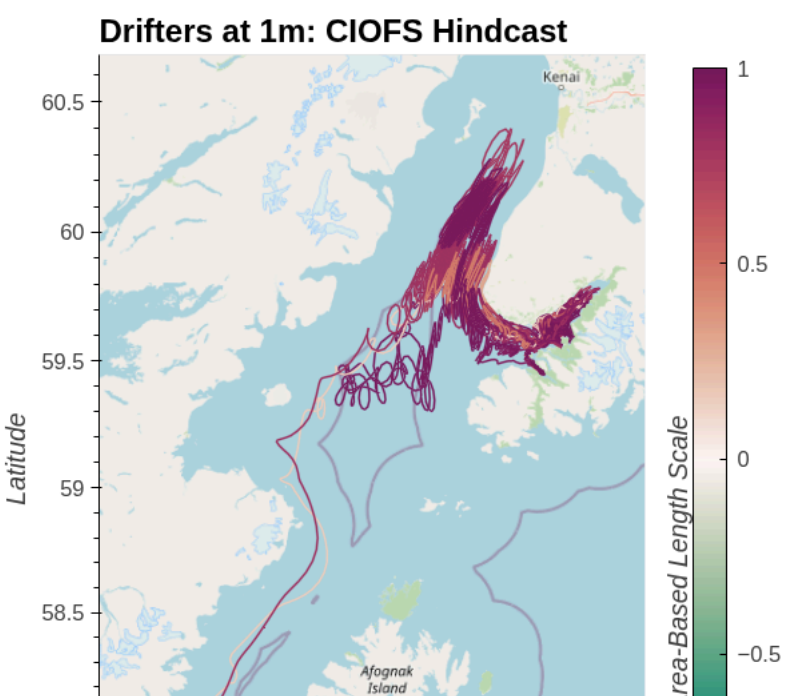

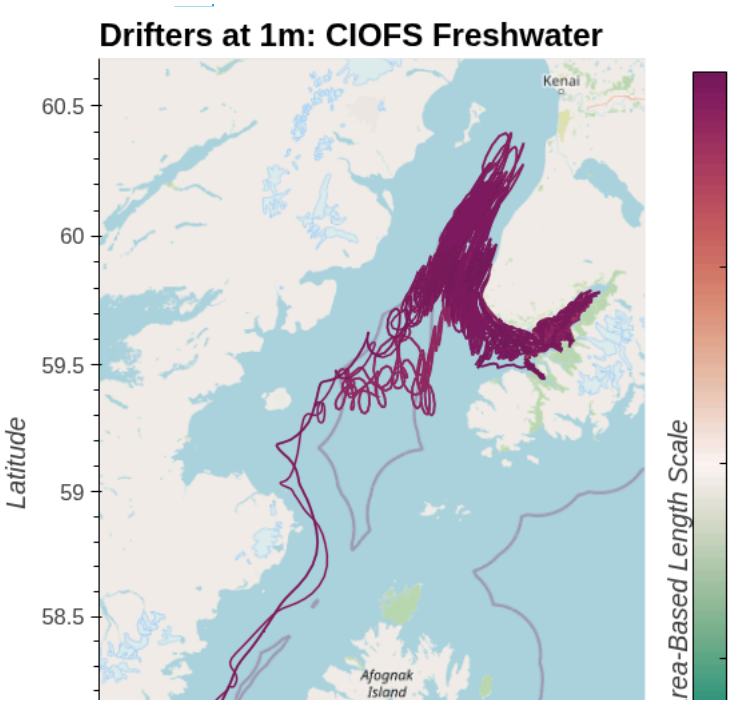

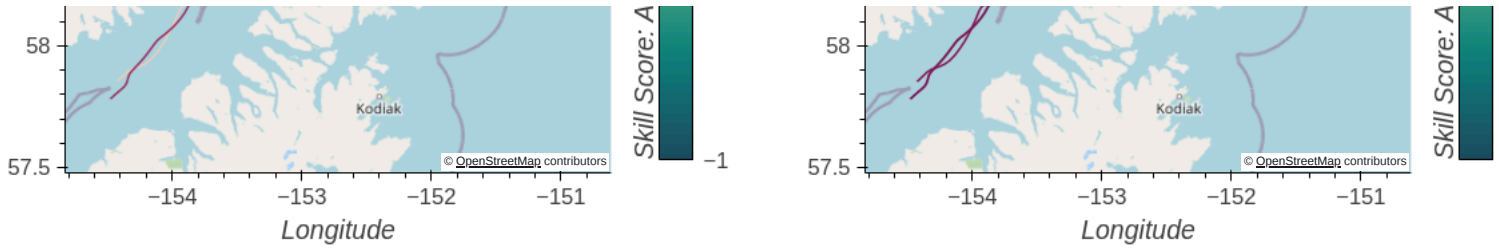

Fig. 13.3 Area-based skill scores for CIOFS Hindcast (left) and CIOFS Freshwater (right) with drifters at 1m depth. (HTML plot, won't show up correctly in PDF.)

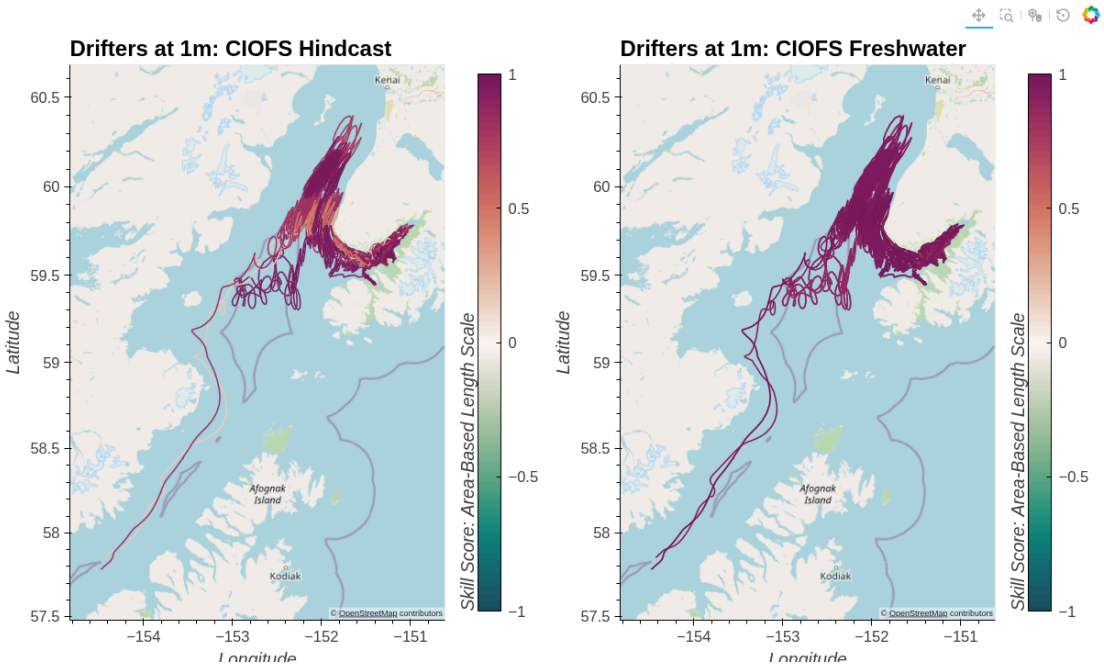

Fig. 13.4 Area-based skill scores for CIOFS Hindcast (left) and CIOFS Freshwater (right) with drifters at 1m depth. (PNG screenshot, available for PDF and for saving image.)

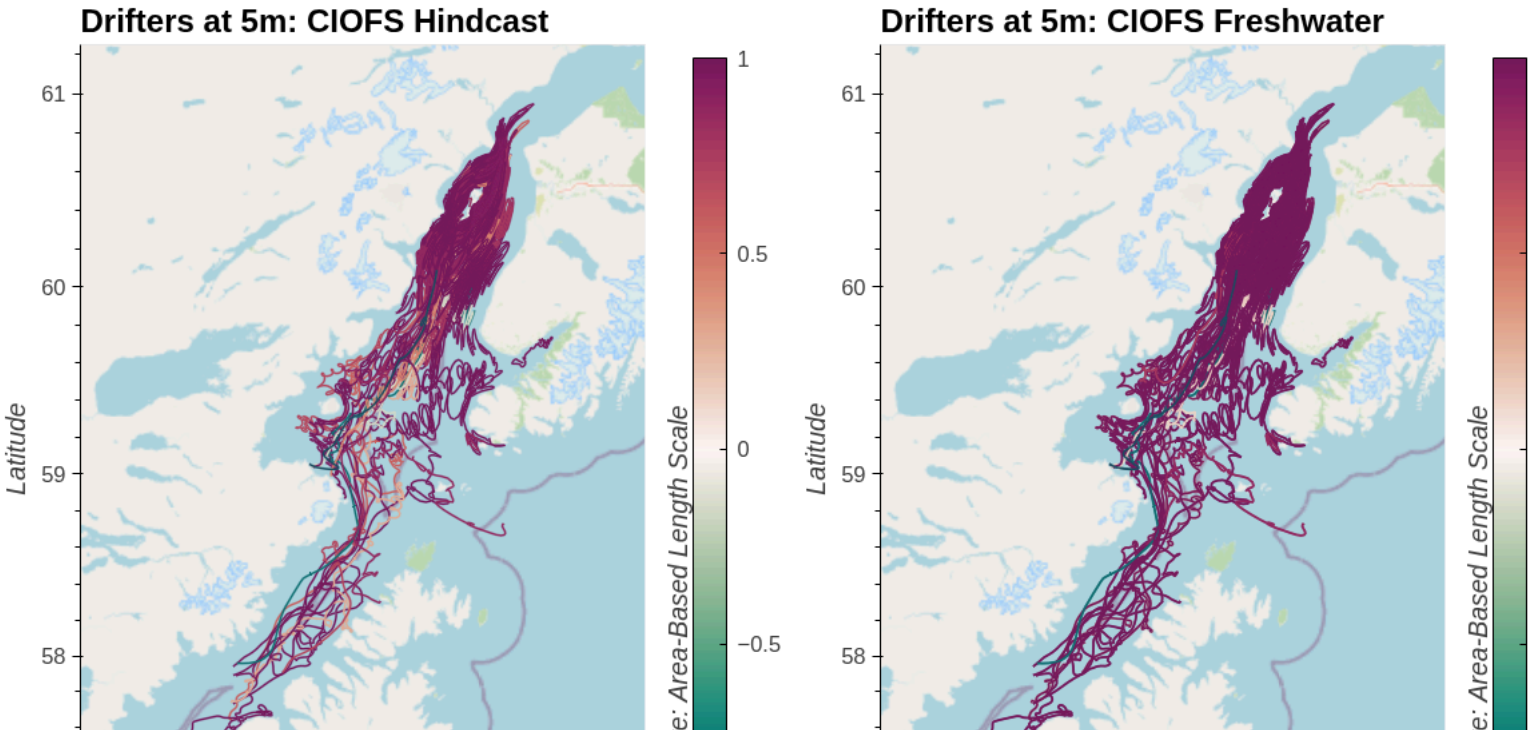

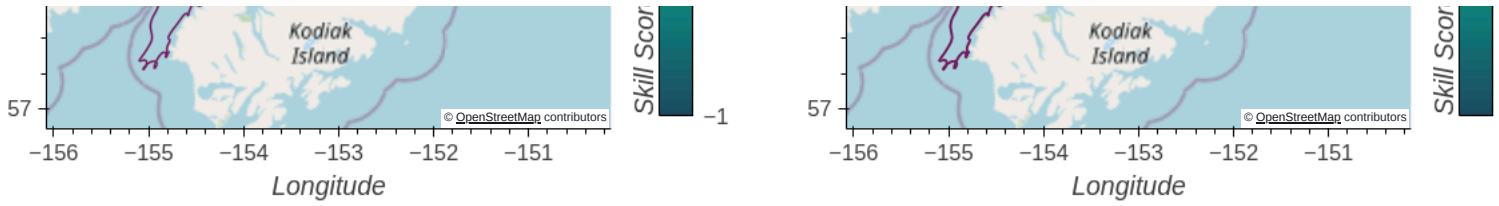

Fig. 13.5 Area-based skill scores for CIOFS Hindcast (left) and CIOFS Freshwater (right) with drifters at 5m depth. (HTML plot, won't show up correctly in PDF.)

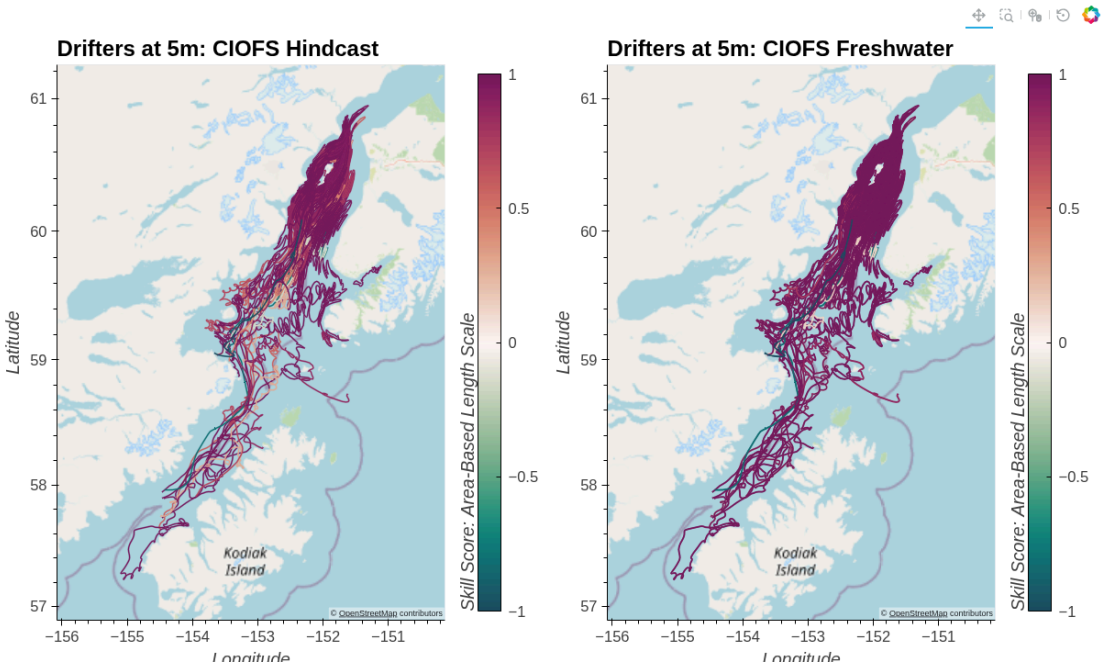

Fig. 13.6 Area-based skill scores for CIOFS Hindcast (left) and CIOFS Freshwater (right) with drifters at 5m depth. (PNG screenshot, available for PDF and for saving image.)

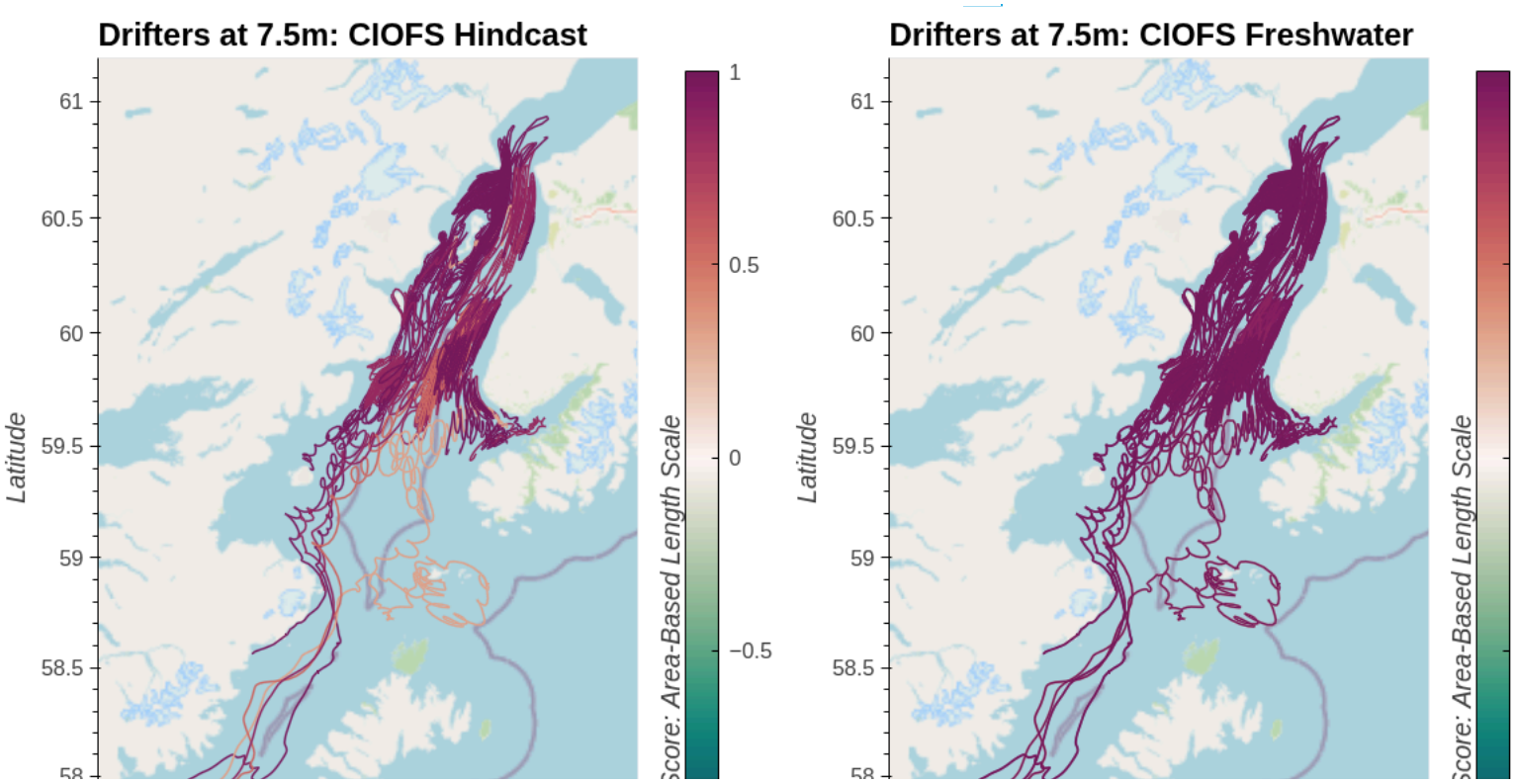

Fig. 13.7 Area-based skill scores for CIOFS Hindcast (left) and CIOFS Freshwater (right) with drifters at 7.5m depth. (HTML plot, won't show up correctly in PDF.)

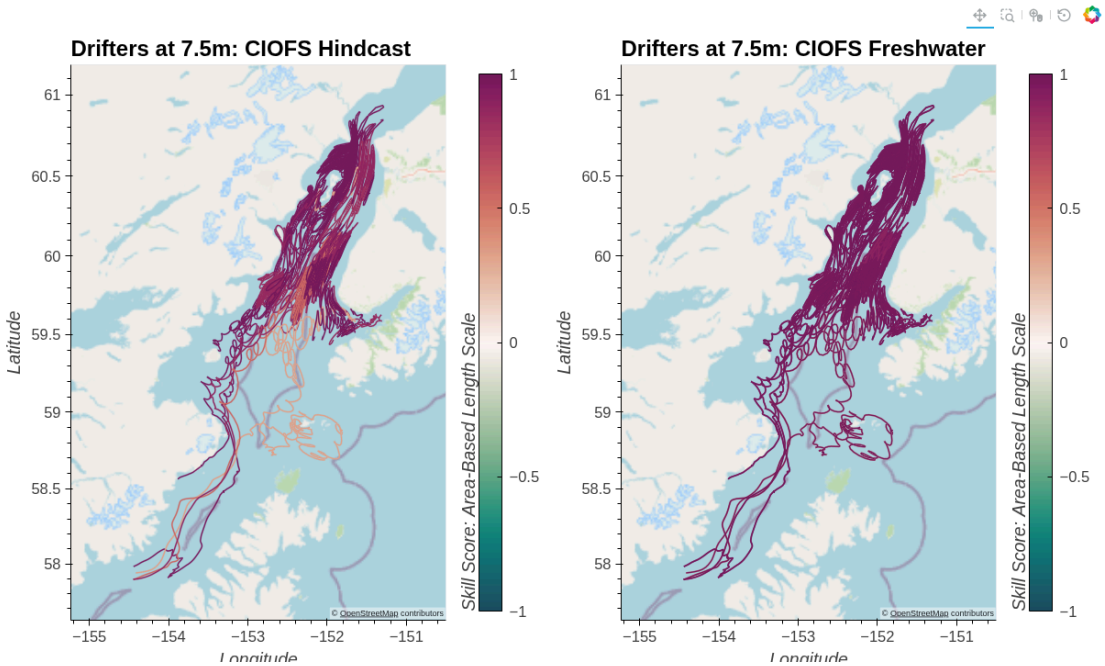

Fig. 13.8 Area-based skill scores for CIOFS Hindcast (left) and CIOFS Freshwater (right) with drifters at 7.5m depth. (PNG screenshot, available for PDF and for saving image.)

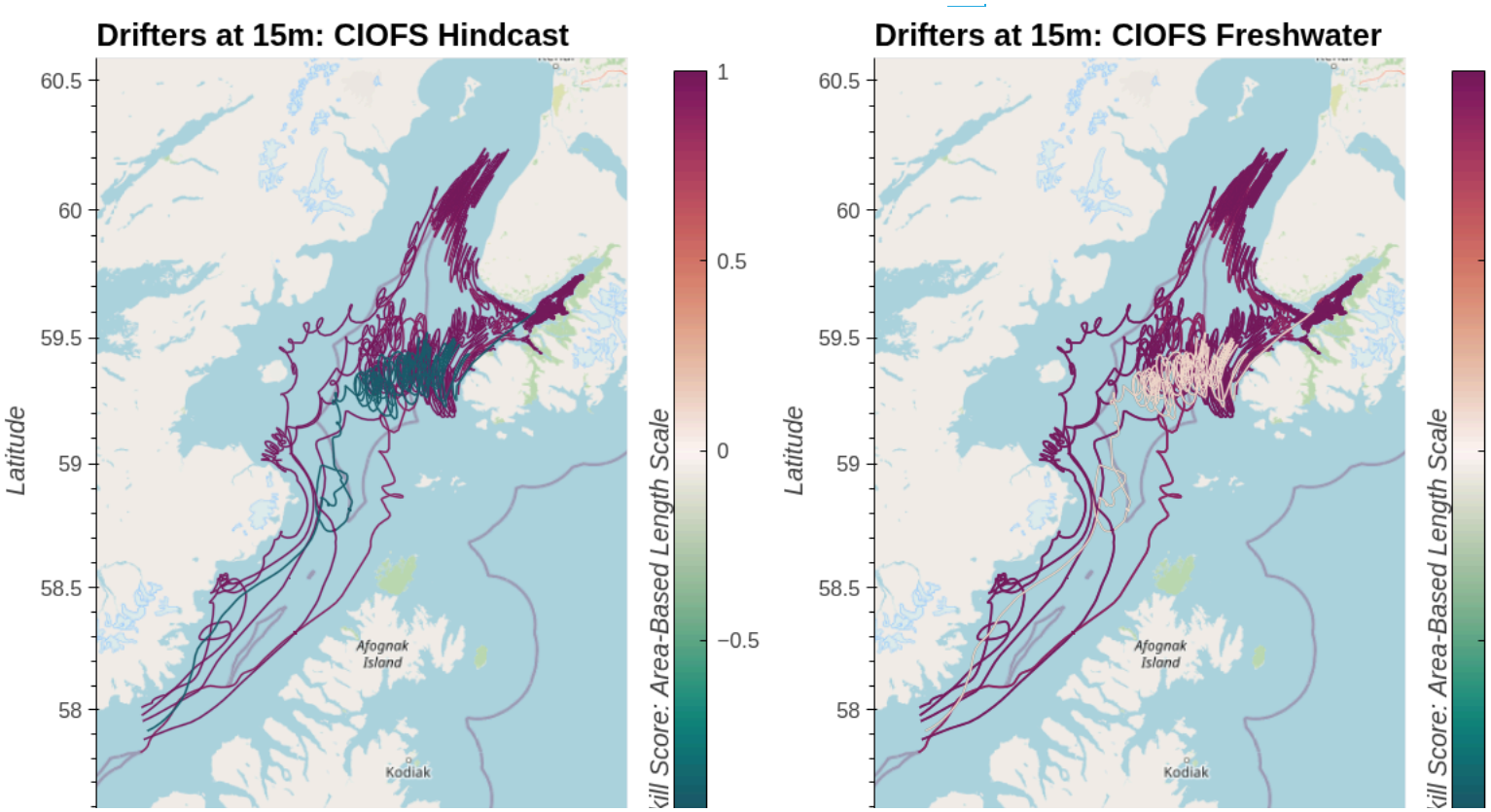

Fig. 13.9 Area-based skill scores for CIOFS Hindcast (left) and CIOFS Freshwater (right) with drifters at 15m depth. (HTML plot, won't show up correctly in PDF.)

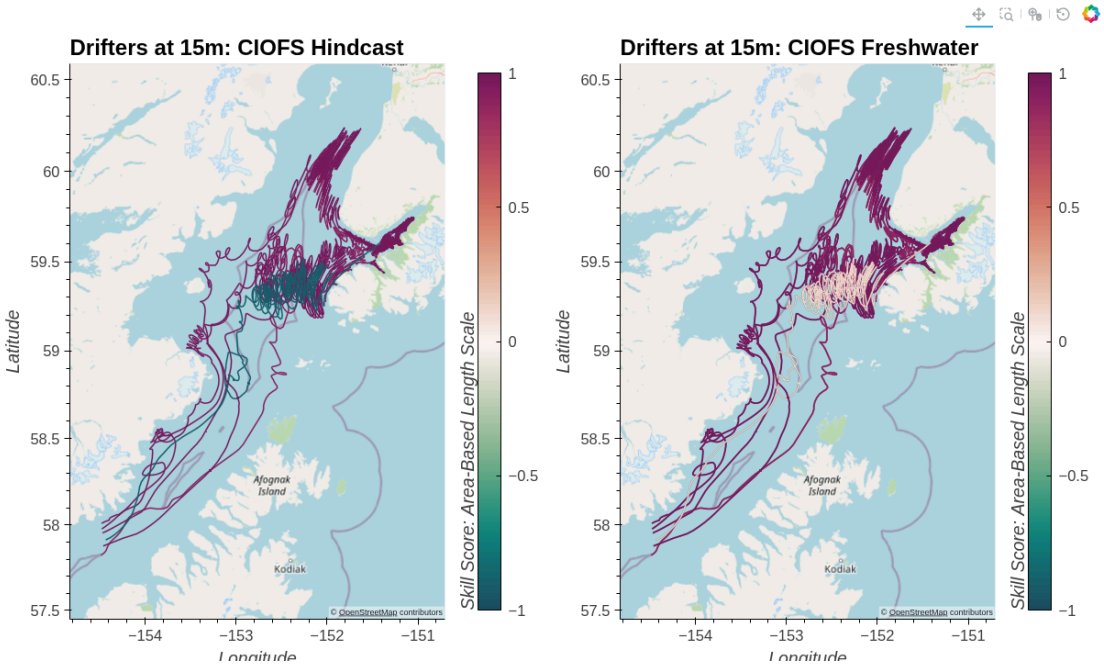

Fig. 13.10 Area-based skill scores for CIOFS Hindcast (left) and CIOFS Freshwater (right) with drifters at 15m depth. (PNG screenshot, available for PDF and for saving image.)

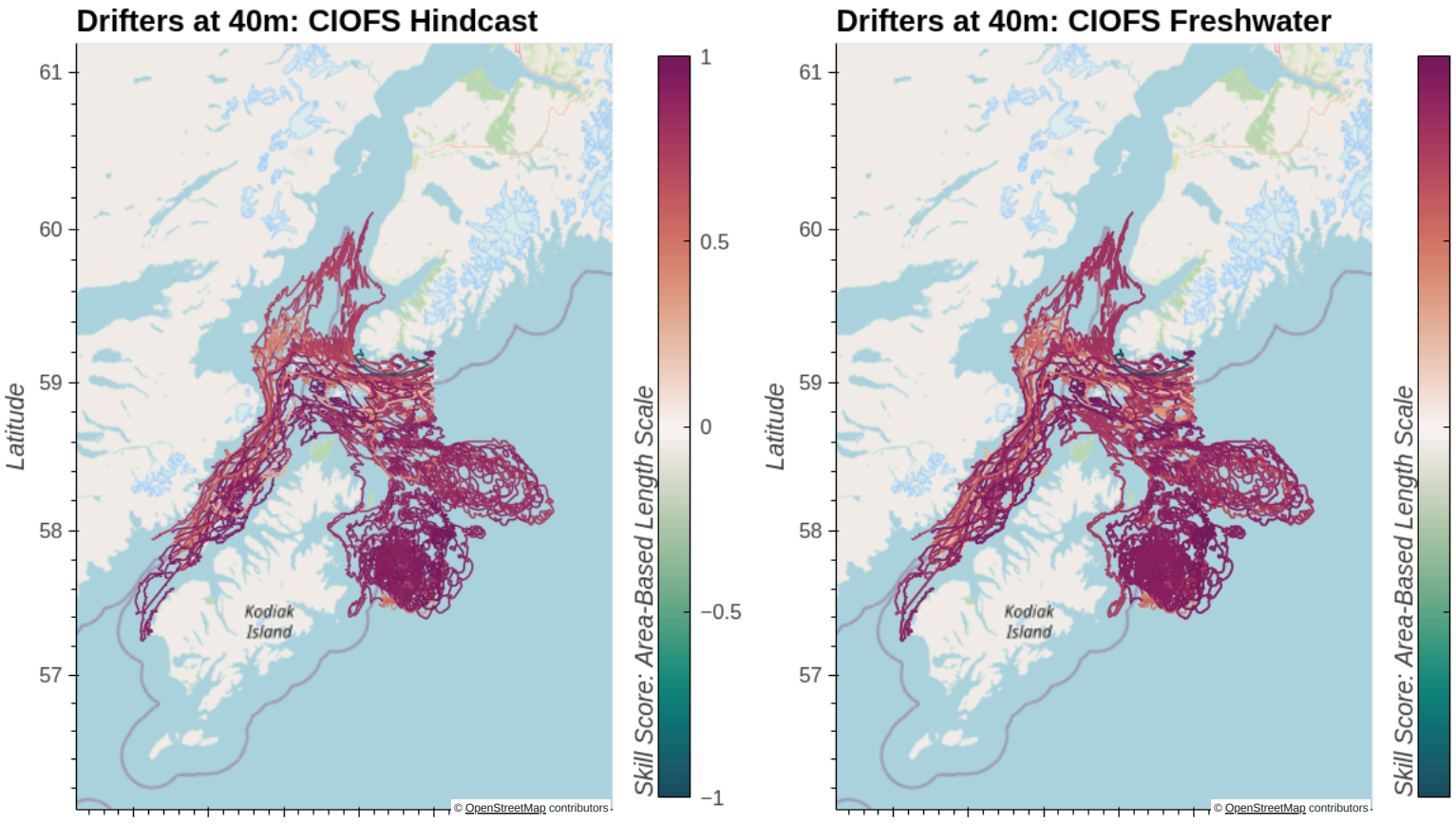

Fig. 13.11 Area-based skill scores for CIOFS Hindcast (left) and CIOFS Freshwater (right) with drifters at 40m depth. (HTML plot, won't show up correctly in PDF.)

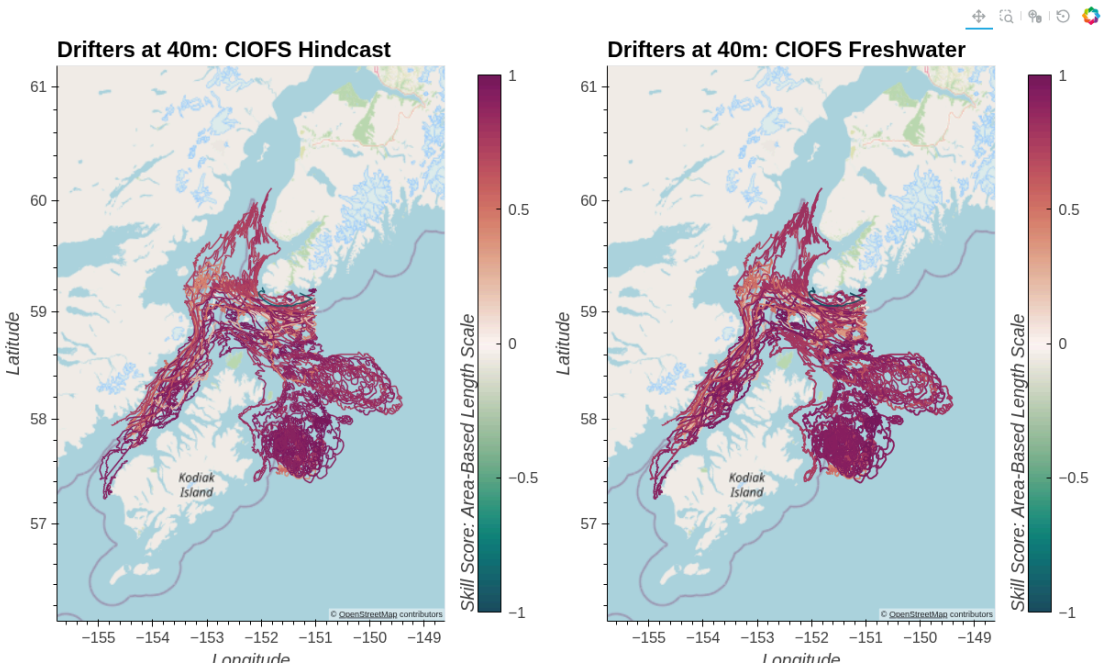

Fig. 13.12 Area-based skill scores for CIOFS Hindcast (left) and CIOFS Freshwater (right) with drifters at 40m depth. (PNG screenshot, available for PDF and for saving image.)

13.2.2. Skill Score: Separation Distance, Mean

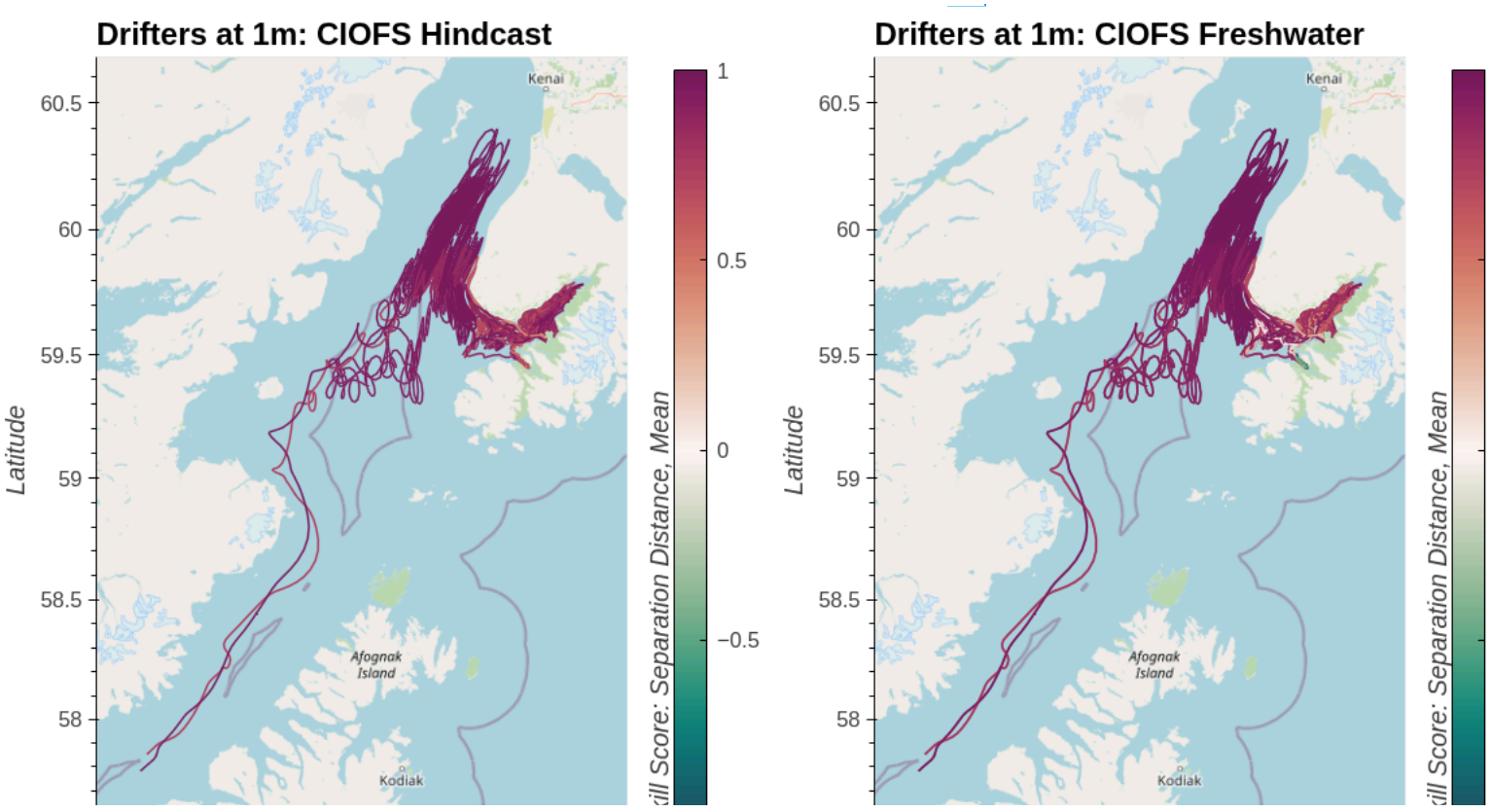

Fig. 13.13 Separation-distance skill scores for CIOFS Hindcast (left) and CIOFS Freshwater (right) with drifters at 1m depth. (HTML plot, won't show up correctly in PDF.)

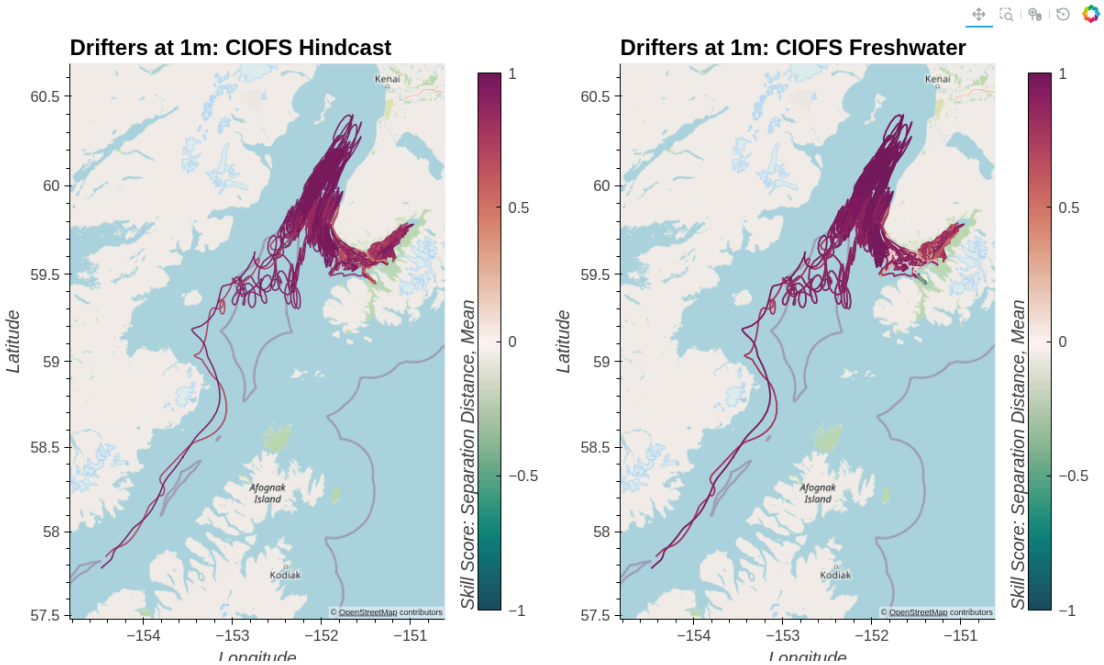

Fig. 13.14 Separation-distance skill scores for CIOFS Hindcast (left) and CIOFS Freshwater (right) with drifters at 1m depth. (PNG screenshot, available for PDF and for saving image.)

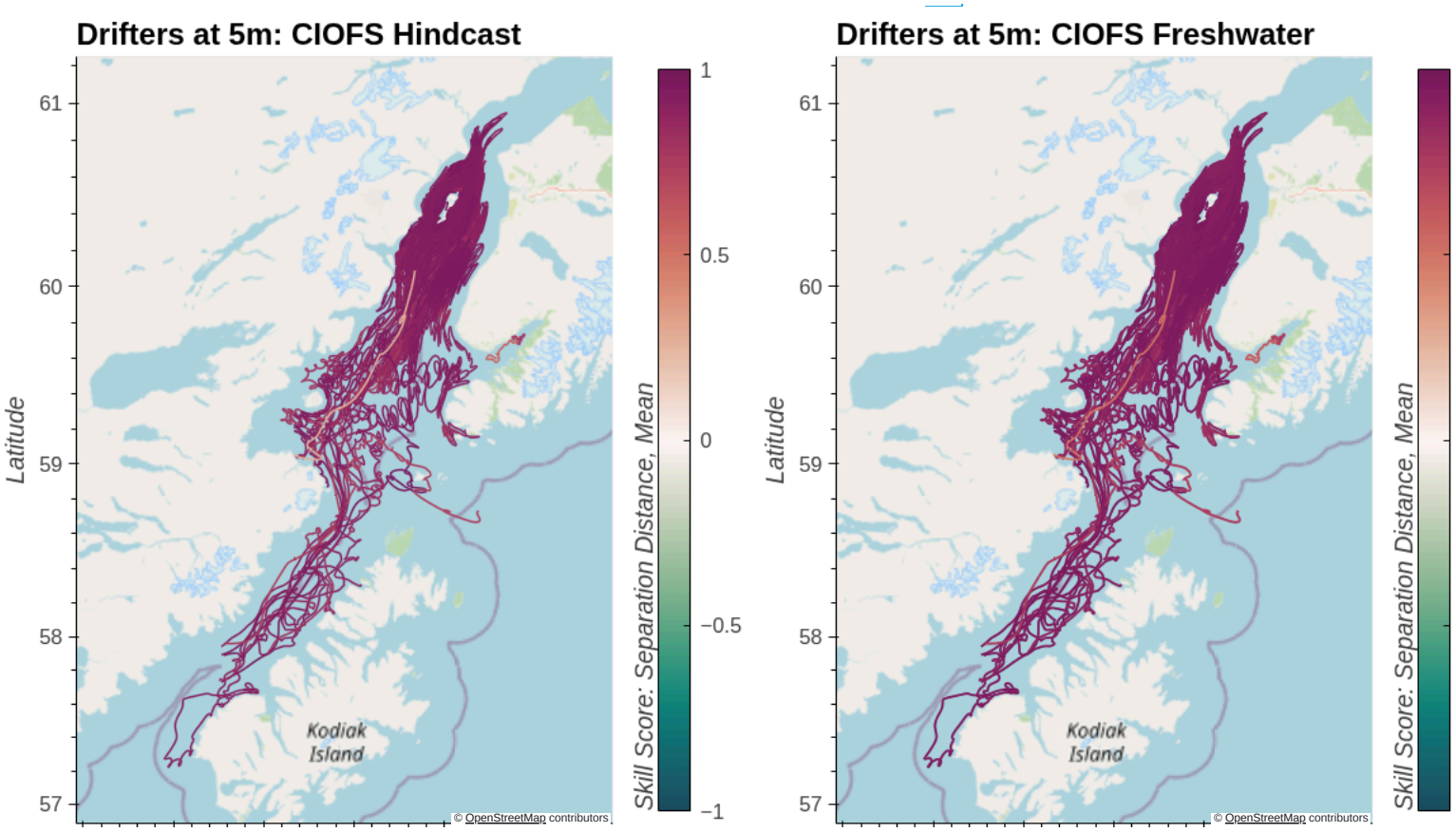

Fig. 13.15 Separation-distance skill scores for CIOFS Hindcast (left) and CIOFS Freshwater (right) with drifters at 5m depth. (HTML plot, won't show up correctly in PDF.)

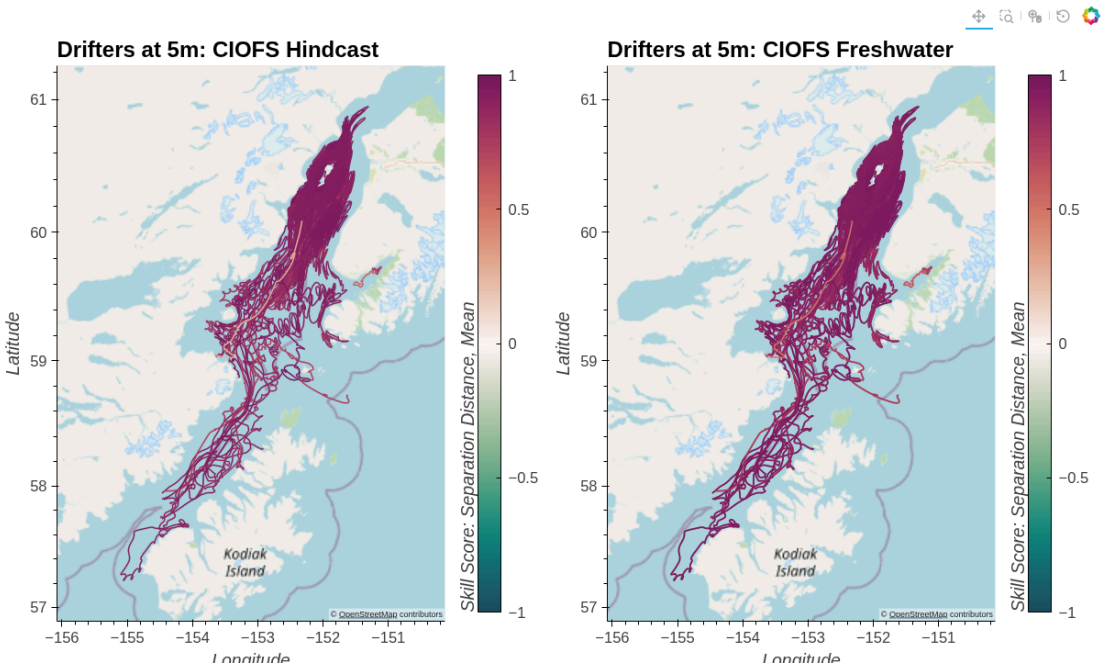

Fig. 13.16 Separation-distance skill scores for CIOFS Hindcast (left) and CIOFS Freshwater (right) with drifters at 5m depth. (PNG screenshot, available for PDF and for saving image.)

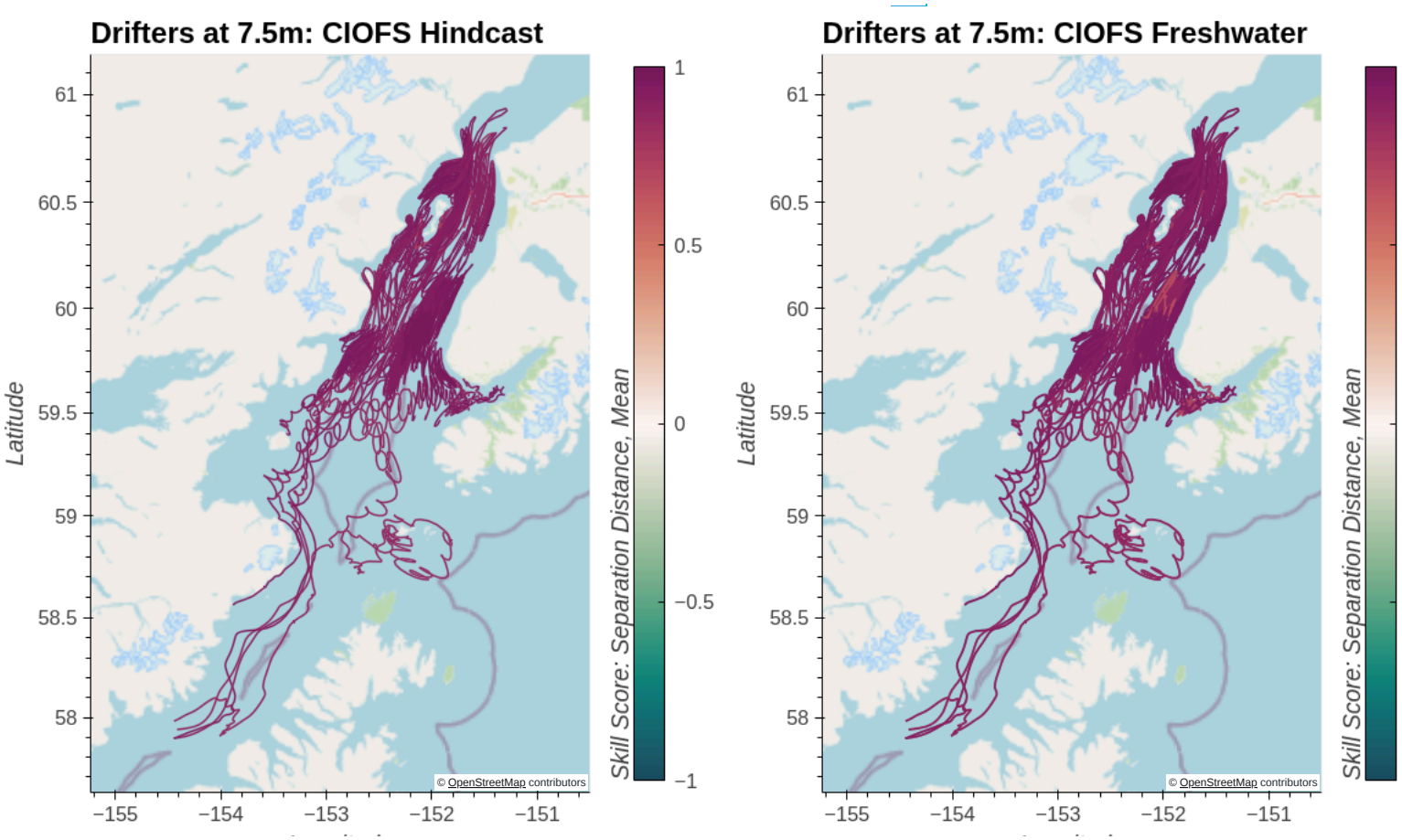

Longitude Longitude

Fig. 13.17 Separation-distance skill scores for CIOFS Hindcast (left) and CIOFS Freshwater (right) with drifters at 7.5m depth. (HTML plot, won't show up correctly in PDF.)

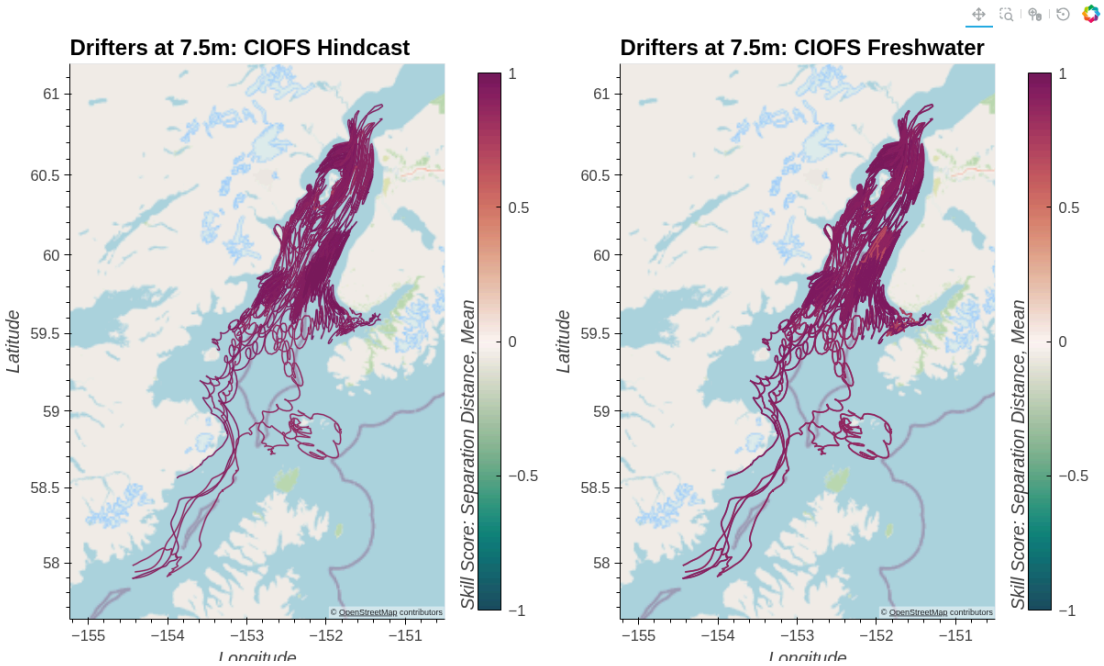

Fig. 13.18 Separation-distance skill scores for CIOFS Hindcast (left) and CIOFS Freshwater (right) with drifters at 7.5m depth. (PNG screenshot, available for PDF and for saving image.)

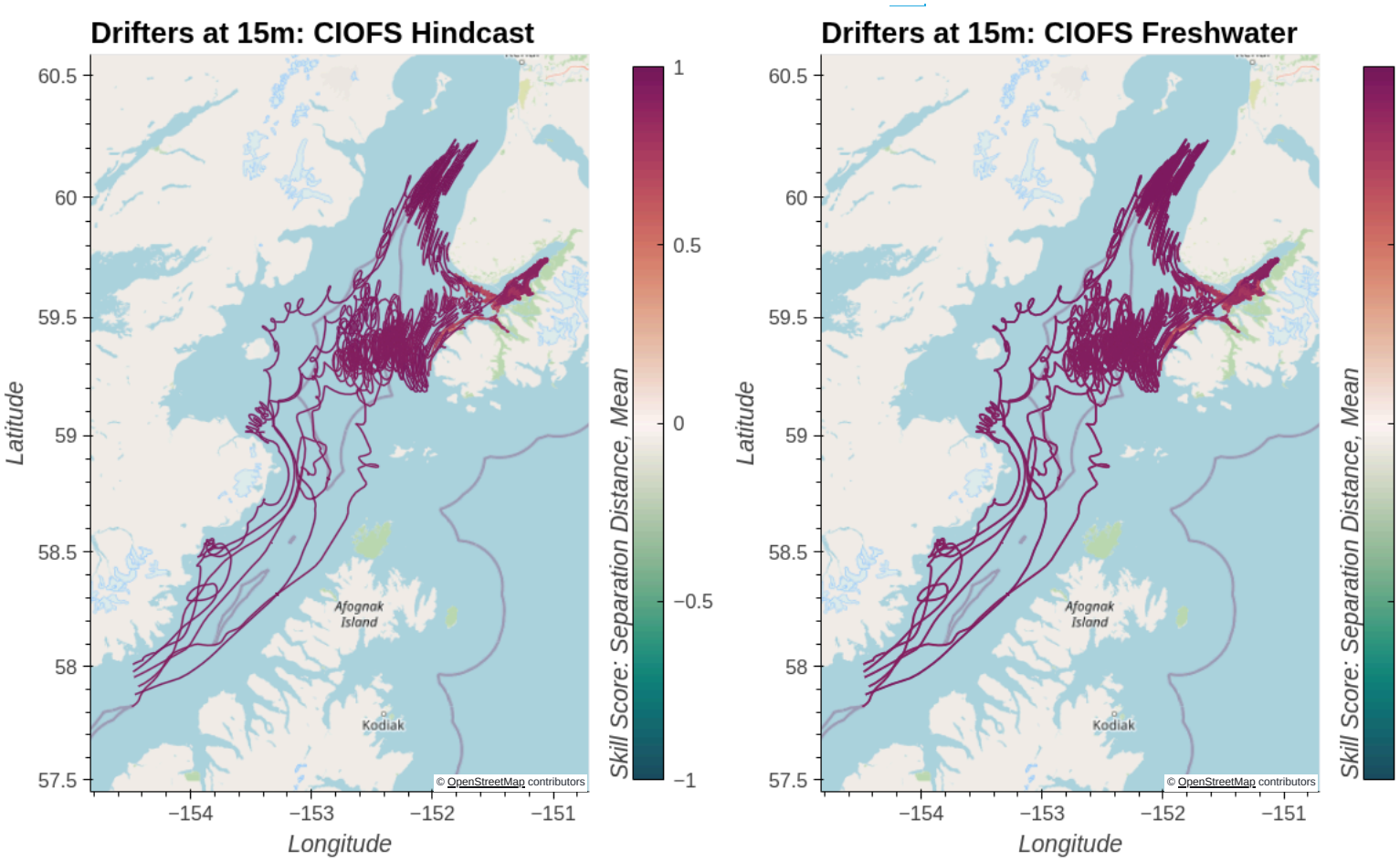

Fig. 13.19 Separation-distance skill scores for CIOFS Hindcast (left) and CIOFS Freshwater (right) with drifters at 15m depth. (HTML plot, won't show up correctly in PDF.)

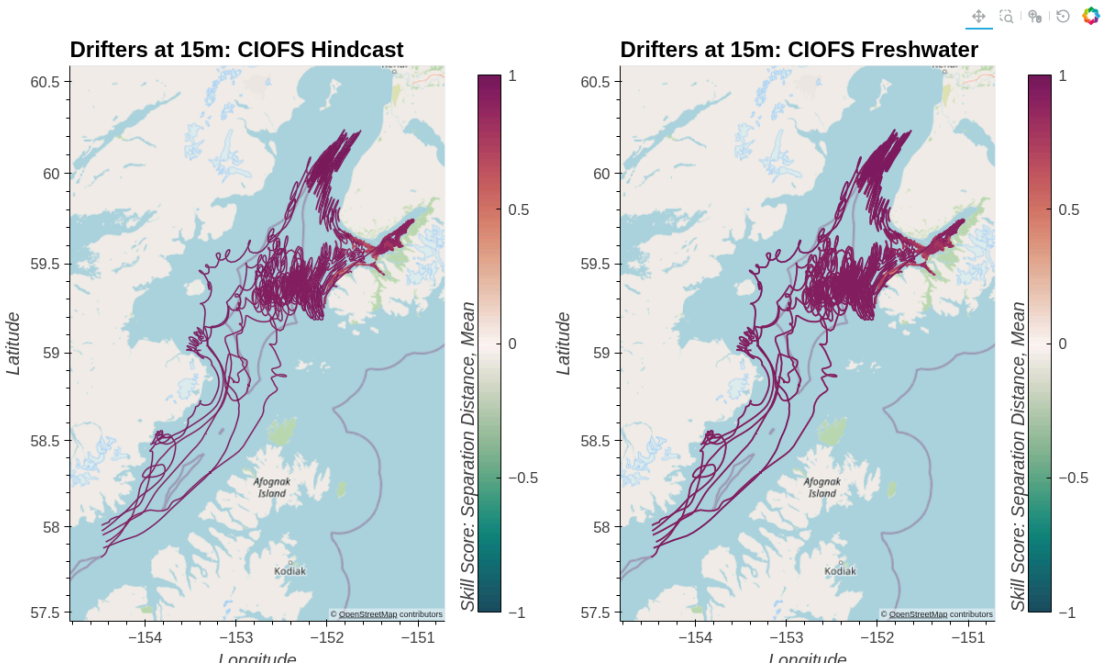

Fig. 13.20 Separation-distance skill scores for CIOFS Hindcast (left) and CIOFS Freshwater (right) with drifters at 15m depth. (PNG screenshot, available for PDF and for saving image.)

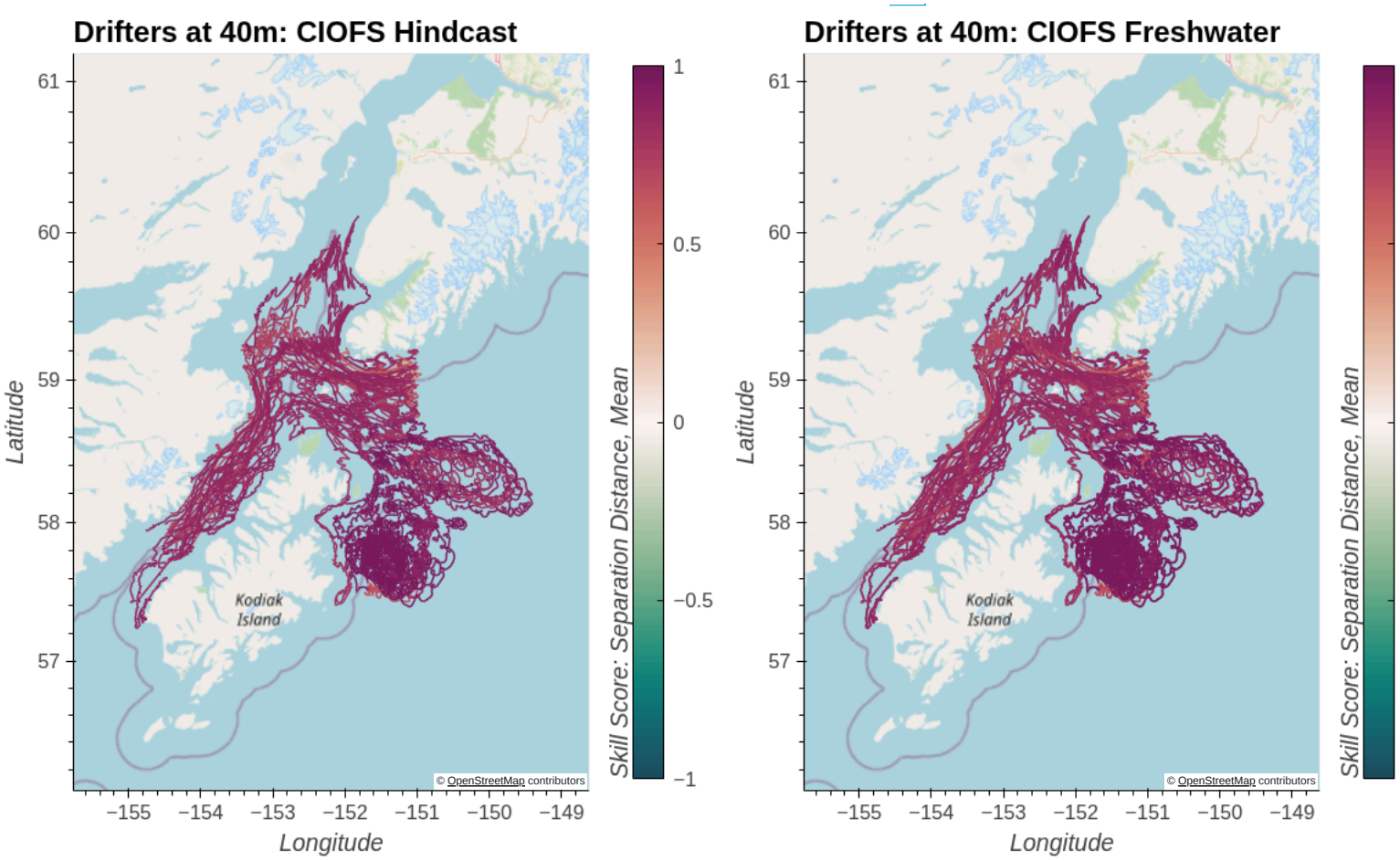

Fig. 13.21 Separation-distance skill scores for CIOFS Hindcast (left) and CIOFS Freshwater (right) with drifters at 40m depth. (HTML plot, won't show up correctly in PDF.)

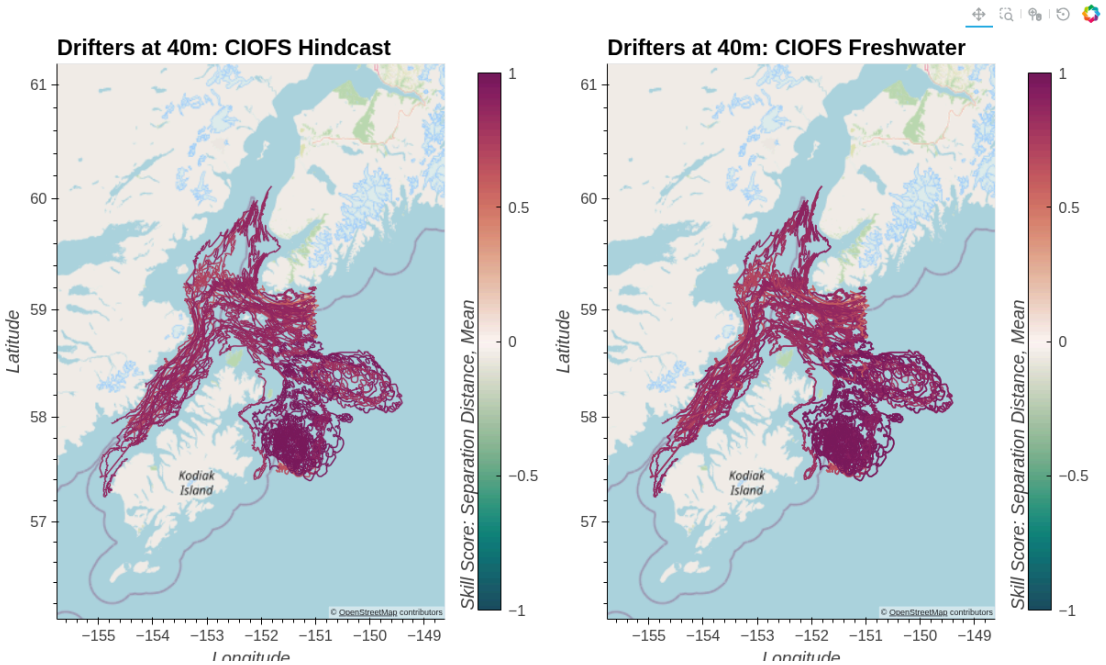

Fig. 13.22 Separation-distance skill scores for CIOFS Hindcast (left) and CIOFS Freshwater (right) with drifters at 40m depth. (PNG screenshot, available for PDF and for saving image.)

14. References

[ADCd.] ADCIRC. ADCIRC Tidal Databases. http://adcirc.org/products/adcirc-tidal-databases/, n.d. [Accessed 03-11-2023].

[BHAL16] JP Beamer, DF Hill, A Arendt, and GE Liston. High-resolution modeling of coastal freshwater discharge and glacier mass balance in the Gulf of Alaska watershed. *Water Resources Research*, 52(5):3888–3909, 2016.

[Cop12] Yannick Copin. Taylor diagram for python/matplotlib. 8 2012. URL: https://doi.org/10.5281/zenodo.5548061, doi:10.5281/zenodo.5548061.

[DHH+20] Seth L. Danielson, David F. Hill, Katherine S. Hedstrom, Jordan Beamer, and Enrique Curchitser. Demonstrating a high-resolution Gulf of Alaska ocean circulation model forced across the coastal interface by high-resolution terrestrial hydrological models. *Journal of Geophysical Research: Oceans*, 125(8):e2019JC015724, 2020. e2019JC015724 2019JC015724. URL: https://agupubs.onlinelibrary.wiley.com/doi/abs/10.1029/2019JC015724, arXiv:https://agupubs.onlinelibrary.wiley.com/doi/pdf/10.1029/2019JC015724, doi:https://doi.org/10.1029/2019JC015724.

[Hedstrom18] Katherine S Hedström. Technical Manual for a Coupled Sea-Ice/Ocean Circulation Model (Version 5). Technical Report, U.S Dept. of the Interior, Bureau of Ocean Energy Management, Alaska OCS Region, 2018. OCS Study BOEM 2018-007. 182 pp. URL: https://www.boem.gov/sites/default/files/boem-newsroom/Library/Publications/2018/BOEM-2018-007.pdf.

[HBB+20] Hans Hersbach, Bill Bell, Paul Berrisford, Shoji Hirahara, András Horányi, Joaqu\'ın Muñoz-Sabater, Julien Nicolas, Carole Peubey, Raluca Radu, Dinand Schepers, Adrian Simmons, Cornel Soci, Saleh Abdalla, Xavier Abellan, Gianpaolo Balsamo, Peter Bechtold, Gionata Biavati, Jean Bidlot, Massimo Bonavita, Giovanna De Chiara, Per Dahlgren, Dick Dee, Michail Diamantakis, Rossana Dragani, Johannes Flemming, Richard Forbes, Manuel Fuentes, Alan Geer, Leo Haimberger, Sean Healy, Robin J. Hogan, El\'ıas Hólm, Marta Janisková, Sarah Keeley, Patrick Laloyaux, Philippe Lopez, Cristina Lupu, Gabor Radnoti, Patricia de Rosnay, Iryna Rozum, Freja Vamborg, Sebastien Villaume, and Jean-Noël Thépaut. The ERA5 global reanalysis. *Quarterly Journal of the Royal Meteorological Society*, 146(730):1999–2049, June 2020. URL: https://doi.org/10.1002/qj.3803, doi:10.1002/qj.3803.

[HBC+15] DF Hill, N Bruhis, SE Calos, A Arendt, and J Beamer. Spatial and temporal variability of freshwater discharge into the Gulf of Alaska. *Journal of Geophysical Research: Oceans*, 120(2):634–646, 2015.

[LW11] Yonggang Liu and Robert H. Weisberg. Evaluation of trajectory modeling in different dynamic regions using normalized cumulative lagrangian separation. *Journal of Geophysical Research: Oceans*, 116(C9):, 2011. URL: https://agupubs.onlinelibrary.wiley.com/doi/abs/10.1029/2010JC006837, arXiv:https://agupubs.onlinelibrary.wiley.com/doi/pdf/10.1029/2010JC006837, doi:https://doi.org/10.1029/2010JC006837.

[McW09] James C. McWilliams. Targeted coastal circulation phenomena in diagnostic analyses and forecasts. *Dynamics of Atmospheres and Oceans*, 48(1-3):3–15, October 2009. URL: https://doi.org/10.1016/j.dynatmoce.2008.12.004, doi:10.1016/j.dynatmoce.2008.12.004.

[NOA19] NOAA. Cook Inlet Operational Forecast System (CIOFS) Information — tidesandcurrents.noaa.gov. https://tidesandcurrents.noaa.gov/ofs/ciofs/ciofs_info.html, 2019. [Accessed 03-11-2023].

[PBL02] Rich Pawlowicz, Bob Beardsley, and Steve Lentz. Classical tidal harmonic analysis including error estimates in MATLAB using T_TIDE. *Computers & Geosciences*, 28(8):929–937, 2002.

[Pea95] Karl Pearson. Note on regression and inheritance in the case of two parents. *Proceedings of the Royal Society of London*, 58:240–242, 1895. doi:10.1098/rspl.1895.0041.

[SM05] Alexander F. Shchepetkin and James C. McWilliams. The regional oceanic modeling system (ROMS): a split-explicit, free-surface, topography-following-coordinate oceanic model. *Ocean Modelling*, 9(4):347–404, January 2005. URL: https://doi.org/10.1016/j.ocemod.2004.08.002, doi:10.1016/j.ocemod.2004.08.002.

[Tay01] Karl E. Taylor. Summarizing multiple aspects of model performance in a single diagram. *Journal of Geophysical Research: Atmospheres*, 106(D7):7183–7192, 2001. URL: https://agupubs.onlinelibrary.wiley.com/doi/abs/10.1029/2000JD900719, arXiv:https://agupubs.onlinelibrary.wiley.com/doi/pdf/10.1029/2000JD900719, doi:https://doi.org/10.1029/2000JD900719.

[TLFD23] K. M. Thyng, C. Liu, M. Feen, and E. L. Dobbins. Cook Inlet Circulation Modeling, Final Report to the Oil Spill Recovery Institute. Technical Report, National Oceanic Atmospheric Administration National Centers for Coastal Ocean Science Kasitsna Bay Lab and Cook Inlet Regional Citizens Advisory Council, 2023. Axiom Data Science, Anchorage, AK. URL: https://ciofs.axds.co/.

[Wil81] Cort J. Willmott. On the validation of models. *Physical Geography*, 2(2):184–194, 1981. doi:10.1080/02723646.1981.10642213.

[Zha19] Aijun Zhang. Cook Inlet Operational Forecast System. Technical Report 096, NOAA National Ocean Service, Center for Operational Oceanographic Products and Services, 2019. doi:10.25923/50yk-ya28.

[NavalRLaboratory21] Naval Research Laboratory. HYCOM global ocean forecast system (gofs) 3.1. 2021. [Dataset]. URL: https://www.hycom.org/dataserver/gofs-3pt1/analysis.

[USGS16] USGS. National Water Information System (USGS Water Data for the Nation). 2016. [online database]; Available: http://waterdata.usgs.gov/nwis/. (July 2016). URL: http://waterdata.usgs.gov/nwis/.